

Highlights 2001

Contents

Published by:

**Berliner Elektronenspeicherring-Gesellschaft
für Synchrotronstrahlung m.b.H. - BESSY**

**Albert-Einstein-Strasse 15
12489 Berlin, Germany
phone +49 (0)30 / 6392 2999
fax +49 (0)30 / 6392 2990
<http://www.bessy.de>
info@bessy.de**

Board of Directors:

**Prof. Dr. W. Eberhardt, Prof. Dr. E. Jaeschke,
T. Frederking**

Editors:

**Regina Bost, Dr. Heike Henneken,
Dr. Markus Sauerborn, BESSY GmbH**

Layout:

Stitz & Betz Kooperations GmbH, Berlin

Printing:

Druckhaus Berlin-Mitte GmbH

**ISSN 0179-4159
BESSY GmbH, 2002**



Berliner Elektronenspeicherring-Gesellschaft für Synchrotronstrahlung m.b.H.

1	Introduction 04	
2		Scientific Highlights 06
3	News & Events 40	
4		Surface Reactions 08
5	BESSY-FEL 54	Superconductivity 18
6		Clusters and Nanostructures 20
		Magnetism 24
		Fundamental Physics 30
		Archeometry 32
		Protein Crystallography 34
		EUV Lithography 36
	Facility Report 46	
		Facts & Figures 60

Introduction

1

2001 was a year of many changes and new developments at BESSY.

The annual report, now called 'BESSY Highlights 2001', your are holding in your hands has a new look.

This new format intends to reflect the full spectrum of science at BESSY including new developments of accelerator and experimental stations. The 'good old' annual report is now published on compact disc.



In May 2001, Prof. Wolfgang Gudat handed over the position as director of science to Prof. Wolfgang Eberhardt, who will keep on developing BESSY's scientific profile and future. The accelerator of BESSY II shows an excellent performance, improving the life time of the electron beam at 200 mA to 10 h. In the past year, nearly 3,900 h total user operation time has been achieved in three shift seven days a week operation mode and more than 160 projects were carried out.

At present, 36 beamlines are in operation. Among the beamlines put into operation in 2001 is a newly designed plane grating monochromator beamline of the Russian-German Laboratory, a joint venture of the University of St. Petersburg, the Freie Universität Berlin and BESSY. The inauguration was accompanied by the 'Third Russian-German' Workshop" on Synchrotron Radiation Research. By the end of the year, the new Infrared beamline run by the IR-Initiative Synchrotron radiation (IRIS) was operational, opening a whole new wavelength range for BESSY users.

The Application Center for Microtechniques started operation in November 2001. This is a cooperation with the Technical University Berlin, dedicated for applied research in lithography, enabling developments for industry and small and medium sized companies.

Also, the conventional facilities of BESSY are expanding. The new wing of the building on Albert-Einstein-Straße has been inaugurated with a ceremony on October 4th, 2001. It includes a lecture hall for 150 people and a library, improving the scientific communication on site as well as 1,000 m² of additional office and laboratory area increased the space capacity for the growing BESSY crew. Another 1,000 m² are dedicated to the Hahn-Meitner-Institute (HMI) including laboratory installations and office spaces, intensifying the BESSY-HMI collaboration.

'Visions of Science: The BESSY-FEL in Berlin-Adlershof' describes the technological challenges and the enthusiasm about the scientific opportunities of the planned free electron laser (FEL) (see CD).

In context with this documentation of the 'Scientific Case', a short description of the project 'Development and Construction of a Free Electron Laser (SASE-FEL) in Berlin-Adlershof' was submitted and successfully presented to the Wissenschaftsrat on October



25th and 26th, 2001. A statement by the Wissenschaftsrat is expected by mid 2002. The importance of the FEL project is also recognized by the Berlin Senate, supporting the technical design study by the Zukunftsfonds for three years.

The BESSY Users' Meeting, traditionally held beginning of December, with more than 300 participants, also had a focus on the perspectives of the planned BESSY-FEL. The annual 'Ernst-Eckhardt-Koch' Prize for the outstanding doctoral thesis was awarded to Dr. Karin Heister (University Heidelberg). For the first time the BESSY innovation prize, also funded by the VDFFB, was donated to Dr. Rolf Follath and Dr. Friedmar Senf (both BESSY).

A look behind the scenes of BESSY attracted more than 3,800 visitors during the first 'Lange Nacht der Wissenschaften' in Berlin. Additionally, more than 70 national and international groups visited BESSY in 2001. The importance of BESSY for the WISTA and greater area of Berlin concerning science and technological development was also expressed by the visits of high ranking persons among them Klaus Wowereit (Mayor of Berlin), Adrienne Goehler (Berlin Senator of Science, Research and Culture), Werner Müller (Federal Minister of Economy), and Hans-Olaf Henkel, the new president of Wissenschaftsgemeinschaft Gottfried-Wilhelm-Leibniz.

The facility BESSY II is one of the most modern and efficient synchrotron radiation sources world wide, which is only possible due to the great dedication of all people involved. We want to thank the entire BESSY staff and all BESSY users for their commitment and the members of our various committees and the funding agencies for their support.

*The BESSY Board of Directors
Berlin, February 2002*

Scientific Highlights

2

The selection of highlights intends to reflect the full spectrum of sciences at BESSY comprising such diverse fields as archeometry, study of magnetism, lithography, and protein crystallography.

The contributions are written in a more popular style than in the 'good old' annual report. We hope that non-experts will find them understandable and interesting to read. These short articles are also meant as appetizers for the long version available on the CD.





Surface Reactions **08**

Superconductivity **18**

Clusters and Nanostructures **20**

Magnetism **24**

Fundamental Physics **30**

Archeometry **32**

Protein Crystallography **34**

EUV Lithography **36**

High-resolution photoemission meets supersonic molecular beam

R. Denecke, M. Kinne, T. Fuhrmann, C. Whelan, J. Zhu and H.-P. Steinrück

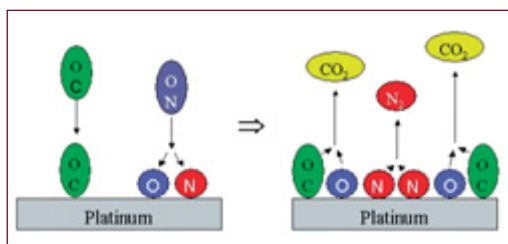


Fig. 1

The fundamental understanding of heterogeneous catalysis requires knowledge of the basic processes taking place at the catalyst surface. These are adsorption and desorption of molecules and their reactions (Fig. 1). However,

most of the current surface science tools are not applicable in the environment where catalysts are working, which is high gas pressures and/or high temperatures on rough surfaces. In order to bridge these two 'gaps' quite some effort can be observed in the surface science community.

High-resolution core-level X-ray photoelectron spectroscopy (XPS) has developed into a powerful tool for studying adsorbates on surfaces. Besides the chemical sensitivity, even more detailed information about surface processes, like the actual binding sites and bonding properties of surface species, can be derived. However, due to the use of electrons and the strong dependence of their mean free path on the pressure, XPS is limited to high vacuum conditions. One way of extending the usable pressure range is by differentially pumping between a reaction cell and the electron analyzer [1]. Our approach is to use a supersonic molecular beam as gas source which allows for relatively high sample pressures (up to 10^{-5} mbar) without flooding the whole experimental chamber – in a way comparable to a water stream from a fire fighter hose. A second aspect is the sharp and tunable kinetic energy distribution in contrast to a broad Maxwellian distribution of energies from a gas volume at a certain temperature. This provides molecules with sufficient energy to overcome activation barriers for adsorption or reaction.

We have recently built a new apparatus integrating both a three stage supersonic molecular beam and a high-resolution photoelectron analyser in a compact transportable set-up [2]. Especially, the advent of third generation synchrotron sources like BESSY II with their high photon flux at high resolution

allows photoelectron spectroscopy to enter the time-resolved measurement mode.

This has been termed fast-XPS [3] or temperature-programmed TP-XPS, if a linear heating ramp is applied to the sample [4]. Besides the possibility to observe chemically induced core-level shifts for almost all core-levels involved (of both adsorbate and substrate) and thus to identify different adsorbed species, quantitative information can be obtained. We will limit the discussion to two examples, CO oxidation on Pt(111) and dissociative CH₄ adsorption on Pt(111).

The first step is the study of CO adsorption on Pt(111). This system is known to provide two adsorption sites (on-top and bridge), which for a total coverage of 0.5 monolayers (ML) are arranged in a $c(4 \times 2)$ structure with equal partial coverages. Fig. 2 shows a series of C 1s spectra recorded during the uptake of CO at a sample temperature of 95 K, with a resolution of 120 meV and the time per spectrum of 3s. Our findings are in general agreement with time-resolved high-resolution electron energy loss spectroscopy results [5]. Quantitative analysis of site occupancy vs. total coverage curves for different temperatures can yield the binding energy difference between the two adsorption sites. For this analysis it has to be ensured that the site distributions are in thermal equilibrium, since an activated transfer between the sites is possible. This is confirmed by the similarity of the site distribution upon varying the pressure of the incident CO molecules using the molecular beam. Using a simple model the binding energy difference is found to be 50 meV, in agreement with previous publications.

The second step is the study of the CO oxidation reaction. In order to understand the fundamental steps we have to use simple and well-defined situations. In the present study we prepared a (2×2) layer of atomic oxygen by saturation dosing O₂ at low temperatures and heating to 300 K. On this layer CO was impinging from the molecular beam. To be able to study reaction kinetics independently of the adsorption process or the diffusion time we used a high local CO

[1] D.F. Oggletree et al., *Rev. Sci. Instr.* (submitted) (and references therein)

[2] R. Denecke et al., *Surf. Rev. Lett.* (in print)

[3] A. Baraldi et al., *R. Rosei, Surf. Sci. Lett.* 367 (1996) L67.

[4] C.M. Whelan et al., *J. Chem. Phys.* 115 (2001) 8133.

[5] A. Cudok et al., *Phys. Rev. B* 47 (1993) 13682 (and references therein).

[6] S. Völkening et al., *J. Chem. Phys.*, 114 (2001) 6382.

[7] A. Luntz et al., *J. Chem. Phys.* 90 (1988) 1274.

Supported by DFG.

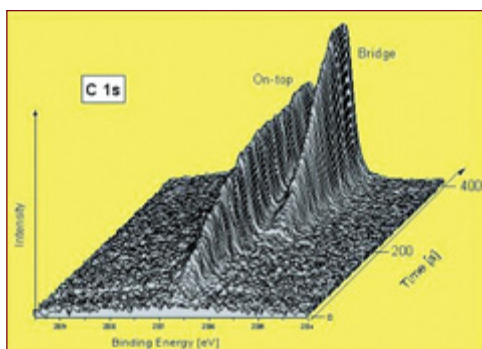


Fig. 2:

C 1s spectra recorded with a photon energy of 380 eV during CO uptake on Pt(111) at 95 K. The resolution is about 120 meV and the time per spectrum is 3 s. The background CO pressure in the chamber was 3×10^{-9} mbar. Adsorption starts on the on-top sites (electron binding energy of 287.0 eV) while the bridge sites (286.3 eV) are only occupied for higher coverages.

pressure (about 1×10^{-6} mbar). Following O 1s intensities as function of time for different temperatures, we get results as shown as density plots in Fig. 3 for two particular cases. From the rate of oxygen coverage change we derive a reaction order close to 0.5, in agreement with STM studies [6]. The latter proposed that the reaction takes place at the perimeter of O islands. Variation of the surface temperature between 275 and 305 K results in changing reaction rates. From an Arrhenius plot of the reaction constants we obtain a value of about 0.5 eV for the activation energy of the reaction, which is in the range of previously reported values [6].

So far we used the high local pressure and fast switching possibility of the molecular beam. For studying activated adsorption processes the variable kinetic energy of the molecules is a key ingredient. One such system we studied is the dissociative adsorption of CH_4 on Pt(111). This initial adsorption step seems to be the limiting factor in the so-called steam-reforming process to produce synthesis gas ($\text{CO} + \text{H}_2$) from natural gas, which in turn is the initial catalytic event in the conversion from natural gas to gasoline. This reaction normally runs at high pressures and is as such not easily observable. However, increasing the kinetic energy of the molecules has been shown to lead to substantial dissociative adsorption [7].

One goal of our investigations is to see, if the chemical nature of adsorbed species depends on the kinetic energy or the excitation of internal degrees of freedom (vibrations, rotations) of the impinging molecules. Therefore, two ways of changing the molecular energy have been employed, namely heating of the nozzle and/or seeding CO in He (in flowing through the nozzle orifice the faster He atoms accelerate the CO molecules by collisions). Comparing experiments with the same kinetic energy but different degrees of excitation of vibrational modes should give an answer about the activation mechanism. We find in agreement with literature, that for low kinetic energy

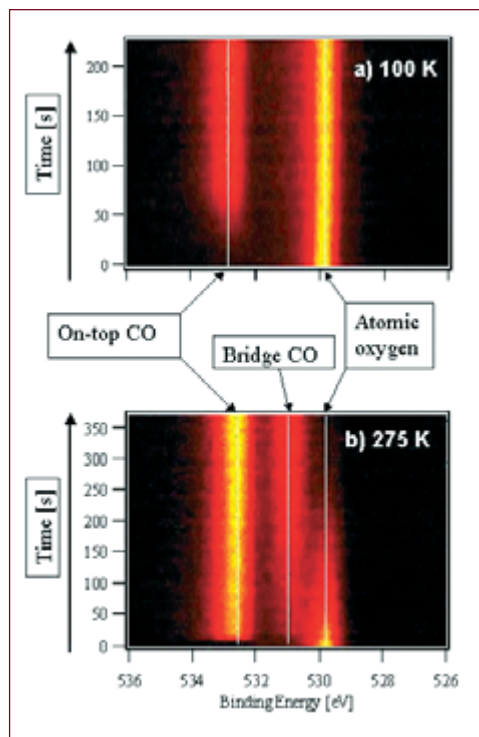


Fig. 3:

O 1s intensities taken with a photon energy of 650 eV shown as density plots. At 100 K (a) introduction of CO leads to occupation of the on-top sites (binding energy of 532.8 eV) only. The bridge sites seem to be blocked by the adsorbed O. No reaction takes place, as can be seen by the constant O coverage (peak at 529.8 eV). Increasing the temperature to 275 K (b) leads to a decrease of the atomic oxygen signal, which is accompanied by an increased CO bridge occupation.

almost no adsorption can be observed (i.e., the sticking coefficient is very low) [7]. If the kinetic energy is increased (to about 1 eV) observable dissociative adsorption takes place. From TP-XPS series, and in comparison with similar measurements for other hydro-carbons, intermediate species of the thermal dehydrogenation can be identified.

In the future this combination of techniques, which can provide time- and temperature-resolved quantitative chemical information about intermediates and products on surfaces will be used in the study of more complex reactions. One such example is the methanol steam-reforming process, which can be used to provide hydrogen for fuel cells in automobiles. A further advantage of the described method is the possibility to simultaneously observe changes in the catalyst surface, which could help to identify the active surface phase (e.g., a PdZn alloy is proposed to be an efficient catalyst for this reaction).

Contact:

Reinhard Denecke,
Physikalische Chemie II,
Universität Erlangen-Nürnberg
reinhard.denecke@
chemie.uni-erlangen.de

Heterogeneous Catalysis: Surface Structures in a high pressure environment

M. Hävecker, R.W. Mayer, A. Knop-Gericke and R. Schlögl

Catalysis is the science and technology of manipulating the rate and course of chemical reactions. Accelerating wanted reactions and suppressing unwanted reactions allow to effectively produce all functional materials, polymers, fertilisers, transportation fuels and biologically relevant molecules, accounting for about 10% of the industrial world GNP. Catalysts are either free molecules (homogeneous catalysis, dominating in the biological area) or surfaces of solids (heterogeneous catalysts, dominating technical catalysis). Highly specific chemisorption and surface diffusion processes occur under operating conditions. These processes need to be known in detail to understand the mode of operation of catalysts and eventually to reach the goal of improving or innovating catalytic processes. As the overall efficiency of technical chemical synthesis is about 50% of the thermodynamic limit, there is ample space for technology to ensure sustainable development of the industry. After 80 years of empirical optimisation further improvements are increasingly depending on knowledge-based approaches.

The only way to get the necessary understanding is the analysis of model systems with reduced structural complexity that allow the application of modern surface science techniques and theoretical methods in describing quantitatively the course of elementary step processes [1]. The limited progress in this approach in understanding more than a few 'bellwether' reactions [2] is due to the issue of complexity of most practical systems and the frequent failure to reduce this complexity without modifying the function of the system.

Active catalysts [3] restructure under operating conditions not only at their surfaces [4] but also as material [5], leading to metastable and usually unknown compounds. An essential pre-information to model studies is thus the knowledge about geometric and electronic structures of the operating system. Techniques are required delivering information about the surface electronic and geometric structure under operating conditions [6].

X-ray absorption spectroscopy of reactants and surfaces at low energy and high pressure is a suitable method. This technique, which can work with model systems as well as with practical catalysts and which exhibits no limitations in the complexity of the catalytic reaction, requires tunable high brilliance synchrotron radiation and a dedicated detection scheme [7]. In the following two examples we show results on the electronic and geometric structure of working catalysts.

We start discussing the role of copper (Cu) in the selective oxidation of methanol. Cu is very reactive to molecular oxygen forming a manifold of surface and bulk oxides. It is further an active and selective catalyst for partial oxidation of alcohols to aldehydes and ketones. Under UHV reaction conditions and after quenching from reaction cell experiments the surface is metallic and covered with patches of Cu_2O [8]. Complete coverage with oxide is strongly inhibiting and leads to a change in selectivity from partial to total oxidation. The pure metal is non-reactive to organic substrates. An in-situ study of polycrystalline Cu foil was carried out looking at the selective oxidation of methanol yielding formaldehyde and as undesired product carbon dioxide and water [8]. The key to a successful operation is the control of reactivity of adsorbed atomic oxygen that should only be mildly active to perform selective oxidation. The problem can be reduced to an in-situ analysis of the atomic oxygen species present on a reacting surface.

Fig. 1 shows in the top panel the XAS Cu L_{III} data of a reacting foil. High activity at a stoichiometric composition of the gas phase can be reached. Under these conditions the surface is metallic (blue coded spectra) despite the presence of substantial amounts of activated oxygen in the system. Excess oxygen oxidises the metallic state yielding a Cu_2O -like thin layer (red coded spectra) over the Cu bulk and strongly suppresses the catalytic function. The corresponding oxygen K-edge data are reported in the bottom panel of Fig. 1.

[1] G. Ertl, *J. Vac. Sci. Technol. A* 1, 1283 (1983).

[2] M. Boudart, *Topic Catalysis* 13, 147 (2000).

[3] G. Mestl et al., *J. Mol. Catal. A* 162, 455 (2000).

[4] P. W. Jacobs et al., *J. Mol. Catal. A* 131, 5 (1998).

[5] A. J. Nagy et al., *J. Catal.* 188, 58 (1999).

[6] J. M. Thomas et al., *Angew. Chem-Int. Ed.* 106, 316 (1994).

[7] M. Hävecker et al., *Angew. Chem-Int. Ed.* 37, 1939 (1998).

[8] T. Schedel-Niedrig et al., *Phys. Chem. Chem. Phys.* 2, 2407 (2000).

[9] A. Knop-Gericke et al., *Topic Catalysis* 15, 27 (2001).

[10] G. Centi, *Catal. Today* 16, 1 (1993).

[11] P. T. Nguyen et al., *Mat. Res. Bull.* 30, 1055 (1995).

[12] V. Eyert et al., *Phys. Rev. B.*, 57, 12727, (1998).

Funded by BASF and DFG

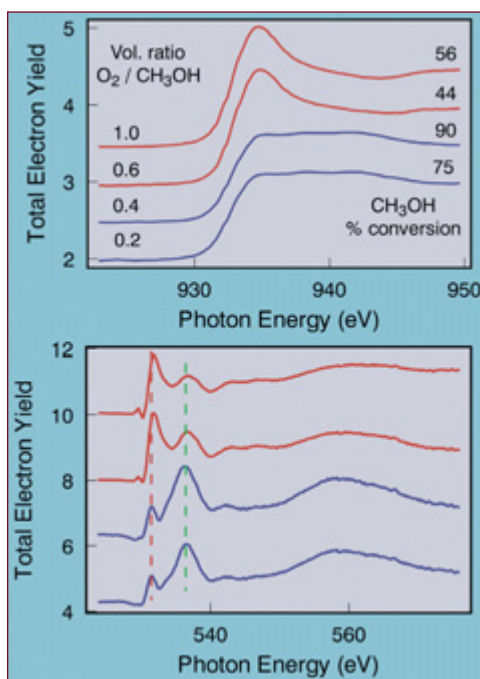


Fig. 1:
Top: Copper L_{III} XAS data of catalyst foil at 0.56 mbar pressure and at 570 K reaction-temperature under methanol: oxygen gas compositions. The methanol conversion discriminates two regimes of operation.

Bottom: Oxygen K edge data corresponding to the in-situ experiment above. The dotted lines indicate contributions from oxide-like species (red) and from weakly adsorbed atomic oxygen (green). The modification of spectral shapes with gas phase composition (see above) is evident.

In the highly active state chemisorbed oxygen is present at the surface as oxide (peak at 532.7 eV) and as a novel species undetectable under ex-situ conditions. Its broad single resonance at 535.5 eV is due to a weakly interacting atomic oxygen species. The variation of the parameters of the working conditions allows to assign specific catalytic functions to these species and to deduce structure-function-relationships [9]. It occurs that the novel oxygen species is responsible for the partial oxidation of methanol whereas the conventional oxide-like species is consumed during total oxidation of methanol. From these data it follows further that total and partial oxidation occur via different mechanisms on two different sites of the same catalyst.

The second example is Vanadyl pyrophosphate (VPP) in the butane oxidation. VPP represents a complex derivative of V^{IV} -oxide which is a uniquely active and selective catalyst for the oxidation of n-butane with air to yield maleic acid anhydride (MAA) [10]. Unfortunately, there exists no other direct oxidative activation of n-alkane molecules that would be an abundant feedstock for chemical industry. In the intense search for such activation reactions it is essential to understand the surface properties of this very special catalyst. The top spectrum in Fig. 2 represents the $V-L_{III}$ edge of the reference oxide V_2O_5 whereas the bottom spectrum stems from an in-situ activated practical VPP material. The spectra can be used to correlate the positions of the different t_{2g} transitions for the structurally inequivalent V-O bonds to their bond distance available from X-ray diffraction analysis [11]. The insets reveal that a good correlation exists between these two quantities.

The validity of the analysis can be checked by cross correlations between the theory-calibrated data set [12] for V_2O_5 and the X-ray diffraction-calibrated data set for VPP yielding excellent agreements for all peaks except for the main resonance which does not correlate to any bulk bond length found in the reliable structure determination of VPP. This discrepancy leads to the conclusion that there should be a further compound present exclusively at the surface of the active catalyst consisting of a structure with a prominent V-O-V bridge geometry of a bond distance of 1.75 ± 0.03 Å. The accurate prediction from quantitative XAS finds its relevance by the fact that there do exist several vanadium oxo-compounds that exhibit this rather rare V-O bond distance and by the fact that working catalysts are surface-deficient in phosphate precluding the stoichiometry of VPP to exist at the working surface. It is evident that these findings are most relevant for the functional analysis of VPP and that only in-situ XAS was able to deliver this information.

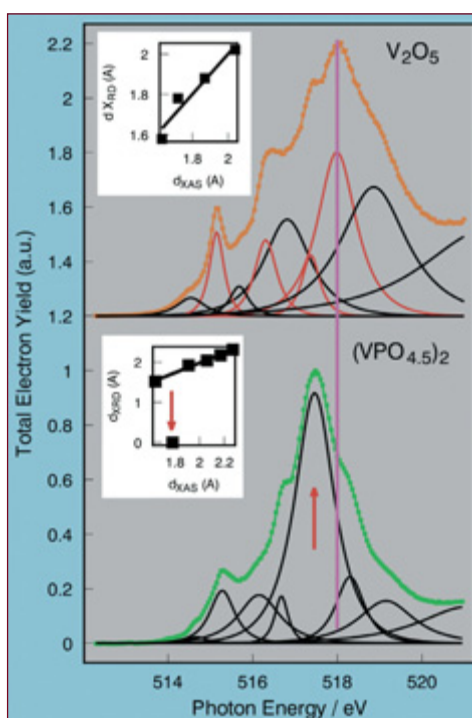


Fig. 2:
Vanadium L_{III} spectra of V_2O_5 (as received, orange) and of vanadyl pyrophosphate ($VPO_{4.5}$)₂ (VPP) (preconditioned under in-situ reaction conditions and measured at 673 K, green). Spectra were taken from powder samples. The deconvolution for V_2O_5 is based upon a theoretical analysis of the lineshape. The insets report the correlations of predicted V-O bond distances (d_{XAS}) with the bulk values from X-ray diffraction data (d_{XRD}). The reference line denotes the position of the resonance arising from the V=O bond in V_2O_5 .

Contact:

Robert Schlögl, Fritz-Haber-Institut der MPG, Berlin
 schloegl@fhi-berlin.mpg.de

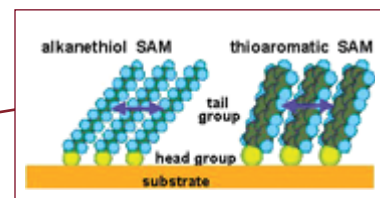


Fig. 2:
Sketch of aliphatic and aromatic SAMs.

New Insights into Self-assembled monolayers

K. Heister, S. Frey, M. Zharnikov and M. Grunze



Fig. 1:
Gold-coated glass chips covered by SAMs are used as carriers for chemical microarrays in biotechnology. A specific surface preparation enables the immobilization of chemical compounds while preventing the nonspecific binding of proteins: Goldfinger® by Graffinity AG

The surface behavior of material is crucial in our lives, whether one considers a biological implant, a catalyst, an electronic chip, or a moving component in an engine. It is therefore vital that the surface properties of materials used in our modern world are thoroughly understood and recipes to tailor these characteristics are found. A perspective tool to design surface properties, such as wetting, lubrication, corrosion, adhesion, and protein affinity (Fig. 1) are so called self-assembled monolayers (SAMs).

SAMs are close-packed 2D arrays of rod-like organic adsorbate molecules. They are chemically bonded to the substrate via their head group while the molecular chain (tail group) points to ambience. Because of this architecture SAMs are an attractive tool to modify surface properties or to laterally structure a surface [1]. The arrangement of the adsorbates is governed by the interplay of the intermolecular forces and the substrate-adsorbate-interaction that promote a high degree of molecular order in the adlayer [2]. To understand the structure-determining balance of forces we applied synchrotron radiation-based surface analysis techniques, like near-edge X-ray adsorption fine structure (NEXAFS) and high resolution photoelectron spectroscopy (HRXPS) and investigated the properties of SAMs with a thiolate head group for different types of tail groups and substrates (Fig. 2).

In HRXPS spectra (Fig. 3) each component of a peak reflects an electronic state of one species of atoms (i.e. bulk vs surface atoms). The method is therefore element specific and sensitive to an atoms chemical surrounding and perturbations of its electron shells e.g. by external excitations. The use of synchrotron radiation allows to measure at photon energies where signal intensity and surface sensitivity are maximised. In combination with high energy resolution ($\Delta E < 0.1$ eV) detailed information of the interactions between SAM and substrate is achieved.

We studied the properties of the aliphatic dodecanethiolates (C12) or the aromatic biphenylthiolates (BPO) on Au and Ag substrates using Au 4f, Ag 3d_{5/2} and S 2p HRXPS. Fig. 3 shows the Au 4f HRXPS spectra for a clean and a SAM-covered Au substrate. For the clean (111) textured Au substrate the emission related to the topmost layer (blue) is clearly separated from the emission originated from the bulk (pink). If this substrate is covered by the aliphatic C12 or the aromatic BPO only one joint peak is perceptible as the emission related to the outermost Au atoms has moved towards the bulk signal at higher binding energies [3]. This strong reaction of the outermost Au layer indicates a strong adsorbate-substrate bond that has been attributed with an Au surface reconstruction. Similar results on Ag substrate confirm the strong bonding of the thiolate head group to the substrate [3]. Focussing on the head group, the S 2p HRXPS spectra (not shown) exhibit a single S 2p doublet (S 2p_{3/2} and S 2p_{1/2}) for both C12 and BPO on Au and Ag with a peak position at lower binding energies on Ag

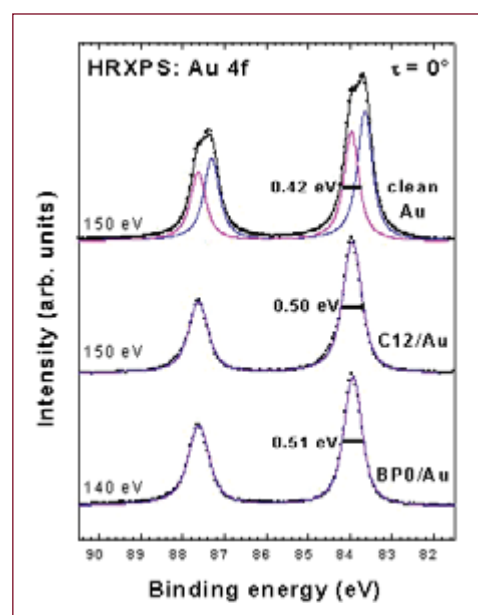


Fig. 3:
HRXPS Au 4f spectra of clean and SAM covered Au surface.

[1] A. Ulman, *An Introduction to Ultrathin Organic Films From Langmuir-Blodgett to Self-Assembly* (Academic Press, Boston, 1991); *Chem. Rev.* 96 (1996) 1533.

[2] M. Zharnikov et al., *Phys. Chem. Chem. Phys.* 2 (2000) 3359.

[3] K. Heister et al., *J. Phys. Chem. B* 105 (2001) 4058.

[4] G. Hähner et al., *J. Vac. Sci. Technol. A* 10 (1992) 2758.

[5] K. Heister et al., *Langmuir* 17 (2001) 8.

[6] H.U. Müller et al., *J. Phys. Chem. B* 102 (1998) 7949.

Supported by BMBF and Fonds der Chemischen Industrie.

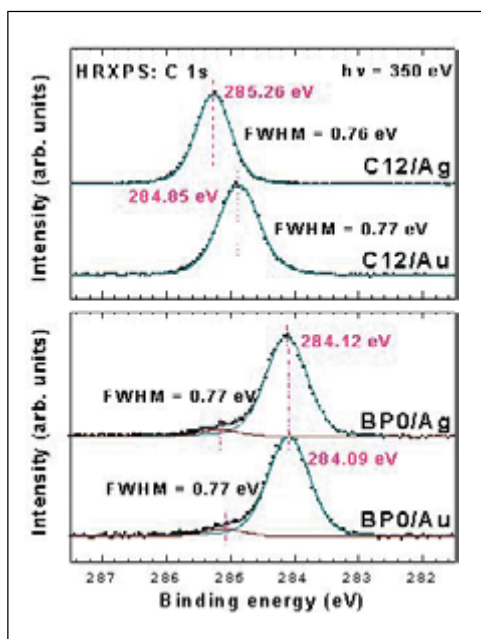


Fig. 4:
HRXPS C 1s spectra of aliphatic and aromatic SAMs on Au and Ag.

than on Au implying a stronger interaction of the head group with the Ag than with the Au substrate.

We used angular-dependant NEXAFS measurements to reveal the orientation of these molecules on the surfaces (not shown). The average tilt angle is less dependent on the substrate in the aromatic films (e.g. 16° for TPT@Ag, 20° for TPT@Au) [6] than in aliphatic thiolates, in which the tilt angle is much larger on Au (30-33°) than on Ag (10-12°) [5]. This indicates, a dominant role of the intermolecular interaction for the film structure of aromatic SAMs [2]. The structural differences are also reflected in the photoemission data showing a correlation between the binding energy of the electron and the structural properties (Fig 4).

The irradiation of aliphatic SAMs by X-rays (necessary for an electron spectroscopy experiment) can damage the SAM significantly due to the excitation of secondary and photoelectrons in the substrate [6]. These electrons cause dehydrogenation of the SAM, desorption of molecular fragments, thickness reduction, the appearance of double bonds between adjacent carbon radicals, and the loss of orientational and conformational order. Furthermore, a new, irradiation-induced sulfur species can be observed in the XPS S 2p spectra at the expense of the pristine thiolate head groups (Fig. 5). The comparison of the binding

energy position of the corresponding S 2p doublet with those of several reference sample reveals a chemical equivalence of the irradiation-induced sulfur species to a dialkylsulfide entity [6]. XPS depth profiling by variation of photon energy and emission angle indicates that these species are predominantly located above the head group-substrate interface. This means that the cleavage of the thiolate-substrate bond leaves a mobile sulfur species which easily bonds to an adjacent carbon radical and forms a sulfide bridge as sketched in Fig. 5 [6]. This process contributes to irradiation-caused crosslinking within the adlayer. At the same time, the damage of the S/substrate interface (along with the decrease of the contact angle) makes irradiated areas sensitive to wet etching, which makes aliphatic SAM suitable for the application as a positive lithographic resist [7].

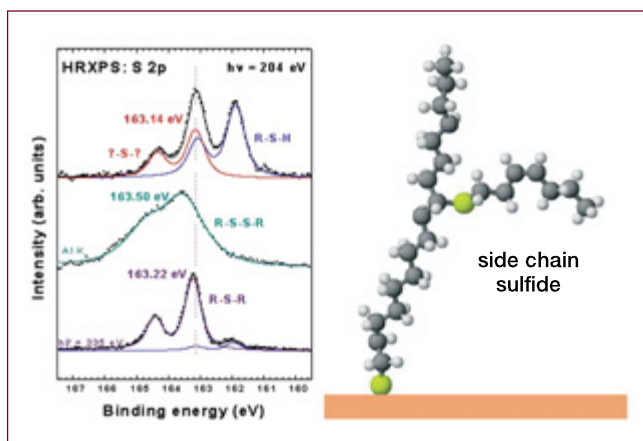


Fig. 5:
HRXPS S 2p spectra of an irradiated aliphatic SAM in comparison to reference systems.

Contact:

Michael Grunze, Universität Heidelberg
Karin Heister, now: Max-Born-Institut, Berlin
michael.grunze@urz.uni-heidelberg.de
heister@mbi-berlin.de

New insight into the properties of condensed organic thin films

A. Schöll, Y. Zou, D. Hübner, Th. Schmidt, R. Fink and E. Umbach

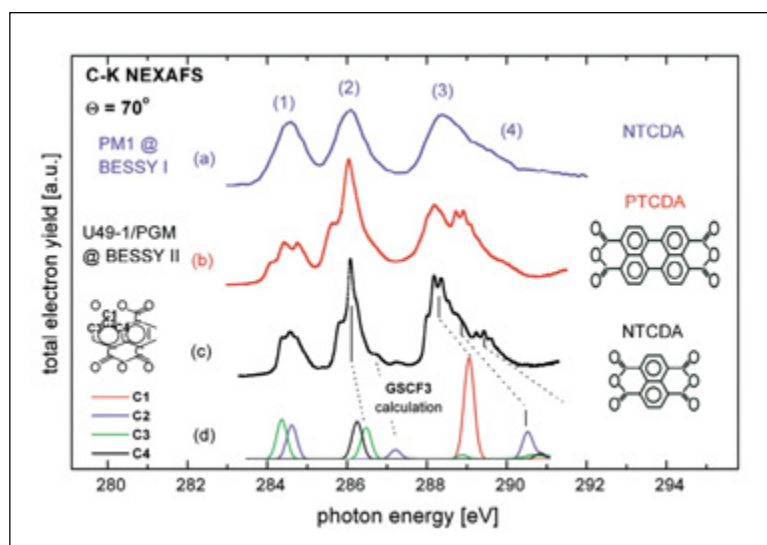


Fig. 1:
C K-edge NEXAFS spectra of bound p-states on expanded energy scale of condensed organic films adsorbed on Ag(111):
a) for NTCDA recorded at the BESSY-I PM-1 beamline
b) and c) for PTCDA and NTCDA [1] measured with improved spectral resolution at the BESSY-II U49/1-PGM beamline.
d) ab-initio calculation for an isolated NTCDA molecule based on the Kosugi code [2].
The structural formulae of the molecules are shown on the right-hand side.

Organic thin films represent a new class of materials that has recently attracted enormous interest due to their outstanding optical and transport properties and their applicability as active components in commercial electronic or opto-electronic devices. These consist either of polymers or of evaporable medium-size organic molecules. A technique that is ideally suited to study such organic systems is near-edge X-ray absorption fine structure (NEXAFS). This technique can distinguish between chemical states, is (semi)quantitative, can be applied as microscopic probe with a spatial resolution of a few (presently few tens of) nanometers, and provides information about molecular orientation and unoccupied electronic orbitals.

High-brilliance third-generation synchrotron sources provide new opportunities, for instance by drastically enhanced spectral resolution and photon fluxes. These improvements can be utilized to get new insight with spectroscopic techniques. NEXAFS experiments of thin films of NTCDA and PTCDA (structural formula see Fig. 1) adsorbed on Ag(111) and Au(111) surfaces were recorded at BESSY II very recently with much higher resolution than ever before.

Fig. 1 compares C K-edge NEXAFS data recorded at BESSY I [1] (spectrum a - resolving power: 3,000) with those recorded at BESSY-II (spectra b and c; resolving power: ~10,000) and with a calculated spectrum of NTCDA.

Just three years ago we were happy to resolve four different C 1s – π -transitions below ionisation threshold (labelled 1-4 in spectrum a), because such spectra could be used to determine the molecular orientation and the chemical bonding to the substrate. However, they were not detailed enough to derive further properties, and even the difference between NTCDA and PTCDA was hardly discernible. With BESSY II the situation has drastically improved as seen in Fig. 1 (spectra b, c).

Now the spectra contain about 20 discernible peaks and shoulders, the difference between PTCDA and NTCDA is obvious, and the structural properties have remarkable influence on the spectra.

What do we learn from such high resolution spectra? First, we now get all electronic transitions with very accurate relative intensities and energies (~10 meV) which, of course, requires some data evaluation. In this way all calculated transitions (spectrum d in Fig. 1) could be identified in the experimental data. Since each transition reflects the local properties around one sort of atoms within the molecule one is now able to distinguish the changes that occur within a molecule due to mutual interactions or due to the involvement of a certain functional group in a reaction or bonding process. Secondly, one can easily attribute the fine structure to strong electron-vibron coupling. Although expected, such fine structure was not observable in NEXAFS data of organic materials until now. It was usually argued that inhomogeneous broadening and the coupling of too many, partly low-energy vibrations would prevent the observation of electron-vibron coupling which apparently is not true. Now it is possible to identify vibrations that couple preferably to certain electronic transitions.

References:

- [1] D. Gador, et al., *Europhys. Lett.* 41(2) (1998) 213.
 [2] N. Kosugi, *Chem. Phys. Lett.* 74 (1980) 490; N. Kosugi, *Theoret. Chim. Acta* 72 (1987) 149.

This work is funded by the BMBF.

Since the latter are atom-specific one gets information of local vibronic properties within the molecule. And thirdly, it is possible to monitor subtle electronic energy shifts, changes of vibrational energies, and coupling strengths as a function of geometric structure, order within the film, and interaction with other molecules or with the substrate.

Much information can be deduced from a simple "fingerprint" analysis, i.e. just by comparing spectra. More details and especially quantitative data can only be obtained by a detailed lineshape analysis, i.e. by curve fitting.

Since several electronic transitions may contribute to one spectral feature and since each electronic transition can generally couple to $3N$ vibrations (N = number of atoms per unit cell) multiplied by the number of vibrational quanta that contribute according to the Franck-Condon factors one has a fit problem with too many parameters. This requires a careful approach the result of which is shown in Fig. 2. The experimental data (dots) are the features labelled 3 and 4 (Fig. 1).

An unambiguous result of this analysis is that features 3&4 contain three electronic transitions (as postulated by the calculations; spectrum d in Fig. 1) each coupled to at least one vibration. The latter are described each by a vibrational progression with fixed energies (harmonic approximation) using the Franck-Condon principle. The resulting vibrational energies are compatible with C-O stretching modes as deduced from infrared and high-resolution EELS experiments. The residuum of such a fit is still unsatisfactory especially at the leading edge which is described only by very few fit parameters. A better description of the leading edge could only be achieved, if a second vibrational progression with identical parameters but a small total energy offset of 80 meV was allowed to couple to the first electronic transition.

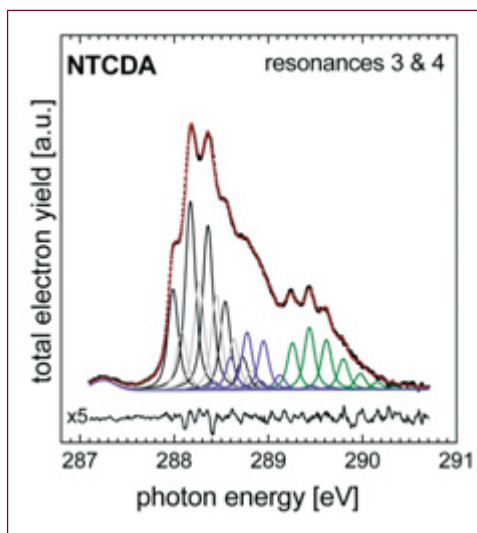


Fig. 2: Least-square fit of vibronic progressions to the experimental data of resonances 3 and 4 (spectrum c in Fig. 1) taking into account three electronic transitions. The relative intensities are scaled by calculated Franck-Condon factors.

This fit is shown in Fig. 2. The second progression is presently interpreted as Davydov splitting which is often observed in optical spectroscopy if the unit cell contains more than one molecule but has never been identified in XUV spectra. However, the observation of a regular structure in the residuum of Fig. 2 (bottom) also indicates that additional vibrations are involved and contribute with significant intensity to the spectrum.

In summary, high-resolution NEXAFS spectra of organic thin films reveal a wealth of fine structures that allow the identification of strong electron-vibron coupling and of additional electronic transitions hitherto undiscovered. The fine structures are very sensitive to molecular details, to the bonding to the substrate, to intermolecular interaction and hence to structural order. It is the first time that in high-energy spectra (in the XUV-range) subtle spectral differences could be attributed to different geometric structures in a van-der-Waals-like system. A careful lineshape analysis reveals further details and yields numbers for electronic levels (very accurately), vibron energies, electron-vibron coupling constants, lifetime widths, inhomogeneous broadening, etc. One could even think to use such measurements as standard to determine the instrumental resolution of a soft X-ray beamline since the lifetime width is smaller at the C 1s as compared to the N 1s edge and since the Gaussian width is fairly below 100 meV in highly ordered thin organic films.

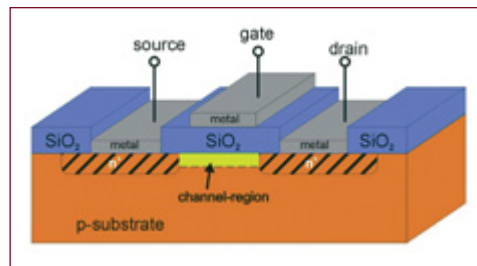
Contact:

Rainer Fink, Experimentelle Physik II, Universität Würzburg
fink@physik.uni-wuerzburg.de

The Local Environment of Silicon upon Oxidation of the Surface

C. Westphal, S. Dreiner and M. Schürmann

Fig. 1:
Schematic drawing of a metal oxide semiconductor field effect transistor. It is composed by a substrate single semiconductor crystal surface which is covered by oxide and metal films



In the past years it became more and more important to develop high-speed low-noise transistors for the on-going miniaturization of integrated circuits. Most modern metal-oxide-semiconductor field effect transistor (MOSFET) are based on silicon technology (Fig. 1). The interface between silicon and silicon oxide in ultra-small silicon based transistors must be smooth on the scale of a few atom distances for an acceptable transistor performance [1].

A rough boundary leads to a scattering of electrons at the insulating SiO_2 layer when the electrons move through the semiconductor. The investigation of the structure at the interface is difficult [2] since characteristic features of its properties are formed by the local arrangement of atoms within the thin interface layer. The interesting part of the structure is located within the solid at the interface, and unfortunately surface-sensitive methods deliver limited information about subsurface structures.

Once the interface is brought to the surface by a preparation technique, e.g. by a sputter process, then an electronic and structural change of its properties happened already. The experimental access to the interface is limited since silicon oxide is an effective insulator and therefore many techniques suffer from charging effects at the surface.

Presently, the following model for the Si(111) surface is accepted and supported by many experimental and theoretical investigations [1,2,3,5]. The interface between silicon oxide and crystalline silicon is rather abrupt and occurs within one atomic layer. The transition is mediated via the sub-oxide species of silicon.

We have studied the Si(111) surface by high-resolution X-ray photoelectron diffraction in angle-scanned mode. This technique offers the advantage of providing chemical selective spectroscopy combined with chemical state specific information. The experiments were performed at the U49 and U41 beamlines at BESSY II. An X-ray photon excites an electron from a core-level. The electron is emitted to a detector far away from the surface (Fig. 2). The electron can be considered as a photoelectron wave propagating around the emitter atom which can be scattered at the nearest neighbors. Here, the primary wave generates a secondary scattered wave front departing from neighbor atoms. Both waves - the direct wave from the emitter atom and the elastically scattered wave part from the neighbor atom - propagate and interfere. They have the same wavelength and a locked phase. At the detector their interference pattern is recorded as a function of emission angle and/or as a function of electron kinetic energy. In our experiments the patterns are recorded as a function of emission angle. Principally, single and multiple scattering processes contribute to the interference pattern. The pattern is a result of the scattering processes and the path length differences for direct and scattered electron waves.

Thin SiO_2 films (thickness $<10 \text{ \AA}$) were grown by thermal oxidation. The spectra were recorded with a hemispherical electron analyzer at room temperature. The data acquisition system was modified for XPD experiments and to minimize idle time. The electron analyzer was operated at 50 meV resolution, the angular acceptance angle was reduced to $\pm 4^\circ$ by a custom-made aperture and the photon energy resolution was $\sim 50 \text{ meV}$. For Si(111), the clean (7x7) sample was kept at 850°C during exposure to pure O_2 at a pressure of $3 \times 10^{-5} \text{ mbar}$ for 2 min. The data recording procedure for 2π diffraction patterns consisted in a series of azimuth scans over 360° . The polar-angle range started at 84° and ended at 0° , all angle increments were set to 2° .

[1] L.C. Feldmann et al, in: *Fundamental Aspects of Ultrathin Dielectrics on Si-based Devices*, edited by E. Garfunkel et al. (Kluwer Academic Publishers, Boston, 1998)

[2] T. Hattori, *Crit. Rev. Solid State Mater. Sci.* 20, 339 (1995), and references therein

[3] M.T. Sieger et al., *Phys. Rev. Lett.* 77, 2758 (1996)

[4] D.-A. Luh et al. *Phys. Rev. Lett.* 79, 3014 (1997)

[5] F.J. Himpsel et al., *Phys. Rev. B* 38, 6084 (1988)

[6] S. Dreiner et al., *Phys. Rev. Lett.* 86, 4068 (2001)

[7] Y. Yu et al., *Phys. Rev. Lett.* 84, 4393 (2000)

[8] J.H. Oh et al., *Phys. Rev. B* 63, 205310 (2001)

Supported by DFG and by BMBF

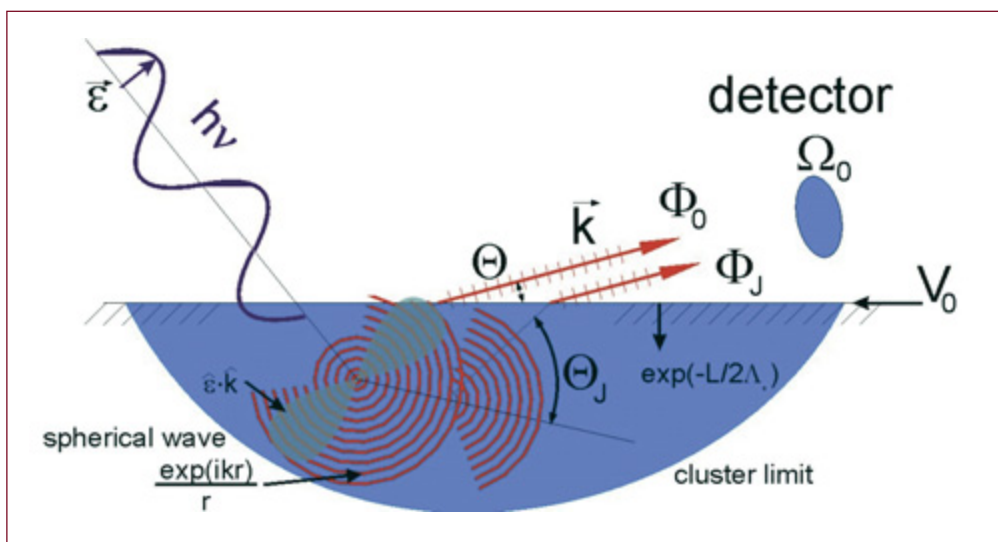


Fig. 2:
Schematic drawing of photoemission including photoelectron diffraction.

Simulations were performed with the MSCD-program package of Chen and Van Hove. The atom configurations were derived from the statistical cross-linking model [4]. In this way atom clusters considering all possible sub-oxides [5] at the interface were obtained.

The photoelectron diffraction patterns were recorded for the Si(111) and Si(001) surfaces. Excellent agreement between experiment and model calculations was obtained [6] for the Si(111) surface. The investigation of the technological important Si(001) surface is more difficult [7] than the investigation of Si(111) surface since at Si(001) the interface is assumed to be gradual over a few layers [7]. The analysis for the Si(001) surface is still in progress. Our data agree well with recent theoretical [7] and experimental results [8].

As an example, Fig. 3 compares the experimental and calculated photoelectron diffraction patterns of the Si²⁺ sub-oxide species. The calculation used a model structure deduced from the statistical cross-linking model. Clearly, all main photoelectron diffraction maxima observed in the experimental patterns are displayed in the calculated result as well. Also, the finer sub-structure features of the experimental pattern is reproduced by the calculated result. This strongly supports an interface structure proposed by the statistical cross linking model.

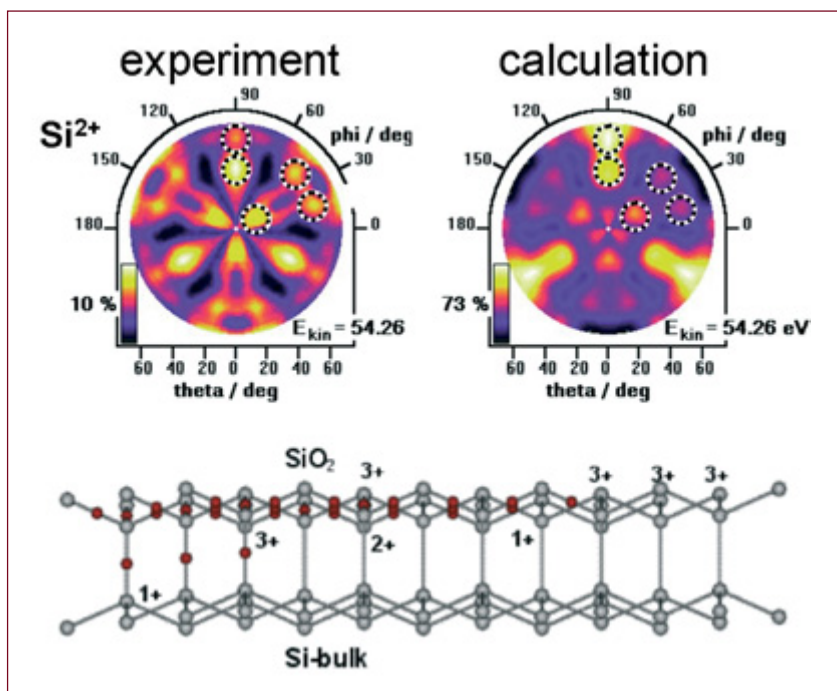


Fig. 3:
Experimental and calculated photoelectron diffraction patterns of the Si²⁺ suboxide of the Si(111) surface. Main diffraction maxima are denoted by circles. A schematic picture of the interface structure is shown.

Contact:

Carsten Westphal, Universität Dortmund, Lehrstuhl für Exp. Physik I

westphal@dx1.HRZ.Uni-Dortmund.de

Do Cu-O layers in high-temperature superconductors 'feel' each other?

**S. V. Borisenko¹, A. A. Kordyuk^{1,2}, M. S. Golden^{1,3}, T. K. Kim¹,
K. A. Nenkov¹, M. Knupfer¹, J. Fink¹, H. Berger⁴ and R. Follath⁵**

¹ *Institute for Solid State and Materials Research, Dresden*

² *Institute of Metal Physics of National Academy of Sciences of Ukraine, Kyiv*

³ *Van der Waals-Zeeman Institute for Experimental Physics, University of Amsterdam*

⁴ *Institut de Physique Appliquée, École Polytechnique Fédérale de Lausanne,*

⁵ *BESSY GmbH*

In less than ten years' time, the scientific community will celebrate the hundredth anniversary of the discovery of superconductivity. It took decades to develop a successful theory describing 'conventional' superconductivity in simple metals. Discovery of high temperature superconductivity (HTSC) in cuprates 15 years ago was not predicted by this theory, implying that a completely novel approach is needed to explain the nature of the phenomenon. The enormous technological potential of the HTSC materials - which now start to find real-life applications in the fields of energy and telecommunication - has initiated extensive efforts by experimentalists and theorists to understand what exactly makes cuprates so special. Despite this research effort, the HTSC have kept their secrets into the new millennium. Our recent experiments on the bilayer cuprates at BESSY suggest that the certain aspects of their electronic structure could be well understood on rather simple and conventional grounds.

Let us have a look inside a virtual single crystal of one of the most studied HTSC cuprates - $\text{Bi}_2\text{Sr}_2\text{CaCu}_2\text{O}_{8+\delta}$ - frequently referred to as Bi2212 (Fig. 1). The most important structural components are the two CuO_2 planes separated by a layer of Ca atoms, as it is in these planes that the superconducting current is believed to flow without experiencing any resistance from the crystal lattice below a certain critical temperature (T_c). The number of such CuO_2 layers varies between different cuprates and T_c is proportional to this number (as long as one doesn't have more than three). Layers of Sr-O and Bi-O are not directly involved in carrying the superconducting current and act as a charge reservoir for the transport layers.

How can the electrons move through this lattice without being scattered by the numerous atoms? It is known that, as in conventional superconductors, the electrons cooperate with each other to form pairs in order to overcome the resistance. The pair formation is driven by the interaction between electrons and phonons (lattice

vibrations), but the real driving force behind the pairing is still unknown or of controversial origin.

Of great help in our search for the pairing mechanism are experimental techniques such as angle-resolved photoemission spectroscopy (ARPES) which gives a very direct and detailed view into the electrons' world. Photoemission is simple: a photon kicks an electron out of the crystal (called a photoelectron) and we measure its energy and momentum with very high precision. From this we can calculate back to the energy and momentum the electron had originally in the crystal. For the kick-off in this game not just any photon will do. We require a highly intense, monochromatic source of photons and a well-defined polarization: all attributes of synchrotron radiation from third generation sources such as BESSY.

As soon as the energies and momenta of the emitted photoelectrons are determined we can convert these data into momentum or energy distribution maps: charting how many electrons are located at certain energy and momentum coordinates. In Fig. 2a two momentum distribution maps are shown in which contours of high intensity represent the Fermi surface, a unique set of locations in momentum space of metal, which mark the boundary between electron-containing and empty states. We want our view into the insides of the high T_c superconductor to be as clear and undistorted as possible. In the case of pure Bi2212, however, the atoms of Bi-O layers, which form the cleavage surface of the crystals (see Fig. 1), are not arranged in registry with the rest of the atoms in the crystal. Thus the top of the crystal acts like natural diffracting grating which distorts our view: the electrons emitted from the CuO_2 planes can be deflected and thus fly out from the crystal in the 'wrong' direction, suggesting that the states in the solid had a momentum they never really had. The result is seen as a multiple reproduction of the main pattern (Fig. 2a, left). We can overcome this problem by doping the Bi2212 crystals with lead (Fig. 2a, right) - no more diffraction

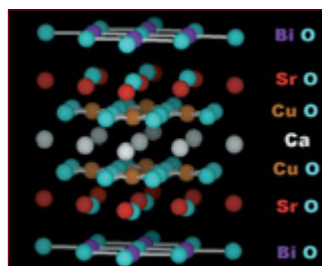


Fig. 1:
Fragment of the crystal structure of Bi2212.

For more background, please see:

A. A. Kordyuk et al.,
<http://www.uni-augsburg.de/abs/cond-mat/0201485>.

A. A. Kordyuk et al.,
<http://www.uni-augsburg.de/abs/cond-mat/cond-mat/0110379>.

Funded by DFG and the Fonds National Suisse de la Recherche Scientifique

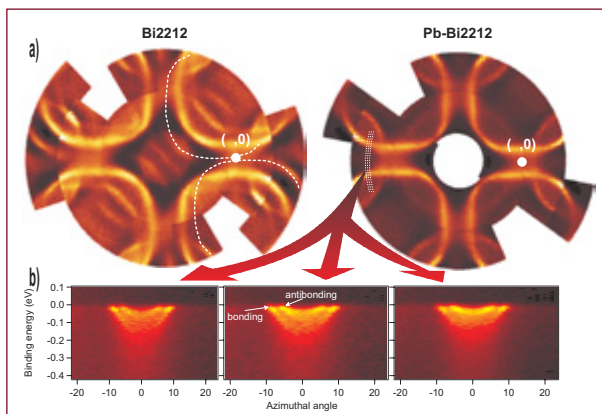


Fig. 2:
a) Fermi surface maps of pristine and Pb-doped Bi2212.

b) Energy distribution maps showing explicitly the two CuO₂-related bands split by the bilayer interaction underdoped Pb-doped Bi2212.

replica are present which could result in an erroneous interpretation of the data.

A key point of some theories of HTSC has been that the electrons responsible for the superconductivity are so strongly confined to the CuO₂ planes due to correlation effects that in Bi2212, for example, each plane does not 'feel' the presence of its neighbour. This behaviour would not be expected and according to even the simplest band-structure calculations, the interaction between the electrons from the two CuO₂ planes should lead to a splitting of the corresponding energy bands and thus of the Fermi surface. However, it is practically impossible to observe such a splitting when looking at the Fermi surface map taken at room temperature.

In Fig. 2b we show three energy distribution maps of Pb-doped Bi2212 taken at low temperature (45K) and very high resolution using 25 eV photons from the U125/1-PGM beamline at BESSY. The data were recorded along lines running essentially perpendicular to the Fermi surface (i.e. along the white dotted lines in the right panel of Fig. 2a). These maps show us clearly that there are two sets of energy/momentum co-ordinates for which states are occupied with electrons.

This has consequences elsewhere in the high T_c canon. As a result of the past non-observation of the two CuO₂-related bands in photoemission, a sophisticated theoretical framework has been built up to explain the fact that at a certain point on a momentum distribution map (the $[\pi/a, 0]$ point, see Fig. 2a), for T < T_c the energy distribution of the photoelectrons is comprised of two peaks, one much larger than the second, with a dip in between. This lineshape has been given the nickname 'peak-dip-hump' ('PDH') and since its first observation more than ten years ago has been the focus of intense experimental and theoretical attention. As one band should give one peak, something special had to be thought up to account for such a complicated two-peak lineshape.

We got suspicious that the accepted interpretation – involving coupling to magnetic

modes or phonons – was starting to show serious cracks when we recorded a series of spectra from the $(\pi/a, 0)$ point in the superconducting state of Pb-doped Bi2212 crystals (Fig. 3). Here we consciously exploited the tunability of the synchrotron radiation and found that depending on the photon energy we could 'select' whether we recorded a beautiful peak-dip-hump (e.g. 20 eV), only hump (39 eV), peak-hump (42 eV) or only peak (50 eV) lineshape: from the same location in momentum space from the same sample. This is in contrast to the existing PDH-interpretation forcing us to search for a new explanation.

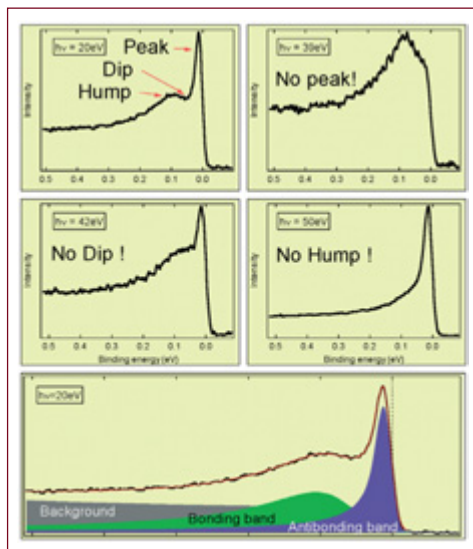


Fig. 3:
 $(\pi/a, 0)$ photoemission spectra from the superconducting state of overdoped Pb-Bi2212 samples for different excitation energies. The red line in the lower panel indicates the sum of the three fit components shown in color.

Looking back at Fig. 2b, we suggested that the two different spectral maxima (the peak and the hump) originate from electrons of two different electronic states such as the bi-layer split CuO₂ bands. As for each photon energy it is not equally easy to kick an electron out of each of these two bands, their relative intensity in the final spectrum varies depending on the energy of the exciting radiation chosen. In the lower panel of Fig. 3 we show how easily one can decompose the complex $(\pi/a, 0)$ lineshape into two main components, each of which is described by an essentially identical spectral function representing the pair of CuO₂-related states residing at different binding energies.

Contact:

Sergey V. Borisenko, Jörg Fink,
 Institute for Solid State and
 Materials Research, Dresden
 S.Borisenko@ifw-dresden.de,
 J.Fink@ifw-dresden.de

Quantum Size Effects in Ultrathin Metal Films

L. Aballe, C. Rogero¹, S. Gokhale², P. Kratzer and K. Horn

¹ Now: Instituto de Ciencia de Materiales de Madrid (Spain)

² University of Pune, Poona (India), now: Indira Gandhi National Open University (India)

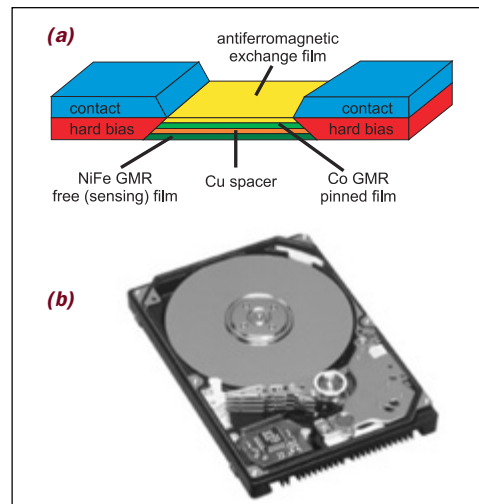


Fig. 1:
(a) Spin valve GMR head.
(b) Modern hard drive read heads are based on quantum size effects in metal films

Quantum size effects in metallic films with thicknesses of only a few atomic layers lead to electronic and structural properties that are very different from those of bulk materials. The increasing miniaturization in the microelectronic industry renders these systems interesting for the development of future devices with a 'tailored' electronic response. One example of the importance of quantum size effects is the thickness-dependent oscillatory coupling between two ferromagnetic layers separated by a nonmagnetic spacer layer [1] (Giant Magneto Resistance effect), which is the basis of novel hard drive reading heads (Fig. 1). The electronic structure of the ultrathin spacer layer, which drastically depends on its thickness, as will be explained below, determines the coupling between the magnetic layers [2], giving rise to a conductivity that strongly depends on the spin of the electrons and is therefore highly sensitive to magnetic fields.

Ultrathin films form a field of intense research at BESSY, and photoelectron spectroscopy with synchrotron radiation is an essential tool for understanding their exotic electronic properties. Layers of metal only a few atoms thick can be deposited on a semiconductor surface using modern evaporation techniques. The conduction electrons of the thin metal layer are confined

to a narrow space between the substrate on the one side and the surface on the other, as in the quantum-mechanical 'particle-in-a-box' or quantum-well problem. Only a few electron wave functions can exist: those for which the wavelength 'fits' an integer number of times in the well, just like a swimmer adjusts the length of his strokes to the swimming-pool size in order to arrive at the edge with the arm preferred for turning, while this is not necessary in the sea. The otherwise smooth band structure of the metal is broken up into distinct states with energy and momentum given by the 'phase-accumulation' condition [3]: those values of the electron's wave number k_{\perp} which add up to a multiple of 2π , including the phase shift upon reflection on either side of the well, i.e. $2k_{\perp}d + \Phi_B + \Phi_C = 2\pi n$, are allowed (n is an integer, d film thickness, and Φ_C and Φ_B are the phase shifts at the metal/substrate interface and metal surface). The data in Fig. 2 are from layers of aluminium on the (111) surface of silicon, a system which, in spite of a disruptive interface reaction, can be prepared in extremely homogenous thickness and high crystalline order by following a specific recipe [4]. Al has an almost perfect coincidence lattice with the Si substrate, which makes epitaxial growth more likely. The basic energetic scheme of the system is illustrated in the inset. In the spectra, each allowed quantum well state appears as a separate peak, and it can be seen how by increasing the film thickness more and more states are allowed. Aluminium has a simple, free-electron-like s - p band that crosses the Fermi energy in the (111) growth direction. It is a model metal ideal for the study of quantum effects, and might be useful as a non-magnetic spacer layer.

Quantum-well states are expected to retain the free-electron like (parabolic) dispersion with the parallel component of the wave-vector $E(k_{\parallel}) = \hbar^2 k_{\parallel}^2 / 2m^*$, since in this direction, parallel to the surface, the overlayer is extended. Here m^* is the effective electron mass. One can imagine a free electron paraboloid broken up into separate parabola, as in Fig. 3(a).

[1] P. Grünberg et al., *Phys. Rev. B* 39, 4282 (1989)

[2] J.E. Ortega et al., *Phys. Rev. B* 47, 1540 (1993)

[3] P.M. Echenique, et al., *J. Phys. C* 11, 2065 (1978), N.V. Smith, *Phys. Rev. B* 32, 3549 (1985)

[4] L. Aballe et al., *Surface Science* 482-485, 488 (2001)

[5] L. Aballe et al., *Phys. Rev. Lett.* 87, 156801 (2001)

Supported by the BMBF and DAAD

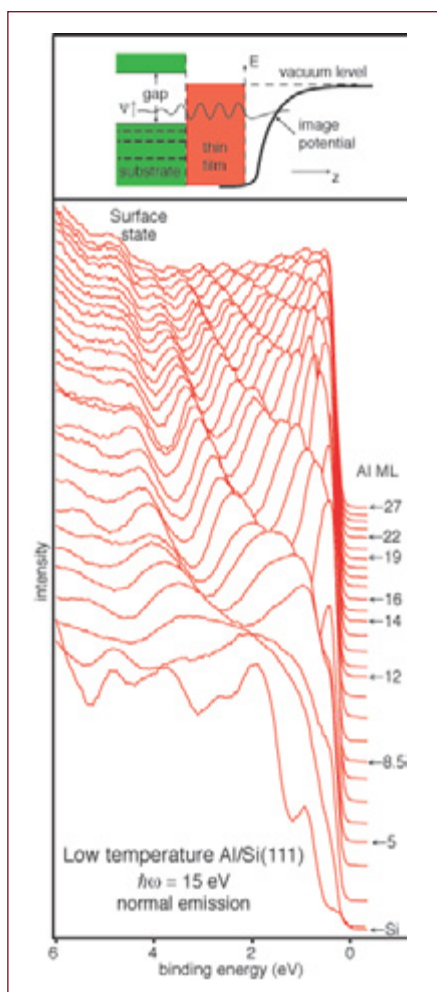


Fig. 2:
Al/Si(111) growth series.
Inset: Schematic representation of a one-dimensional quantum-well.

There is a breaking up into separate states in the confinement direction but continuous parabolae along the film plane. An in-plane dispersion series from a 23 monolayer thick Al film in Fig. 3(b) shows the free-electron-like dispersion of six quantum well states, as well as that of the surface state at the Brillouin zone centre and the surface resonance at the zone boundary.

In the image on Fig. 3(c), the spectral intensities of a dispersion series of a thinner Al layer have been transformed into a greyscale, where white corresponds to the highest intensity. Here, beyond the parabolic shape of the bands, highlighted by thin black lines, there are subtle intensity modulations and peak shifts that were not obvious in the line spectra. These deviations from the ideal free-electron-like dispersion, indicated by red markers, have been found for different film thicknesses and excitation energies. They closely correspond to $E(k_{\parallel})$ regions of high density of the *silicon* states, basically the

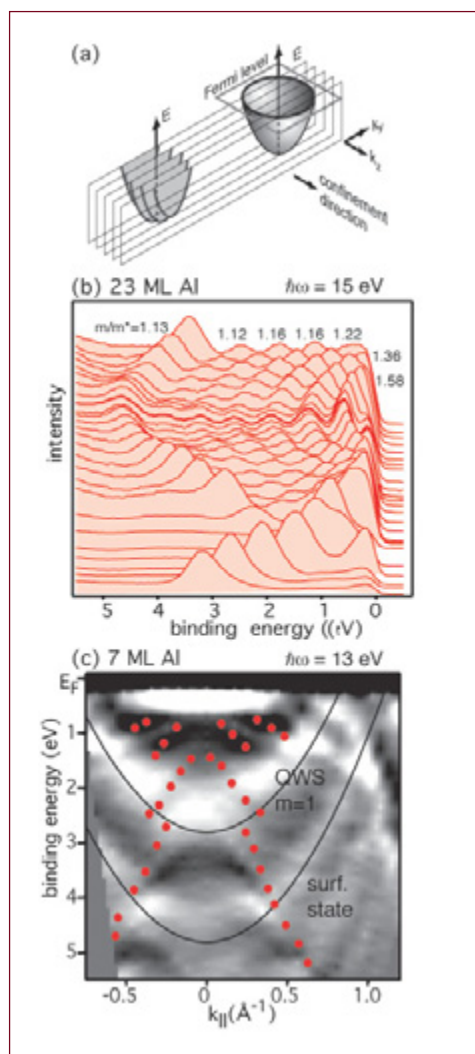


Fig. 3:
(a) Dispersion paraboloid cut into separate parabolae.
(b) In-plane dispersion of quantum well states in a 23 ML film of Al/Si(111).
(c) Greyscale image of 1st derivative of the photoemission intensity in a 7 ML film, enhancing subtle features underlying the strong peaks.

substrate band edges [5]. In such regions there is a decrease in reflectivity and an abrupt change in the phase shift upon reflection at the interface: the substrate is neither a 'hard wall' nor a homogeneous 'soft wall'; it has distinct regions with different reflection conditions. The modified boundary conditions influence the allowed energy and wave-vector values in the metal overlayer through the different interference condition, and so the band edges of the substrate become accessible to photoemission [5]. An interesting aspect of this observation lies in its ground state character: no optical transition from the substrate band edges is involved. It also demonstrates that the details of the substrate electronic structure need to be taken into account for a complete description of the overlayer electronic structure, and that the lateral momentum is conserved to a high degree upon crossing the interface, even though it is lattice-mismatched.

Contact:

Lucía Aballe, Fritz-Haber-Institut
der Max-Planck-Gesellschaft,
Berlin
aballe@FHI-Berlin.mpg.de

Magnetic Clusters – Every Atom Counts

J. T. Lau and W. Wurth

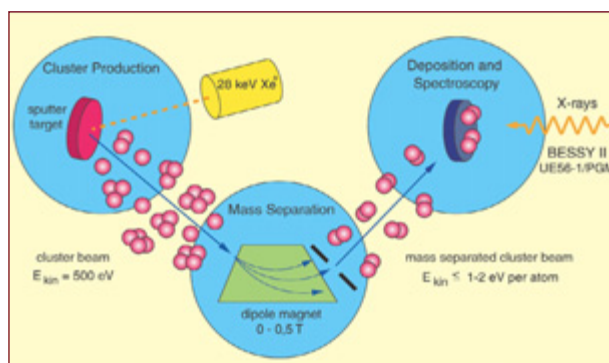


Fig. 1
Experimental set-up for cluster separation, deposition and XMCD measurement

The increasing demand for high density memory and storage media requires a detailed understanding of the properties of advanced low-dimensional magnetic materials in the nanometer regime.

Single atoms differ from bulk matter with respect to their magnetic properties. Since magnetic moments are maximised in free atoms according to Hund's rules, almost all elements across the periodic table carry non-vanishing magnetic moments in the gas phase. In bulk metals, however, these moments are weakened through interaction of the atoms, leaving iron, cobalt, and nickel as the only ferromagnetic elements at room temperature.

To understand the evolution of magnetic and electronic properties with increasing size from sub-nanoscale to macroscopic objects, clusters are ideal systems. Clusters are agglomerates of atoms or molecules, and span the entire range from two or three atoms to nanocrystals and droplets. Therefore they fill the gap between single atoms and bulk matter. For small clusters, every single atom that is added to the cluster can dramatically change its properties.

By simply choosing the number of atoms in a cluster, materials with certain properties can be tailored. This is not only true for magnetic properties, but for many other properties that are governed by the quantum behaviour of electrons, like the optical properties of semiconductor quantum dots or the chemical reactivity of catalytically active nanoparticles.

Magnetic clusters have extensively been studied in the gas phase. In Stern-Gerlach experiments on cluster beams, small transition metal clusters have been shown to exhibit so-called super-paramagnetic behaviour [1]. Here, the magnetic moments of the constituent atoms are coupled to a large overall moment like in a ferromagnet. However, this moment is not locked in a certain direction but fluctuates in space. The magnetic moments of individual atoms in these gas phase clusters are greatly enhanced over the respective values for atoms in bulk matter and show significant size dependent variations. The bulk values of the magnetic moments are only approached for clusters that consist of several hundred atoms. With their unique behaviour, free clusters are interesting objects for scientific research. For potential applications, however, these clusters need to be supported on a substrate, which can substantially alter their properties.

Supported clusters and nanostructures are receiving tremendous interest due to advances in theoretical and experimental techniques [2]. Research in this field of magnetism has been particularly stimulated by the availability of intense beams of circularly polarised soft X-rays from third generation synchrotron radiation facilities like BESSY II, where magnetism can be investigated in detail in a polarisation dependent absorption experiment as described below. With its element specific excitation and its sensitivity on very small amounts of material, soft X-ray magnetic circular dichroism (XMCD) has an enormous advantage over other techniques in the study of nanoparticles on a surface which makes XMCD an ideal tool to study nanomagnetism.

With our experimental set-up shown in Fig. 1, small metal clusters can be produced in sufficient quantity for size separation and deposition on a single crystal surface [3]. Since the properties of these clusters are very sensitive even to minor amounts of contaminants, the cluster deposition and spectroscopy takes place in an ultraclean vacuum environment.

[1] M. L. Billas et al., *Science* 265, 1682 (1994).

[2] J. Stöhr, *J. Magn. Magn. Mater.* 200, 470 (1999) and references therein.

[3] J. T. Lau et al., submitted for publication.

Funded by BMBF.

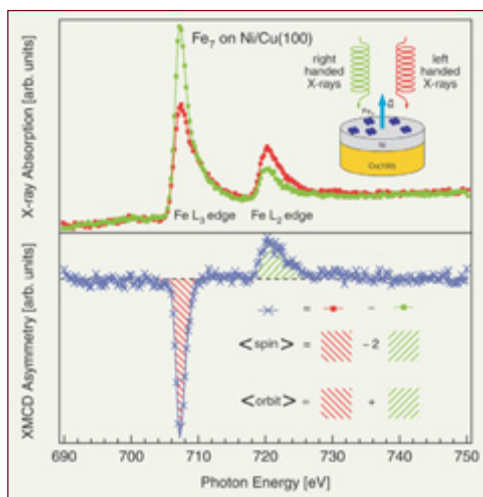


Fig. 2

The upper panel shows that excitation with right or left handed X-rays, shown in red and green colour, respectively, yields different X-ray absorption spectra at the iron L_3 and L_2 edges of clusters consisting of seven iron atoms. By subtracting the green spectrum from the red one, an asymmetry spectrum, shown in blue colour in the lower panel, is generated from which quantitative information on the magnetic moments of the clusters can be obtained.

The set-up is equipped for soft landing of the clusters on the substrate to keep their initial size in the process of deposition. To inhibit cluster diffusion and agglomeration, the sample is cooled down to temperatures as low as -260°C .

The magnetic moments of the deposited clusters need to be aligned by an external magnetic field which is provided by an ultrathin nickel film epitaxially grown on a copper single crystal. A schematic diagram of the cluster sample is depicted in the inset of the upper panel of Fig. 2. The ultrathin (20-30 atomic layers) nickel film can be magnetised remanently to act as a magnet with a magnetic field perpendicular to the film surface. By coupling the magnetic moments of the small iron clusters to the magnetic field of the ultrathin nickel film, a directional preference is superimposed on the clusters. With the incoming X-ray beam aligned parallel to this magnetisation direction, the magnetic moments of the clusters can be determined from X-ray absorption spectra.

In exciting the magnetised clusters with circularly polarised X-rays, either spin up- or spin down-electrons from deep lying electronic core levels can preferentially be promoted to empty valence states. With the spin polarisation of the promoted electron, the spin of the empty states can be probed and information can be gained on a spin imbalance that gives rise to a magnetic moment. This is illustrated in the upper panel of Fig. 2.

From these spectra the magnetisation direction of the clusters can be obtained simply by comparison with corresponding spectra taken for the nickel film. Small iron clusters are coupled ferromagnetically to the nickel substrate, i.e. their magnetic moment

points into the same direction as the moment of the substrate. Within the theoretical framework of XMCD, the size of spin and orbital magnetic moments of the clusters linked to the spin and orbital angular momentum of the electrons, respectively, can be determined using sum rules [2], which correlate these properties to the shaded areas of the asymmetry spectrum as indicated in the lower panel of Fig. 2.

Fig. 3 shows the variation in the spin moment with cluster size in the order of 20 %. Magnetic spin moments indicate almost complete spin polarisation of the empty valence electron states and hint at significantly enhanced magnetic moments for the cluster atoms as compared to the bulk value. The variation of the orbital moments is even larger, reflecting the strong dependency of magnetic properties on cluster size. By adding or removing a single atom, the orbital moment of a cluster changes dramatically. Again, the values of the orbital moments are strongly enhanced as a consequence of the small dimensions of the clusters and the reduced coordination of their constituent atoms. Through spin-orbit coupling, an enhanced orbital moment can give rise to enhanced magnetic anisotropy, which in turn determines easy axes and preferred magnetisation directions of the nanoparticles.

Our results show that the magnetism of sub-nanoscale particles depends strongly on the exact number of atoms in the particles. For these particles every atom counts when it comes to understanding or even tailoring their magnetic properties which makes them fascinating objects for the study and for possible applications of nanomagnetism.

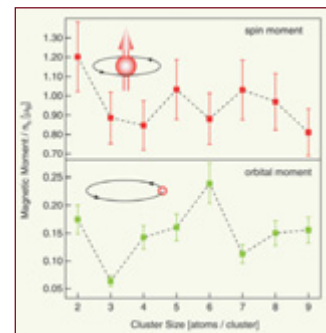


Fig. 3

The results of a thorough sum rule analysis of experimental data for deposited iron clusters obtained at BESSY II beamline UE56/1-PGM. The upper panel shows the magnetic spin moments of small iron clusters, whereas the lower panel shows their orbital moments.

Contact:

Wilfried Wurth, Institut für Experimentalphysik, Universität Hamburg
wilfried.wurth@desy.de

Layer-resolved imaging of non-collinear magnetization in Ni/Cu/Co trilayers

W. Kuch, Xingyu Gao and J. Kirschner

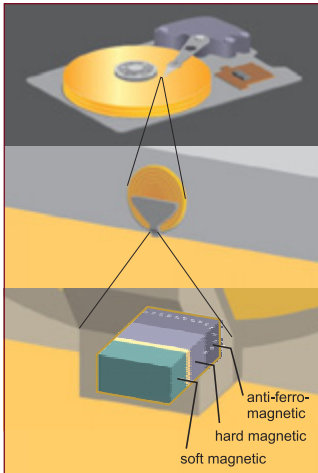


Fig. 1:
Structure of a magnetoresistive write/read head for computer hard disks. The actual head is sitting on the front of the glider. Functional elements are two magnetic layers.

Fundamental research and industrial development in the field of thin film magnetism have soared dramatically during the last decade. This is to a large extent due to the discovery in the late eighties of giant resistivity changes in magnetic trilayers, in which two magnetic layers are separated by a non-magnetic spacer layer [1, 2]. Less than ten years after this discovery, the first commercial applications of the effect were on the market. Fig. 1 shows as an example a computer hard disk read head, as it is delivered nowadays in millions of laptop and desktop computers. Because of the high fundamental interest and the technological importance, the magnetic coupling between two ultrathin magnetic layers, separated by a non-magnetic spacer layer as in the bottom panel of Fig. 1, is a field of intense research. In such trilayers the competition between different energy contributions of magnetically coupled systems can lead to non-collinear and canted magnetic configurations [3].

The study of such phenomena and systems requires a method that allows access to the microscopic magnetic domain pattern of each of the magnetic layers separately. Photoelectron emission microscopy (PEEM) using X-ray magnetic circular dichroism (XMCD) in soft X-ray absorption as a contrast mechanism is such a technique [4]. In this method, the local intensity of emitted low-energy secondary electrons for resonant excitation of elemental X-ray absorption edges is imaged by a set of electrostatic lenses.

The local secondary electron intensity is a measure for the local X-ray absorption, which depends on the relative orientation of the magnetization direction and the direction of the incoming, circularly polarized X-rays. The element-sensitivity of XMCD can be used to obtain layer-selective magnetic domain images if the different layers contain different elements. XMCD-PEEM is therefore ideally suited to study non-collinear magnetic configurations in coupled magnetic systems.

We present here a layer-resolved XMCD-PEEM study of the magnetic domain patterns of Co/Cu/Ni trilayers, epitaxially grown on Cu(001). Ni and Co films on Cu(001) are known to exhibit different magnetic properties: Whereas Co films are always magnetized in the film plane [5], Ni films show a perpendicular magnetization in an extended thickness range [6]. Definite conclusions about canted and non-collinear magnetization configurations can be drawn, independent of domain formation, from comparing magnetic domain patterns of the Ni and Co layers at the same sample position. We show that for appropriate layer thicknesses reorientation transitions between collinear and non-collinear configurations occur, in the course of which the Ni layer assumes a canted magnetization.

The measurements were performed at the helical undulator beamline UE56-2 (Max-Planck-CRG). Circularly polarized light of the fifth harmonic with a degree of polarization of about 80% was incident to the sample under an angle of 60° from the surface normal. A commercial electrostatic PEEM was used (Focus IS-PEEM). Parameters were set to result in a lateral resolution of 400 nm and a field of view of $60 \mu\text{m}$. Ni was deposited as a continuous layer on the clean Cu(001) single crystal. Co and Cu layers were shaped into $320 \mu\text{m}$ wide crossed wedges with a $180 \mu\text{m}$ wide plateau of constant thickness at the upper end of the wedge.

Fig. 2 shows domain images of a Co/Cu/Ni trilayer at low Co thicknesses and a constant Cu thickness of 4 atomic monolayers (ML). The Co thickness increases from bottom to top, as indicated at the left axis. Panels (a) and (c) on the left hand side show the domain pattern of the Co layer, panels (b) and (d) on the right hand side the domain pattern of the Ni layer. The top and bottom images show approximately the same position of the sample for different azimuth angles of the light incidence, as indicated by the arrows labeled ' $h\nu$ '.

- [1] M. N. Baibich et al., *Phys. Rev. Lett.* 61, 2472 (1988).
- [2] G. Binasch et al., *Phys. Rev. B* 39, 4828 (1989).
- [3] A. Taga et al., *Nature* 406, 280 (2000).
- [4] J. Stöhr et al., *Science* 259, 658 (1993).
- [5] P. Krams et al., *Phys. Rev. Lett.* 69, 3674 (1992).
- [6] B. Schulz et al., *Phys. Rev. B* 50, 13467 (1994).
- [7] W. Kuch et al., *J. Magn. Magn. Mater.* in print.
- [8] W. Kuch et al., *Phys. Rev. B* 65, 064406 (2002).

Funded by the BMBF.

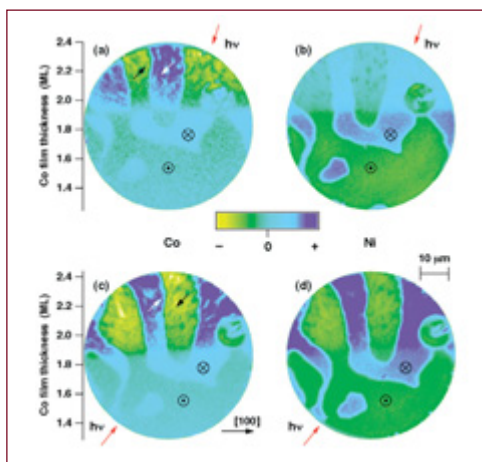


Fig. 2:
 Layer-resolved domain images of a wedged Co/4 ML Cu/15 ML Ni trilayer on Cu(001). The Co thickness increases from bottom to top. (a), (c): Co layer. (b), (d): Ni layer. (a), (b) and (c), (d) are images obtained for different light incidence angles, as indicated by arrows labeled 'hv'. In the lower part of the imaged area Co and Ni magnetizations are collinearly aligned out-of-plane, in the upper part the Ni magnetization is at a canted non-collinear direction

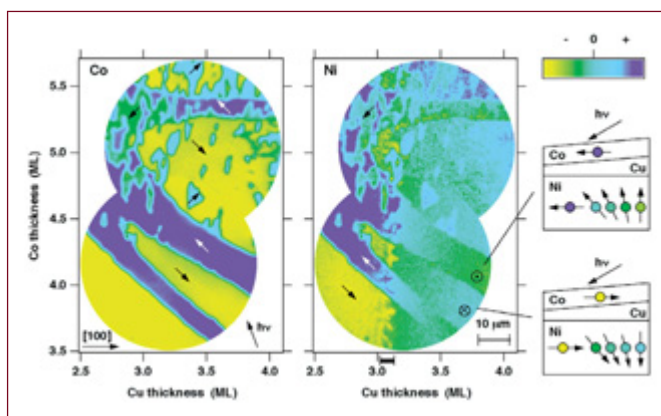
The images are a color-coded representation of the projection of the local magnetization direction onto the light incidence direction, as indicated by the legend in the center of the image. The two angles of the magnetization vector in space can be determined from these two measurement geometries. In particular, for pure out-of-plane magnetization no change in contrast is expected upon changing the incidence azimuth. For in-plane magnetization, on the contrary, a contrast reversal occurs for reversing the X-ray incidence direction.

Comparing the images of Fig. 2 it is seen that in the lower part of the images the Co and Ni magnetizations are aligned in a collinear out-of-plane configuration. In the upper part, the Co layer exhibits an in-plane magnetization, as evidenced from the reversing contrast between panels (a) and (c). In this region the Ni does exhibit a change in contrast, but not a reversal as expected for in-plane magnetization. Here consequently the Ni magnetization is neither purely out-of-plane nor fully in-plane, but something in between. In the upper part of the images a non-collinear magnetization configuration is present, in which the Co layer is magnetized in-plane, whereas the Ni layer is magnetized along canted axes [7]. For the very low Co thicknesses present in Fig. 2, the Curie temperature of the Co layer is close to room temperature. The magnetic anisotropies are strongly reduced close to the Curie temperature, so that the magnetization of the Co layer is here easily rotated out-of-plane by the interlayer coupling.

Fig. 3 shows color-coded domain images for a Co layer and a Ni layer of a crossed Co/Cu double wedge on 15 ML Ni/Cu(001).

As in Fig 2, reorientation transitions between collinear and non-collinear configurations of the Co/Cu/Ni trilayers have been observed, but while the collinear configuration was out-of-plane in Fig. 2, it is in-plane in Fig. 3. In both cases the Ni was magnetized along a canted direction in the non-collinear configuration. This canting can be understood considering the competition between the magnetic anisotropies of the Co and Ni layers and the magnetic interlayer coupling across the Cu spacer layer. Whereas the perpendicular anisotropy of the Ni layer tends to orient Ni out-of-plane, the interlayer coupling tries to align it parallel with the Co moment, thus leading to a canted configuration [8].

Fig. 3:
 Layer-resolved domain images (left: Co, right: Ni) of a crossed Co/Cu double wedge on 15 ML Ni/Cu(001). The Cu thickness increases from left to right, the Co thickness from bottom to top. In the leftmost part of the images Ni and Co magnetizations are in-plane and collinear. In the right part of the images, the Ni magnetization exhibits a gradual canting as a function of Cu spacer layer thickness, leading to a non-collinear configuration. The gradually changing magnetic contrast is schematically explained at the right hand side.



Contact:

Wolfgang Kuch,
 Max-Planck-Institut für Mikrostrukturphysik, Halle
 kuch@bessy.de

Strong magnetic anisotropy of projected Cr 3d moments of CrO₂-films

E. Goering, A. Bayer, S. Gold and G. Schütz

Magnetism is a fascinating field for scientific research and industrial development and has stimulated imagination and curiosity at scientists, children and other people since the early discovery of magnetite. One reason for this attraction is directly associated to new technological developments achieved in the last century, which have a large impact in our whole life. Those research activities are often related to questions of basic research, which have been converted very rapidly into technological devices. Famous examples are the development of giant-magneto-resistive (GMR) read heads in modern hard disc storage devices with capacities in the order of 100 GByte, new magnetic random access memory (MRAM), which is non-volatile and fast, which could lead to a new key technology for this decade, or storage media itself like magneto-optical discs or hard disc coatings, with an unusual preferred magnetization direction along the surface normal. In the majority of technological applications, magnetism is based on elements of the 3d metal series (Fe, Co and Ni) or the 4f Lanthanides (like Nd, Sm and Gd).

All those technological applications are primary related to artificial multilayers of ferromagnetic and nonmagnetic layers, and there are two major questions: How could we understand and control magnetic coupling mechanisms between those layers, and how could we direct the orientation of the spontaneous magnetization (easy axis) for each layer due to changes in the magneto-crystalline anisotropy-energy (MAE) [1, 2]? The key to address those questions is the understanding of microscopic magnetic properties, like the magnetic spin μ_s and the orbital momentum μ_L for each magnetic layer, and for every ion in the system separately. Those properties could be probed quantitatively with X-ray Magnetic Circular Dichroism (XMCD). The quantitative influence of orbital moments [1], inner 3d shell spin-orbit-coupling, and the magnetic dipole term T_z [2], which is related to a quadrupolar spin distribution at the Cr site, to the MAE is still unknown but very

important and of fundamental interest towards satisfying understanding of the magnetism of 3d metal systems.

CrO₂ is a well known material for tape recording applications. In the last few years CrO₂ has attracted revived interest due to its remarkable high spin polarization of about 100% at the Fermi energy [3-5]. The reason for this revival is mainly related to new and promising future technological applications on the basis of CrO₂-electrodes such as magnetic tunneling and spin injection 'transistors' (spintronics).

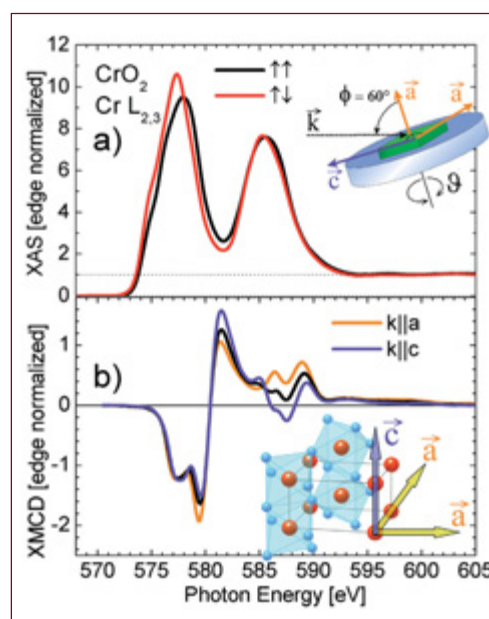


Fig. 1:
a) CrO₂ XAS for parallel (black) and antiparallel (red) alignment of the photon beam to the sample magnetization; inset shows the experimental geometry of the crystallographic axes of the sample relative to the incoming photon beam;
b) XMCD-signal [(black)-(red)] at 5kOe applied magnetic field for different azimuthal angles ϑ and fixed $\phi = 60^\circ$ for enhanced a- (orange), c- (blue) and intermediate (black) axis projections; the inset shows the rutile structure of CrO₂.

[1] Bruno, P.; *Phys. Rev. B* 39 (1989) 865

[2] Van der Laan, G.; *J. Phys.: Condens. Matter* 10 (1998) 3229

[3] Korotin, M. A. et al.; *Phys. Rev. Lett.* 80 (1998) 4305

[4] Schwarz, K.; *J. Phys. F: Met. Phys.* 16 (1986) L211

[5] Soulen, R. J. et al.; *Science* 282 (1999) 85

[6] Carra, P. et al.; *Phys. Rev. Lett.* 70 (1993) 694

[7] Thole, B. T. et al.; *Phys. Rev. Lett.* 68 (1992) 1943

[8] Goering, E. et al.; *J. Sync. Rad.* 8 (2001) 422

[9] Van der Laan, G.; *Phys. Rev. B* 55 (1997) 8086

[10] Goering, E. et al.; *Phys. Rev. Lett.* accepted (2001)

[11] Goering, E. et al.; *BESSY Annual Report* (2002)

[12] Goering, E. et al.; *Applied Physics A* accepted (2002)

[13] Goering, E. et al.; *J. Appl. Phys.* 88 (2000) 5920

Funded by DFG

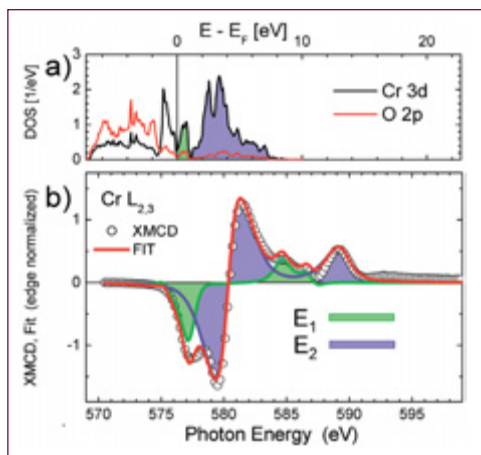


Fig. 2:
a) Cr 3d (black) and O 2p (red) DOS from ref. [3];
The narrow green shaded area is related to t_{2g} -majority and the blue shaded area to e_g -majority ($t_{2g}e_g$)-minority states;
b) Cr $L_{2,3}$ XMCD (open circles) and moment analysis fit result (red) corresponding to two different energy contributions (green and blue).

XMCD is the influence of the sample magnetization in the vicinity of an absorption edge on the absorption coefficient of circular polarized synchrotron light. The resonant excitation of Cr $2p$ electrons into the unoccupied conduction band is shown for CrO₂ in Fig. 1a. Two resonance lines are observable (L_3 at 577 eV and L_2 edge at 585 eV). The difference between parallel and antiparallel alignment between the photon direction and the sample magnetization of this $2p \rightarrow 3d$ transition probes the projected magnetism of Cr, and is shown in Fig. 1b for different orientations of the sample relative to the direction of the photon beam. The orange (blue) curve represents the magnetic behavior of Cr along the rutile a -axis (c -axis).

By the use of so-called 'sum rules' absolute magnetic moments could be extracted in an element and symmetry specific way [6, 7]. Therefore, it is necessary to separate L_3 and L_2 edge XMCD intensity, but this is not possible for CrO₂. We have recently developed so-called 'moment analysis' which takes care of spectral overlap by a fitting procedure [8]. XMCD data has been fitted (Fig. 2b) by superposition of two sets of ground-state-moments [9] corresponding to the projected DOS, shown in Fig. 2a [3]. All spectral XMCD features could be reproduced nearly perfectly by this fitting procedure. Fit results of each orbital contribution (E_1 and E_2) and the total projected 'effective spin moment' are presented in Fig. 3. Strong anisotropy is present, even for the spin moment, which is not expected for a clearly saturated sample [10, 11]. This 'spin anisotropy' has been identified with a strong magnetic dipole term $\langle T \rangle$ [6, 10, 12]. Taking into account O $2p$ hybridization gives a full isotropic Cr $3d$ spin moment of $1.90 \mu_B$. This is strong evidence that hybridization plays an important role in this system and a localized ionic picture of the Cr $3d$ magnetism is not appropriate (for details [10-12]).

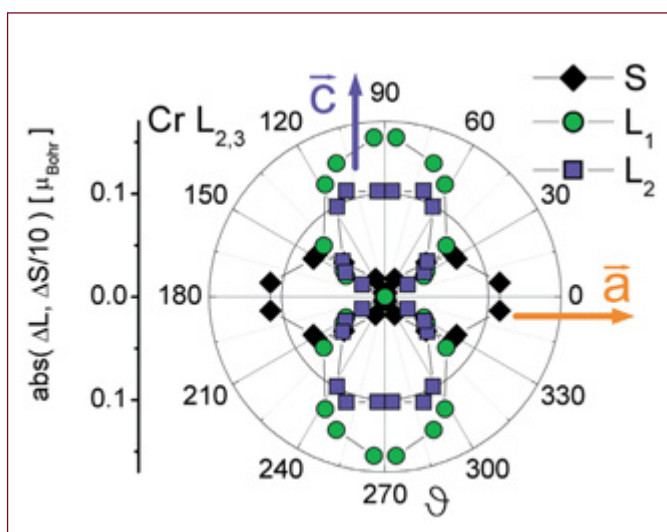


Fig. 3:
Differences of azimuthal angular dependencies of the fitted XMCD related effective spin moments $\langle S \rangle$ (black diamonds) and the two antiparallel orbital Cr 3d projections $\langle L_1 \rangle$ (green circles) and $\langle L_2 \rangle$ (blue squares).

In addition *in situ* element specific magnetization curves [13] have been measured at each ϑ to extract the strong uniaxial anisotropy energy of $K_1 = (5.8 \pm 0.5) \cdot 10^4 \text{ J/m}^3$, with easy axis along the crystallographic c -axis. We used our measured $\langle S \rangle$, $\langle L \rangle$ and $\langle T \rangle$ values to calculate the MAE by a recently modified 'Bruno'-model [2] and could reproduce the hysteresis derived MAE quantitatively. Therefore, we conclude that the magnetic dipole term $\langle T \rangle$ related to the magnetic anisotropy dominates the MAE of CrO₂, which has not been observed before [10; 11].

Contact:

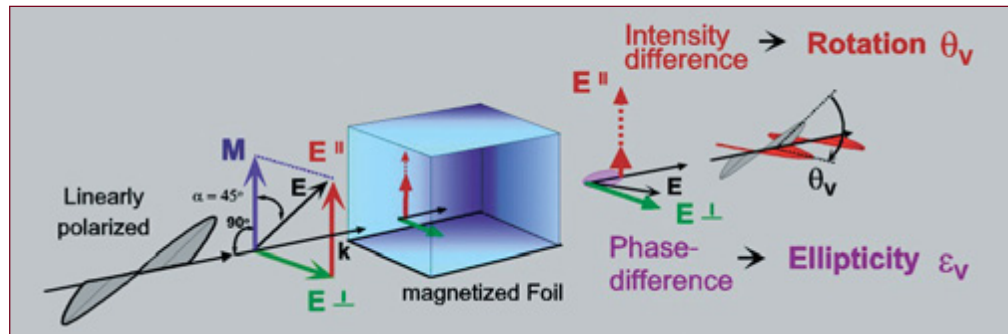
Eberhard Goering, Max-Planck-Institut für Metallforschung, Stuttgart
 goering@mf.mpg.de

Observation of the X-Ray Magneto-Optical Voigt Effect

¹ IFW-Dresden

H.-Ch. Mertins, P.M. Oppeneer¹, J. Kunes¹, D. Abramsohn and A. Gaupp, F. Schäfers and W. Gudat

Fig. 1:
The X-ray Voigt effect on a magnetic thin film. The linearly polarized X-ray beam is at normal incidence to the film which is magnetized in-plane. The polarization plane of the transmitted light is tilted over the Voigt rotation angle θ_V , and the transmitted light becomes elliptically polarized.



Magneto-optical (MO) effects are widely used for the investigation of new magnetic materials and for the development of magneto-electronic devices like ultrahigh density magnetic and MO-recording media [1]. These techniques are well established using visible light, but they received new attention after the observation of MO effects in the X-ray range. Here these effects are some orders of magnitude larger than in the visible due to the strong spin-orbit interaction of the electronic states involved. This is most pronounced for the 2p core electrons of the transition metals Fe, Co, Ni and the 3d electrons of rare earth materials. Spectroscopy experiments at corresponding energies have been made possible with polarised, tunable high-brilliance undulator radiation, allowing an element selective investigation of composite materials, alloys or layered systems, something which is impossible using visible light.

MO spectroscopies can be classified into intensity measurements like the commonly used X-ray magnetic circular dichroism (XMCD) and polarisation experiments. The latter, which is the topic of this report, is based on the relatively new technique of soft X-ray polarisation analysis. At BESSY this technique was made possible by the development of multilayer optics which are operated in a novel high precision UHV-polarimeter chamber [2]. This versatile chamber allows for investigations of any new kind of material with respect to transmission, reflection and ellipsometry parameters. In this way the X-ray magneto-optical Faraday effect was observed at BESSY [3].

The advantage of the polarisation analysis over an intensity measurement is the knowledge of the polarisation state of light after its interaction with the sample, i.e. the intensity and the phase. This in turn directly yields the complex optical constants [3, 4] which give the full description of the interaction between polarised light and magnetic matter allowing a separation between pure magnetic and non-magnetic charge effects.

Recently, we observed the Voigt effect, a MO phenomenon which is new in the X-ray range and is quadratic in the magnetisation M [5]. Therefore it holds great potential for future investigations of anti-ferromagnetic materials, which are not accessible using XMCD or X-ray Faraday effect because the latter spectroscopic techniques are only sensitive to $\langle M \rangle$. Technologically important materials of current interest as magneto-resistive, spin-valve and exchange-bias materials [1] can be investigated by such new type of X-ray spectroscopies on an element selective level. X-ray magnetic linear dichroism (XMLD) is another suitable technique for anti-ferromagnetic materials.

The Voigt effect is observed with linearly polarised light. After passing the magnetised sample, the plane of polarisation is rotated by an angle θ_V and it is changed to elliptical, as expressed by its ellipticity $\tan(\epsilon_V)$ (Fig. 1). The measured X-ray Voigt rotation spectrum θ_V for a Co thin film is shown in Fig. 2. Each point is the result of a polarisation analysis of the transmitted light. Due to the resonant excitation from 2p states to the fairly

[1] G.A. Prinz, *Science* 282, 1660 (1998).

[2] F. Schäfers et al., *Appl. Opt.* 38, 4074 (1999).

[3] H.-Ch. Mertins et al., *Phys. Rev. B* 61, R874 (2000)

[4] J. Kunes et al., *Phys. Rev. B* 64, 174417-1 (2001)

[5] H.-Ch. Mertins et al., *Phys. Rev. Lett.* 87, 047401-1 (2001).

Funded by EU, BMBF, and DFG.

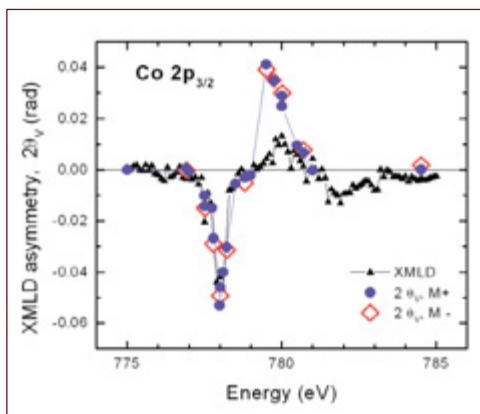


Fig. 2:
The X-ray Voigt rotation measured at the Co L_3 -edge with two antiparallel directions of the magnetization M . Their equivalence proves the quadratic dependence of the Voigt rotation on M . For comparison the XMLD asymmetry is also shown. Both spectra ought to agree according to theory, but do not near 780 eV where the XMLD is diminished by fluorescence.

localised 3d states, the rotation data display maxima immediately below and above the absorption edge. The maximum value of up to $7.5^\circ/\mu\text{m}$ is almost an order of magnitude larger than that observed in the visible. To demonstrate the quadratic magnetic response we made the same experiment under inverted magnetic field. The Voigt rotation was found to be independent of the magnetisation direction, as theoretically expected [5]. For comparison to the X-ray Voigt rotation, we determined the corresponding XMLD asymmetry parameter (intensity measurement) by recording the transmission spectra T_{\parallel} and T_{\perp} (see Fig. 2). As expected, the two quantities agree well, except for the high-energy side of the $2p_{3/2}$ resonance structure. Here the XMLD experiment is disturbed by fluorescence, which is excited at the high-energy side of the Co $2p_{3/2}$ edge. The measurement of the Voigt rotation is less liable to fluorescence disturbances, because the analyser is energy selective and set to select the incident light and to suppress the fluorescence light with its different energy.

Furthermore, our ab-initio calculations revealed an unprecedented sensitivity of the X-ray Voigt effect to the spin polarisation of the core states, including the $2p_{3/2}$ spin polarisation the predicted and the measured Voigt rotation are in excellent agreement [5] (Fig. 3). A value of 0.79 eV was determined for the spin splitting of the $3/2$, $-3/2$ sub-levels of Co. Conversely, the Voigt effect as

calculated without core spin polarisation, but with exchange-split valence states, is practically zero and bears no correspondence to the experiment.

Thus, combined with ab-initio calculations, the X-ray Voigt effect provides a powerful new instrument to investigate the core polarisation. Its dependence on the square of the magnetisation opens up new ways to study anti-ferromagnetic materials on an element selective level.

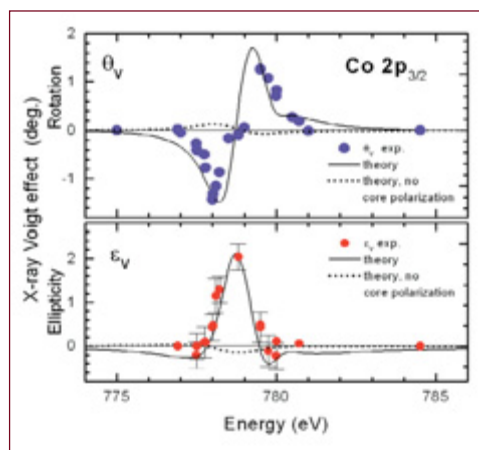


Fig. 3
Calculated and measured X-ray Voigt effect at the L_3 -edge of a 200 nm Co film.
Top: experimental Voigt rotation θ_V and the calculated spectrum. The full curve is computed with spin polarization of the $2p_{3/2}$ core states, while the dashed curve is obtained without core polarization.
Bottom: likewise, but for the Voigt ellipticity ε_V .

Contact:

Hans-Christoph Mertins,
BESSY GmbH, Berlin,
mertins@bessy.de

Complete characterization of the atomic Auger decay

M. Drescher, B. Schmidtke, T. Khalil, N. Müller and U. Heinzmann

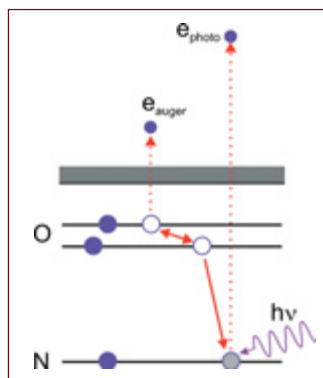


Fig. 1:
Scheme of the photoexcitation and NOO Auger decay in xenon.

We photo-excited the rare gas xenon in order to study the subsequent radiationless NOO Auger decay (Fig. 1) with spin- and angle-resolved electron spectroscopy. The interest is to obtain a quantum mechanically complete characterization of the Auger decay, i.e. extract all relevant transition matrix elements from experimentally accessible observables. Such full description of the outgoing electron wave represents the most comprehensive picture of the process under study. A recent – and unexpected – finding states that a complete experiment for the photoionization of closed-shell atoms is not possible by exclusively measuring the properties of the photoelectron [1]. Also, for the subsequent Auger decay a mathematical analysis clearly indicates that the Auger-electron related observables are intertwined [2]. However, our studies reveal that for distinct cases and by introducing rather weak simplifications, definite numbers for the matrix elements can be extracted.

The exceptionally high photon flux and the polarization characteristics of the new helical undulators at BESSY in combination with a rotatable electron spectrometer and a dedicated spin polarization detector allow measurement of the angle-dependent spin polarization of photo- and Auger electrons from atomic gas targets. In the experiment reported here we used circularly polarized radiation from the beamline UE56/1-PGM. Combining the angle-resolved spin polarization analysis with data for the intensity angular distribution and the total cross section constitutes a full determination of the electron properties.

Due to the low density in the gas target of some 10^{-3} mbar, a high photon flux is essential for a combined energy-, angle-, and spin resolved electron analysis. With the degree of circular polarization from the beamline approaching unity at the typical excitation energies around 130 eV, the spin polarization sensitivity of the apparatus is mainly determined by the analyzing power of

the spherical retarding field Mott polarimeter which was measured to be close to 0.2 by using the spin polarization transfer to the Xe-4d¹ photoelectrons as a reference. The helicity of the radiation was changed every few minutes by moving the undulator shift in order to eliminate apparatus asymmetries. Variation of the detection angle in the reaction plane was realized with a rotatable spectrometer followed by a space-fixed Mott analyzer. In its latest version the spin analyzer is mounted on a rotatable chamber (Fig. 2); in this case two spin polarization components can be measured simultaneously in the electron-fixed coordinate frame. Particular attention has been paid to a careful compensation of residual magnetic fields by Helmholtz-coils in order to avoid a rotation of the spin polarization vector in space.

If one concentrates on relative amplitudes by normalizing to the total cross section the full quantum mechanical description of the transition requires a set of two amplitude ratios $\eta_1 = D(s_{1/2}) / D(d_{5/2})$ and $\eta_2 = D(d_{3/2}) / D(d_{5/2})$ as well as two phase shift differences $\delta_1 = \Delta(s_{1/2}) - \Delta(d_{5/2})$ and $\delta_2 = \Delta(d_{3/2}) - \Delta(d_{5/2})$. On the experimental side, from the angular distribution of the transferred spin polarization of Xe N₄O_{2,3}O_{2,3} (³P₁) Auger electrons in the reaction plane (Fig. 3) we could directly extract the independent intrinsic Auger parameters β_1 , γ_1 and α_2 using a fitting procedure. Since the four desired quantum mechanical quantities $\eta_{1,2}$ and $\delta_{1,2}$ are opposed by only 3 non-redundant experimental parameters, the solution of the inversion problem corresponds to a one-dimensional subspace of a four-dimensional space. The projections of this steady solution curve onto three relevant quantum mechanical quantities are plotted in Fig. 4 as function of the fourth one (chosen as the so-called 'relativistic' phase-shift δ_2). An inspection reveals that for the range around $\delta_2 = 0$ the solution is actually confined to a narrow range of allowed values.

[1] B. Schmidtke et al., *J. Phys. B* 33, 2451 (2000)

[2] B. Schmidtke et al., *J. Phys. B* 33, 5225 (2000)

[3] B. Schmidtke et al., *J. Phys. B* 34, 4293 (2001)

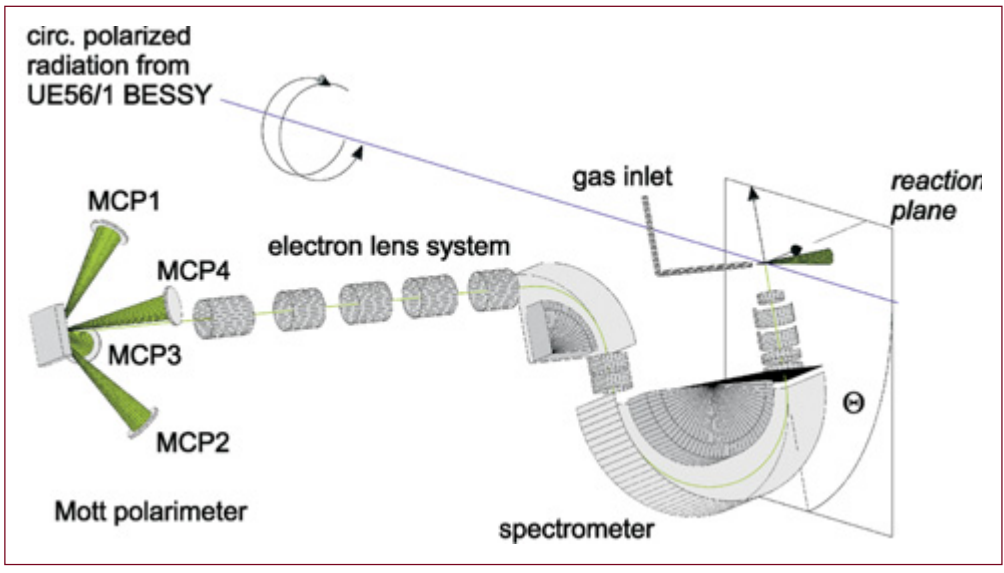


Fig.2: Experimental set-up for the simultaneous measurement of two spin polarization components in the electron-fixed coordinate frame.

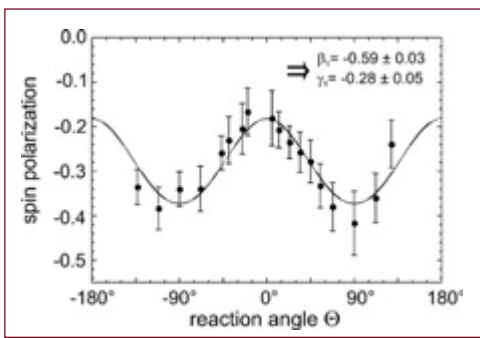


Fig.3: Angular distribution of the transferred spin polarization of the $Xe N_{4,2,3} O_{2,3} (^3P_1)$ Auger decay after excitation at 125 eV photon energy. The full line represents the fit for an extraction of intrinsic parameters.

If we therefore assume that electron waves with the same orbital angular momentum (here: $l=2$) but different total angular momenta ($j=3/2$ or $5/2$) leave the atom with virtually the same phase – which according to theory is a rather weak postulate – we finally end up with definite values for the other three matrix element components.

Spin- and angle-resolved photoelectron spectroscopy provides valuable non-redundant information about the Auger decay process. Backed by the new efficient helical undulator beamlines this technique will provide further insights in even more subtle – but fundamentally relevant – phenomena in atomic photoionization.

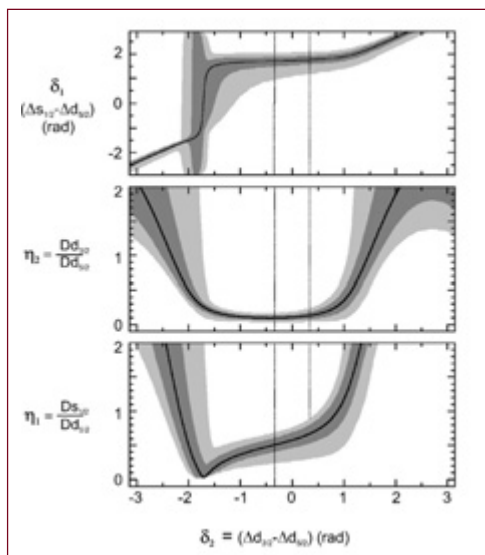


Fig.4: Solution space of the Coulomb matrix element ratios and phase shift differences for the $Xe N_{4,2,3} O_{2,3} (^3P_1)$ Auger decay. The area in dark (light) gray may be occupied if the measured intrinsic parameters are varied within a range of 0.5σ (1σ).

Contact:
 Markus Drescher,
 Universität Bielefeld, Fakultät
 für Physik, Bielefeld,
 drescher@physik.uni-
 bielefeld.de

A closer look at Albrecht Dürer's drawings (1471-1528)

¹ *Bundesanstalt für Materialforschung und -prüfung (BAM), Berlin*

I. Reiche, A. Berger¹, W. Görner¹, S. Merchel¹, M. Radtke¹, J. Riederer and H. Rieseemeier¹



From July 1520 to August 1521, Albrecht Dürer and his wife Agnes travelled together to the Netherlands. During the journey Dürer drew his impressions into a travel book using silver pencil, a technique very much appreciated by artists of the Renaissance. The sheets of Dürer's travel book, about fifteen silver point drawings each 13 to 16 cm² in size, have been separated in the 19th century and individual drawings are now distributed and conserved in different international art collections.

Silver point drawings are among the most precious and rarest treasures of graphical collections. They are characterised by a grey-brownish colour and a very fine and precise line. Silver pencils were used since antiquity until the 16th century and then replaced by graphite pencils.

Art historical investigations on the silver point drawings generally allow a determination of the drawings' origin. However, some cannot be attributed unambiguously to a certain artist or school. Further information on provenience and authenticity can only be gained from scientific analyses.

So far, only few studies on the chemical composition of these silver drawings have been realised since a suitable analytical technique has to combine two features: It has to be very sensitive due to the extremely thin silver deposits on the paper and it should not damage the art object.

First scientific investigations on silver point drawings, mostly Italian and Flemish but also on seven Dürer drawings were performed by Duval in 1999 at the Research laboratory of the French Museums, Paris using 3 MeV Proton Induced X-ray Emission (PIXE).

Similarly the aim of our project is to characterise silver point drawings of Dürer's travel book by Synchrotron induced X-ray fluorescence (Sy-XRF), another non-destructive analytical method. A major advantage of Sy-XRF is the accessibility in Berlin which prevents art objects from being transported over long distances.

In Sy-XRF, synchrotron radiation is used to introduce vacancies in the inner electron shell of atoms, which are refilled by outer shell electrons. The surplus energy, the difference in the binding energy between outer and inner shell electron, is emitted as element characteristic X-ray fluorescence, allowing identification and quantification of an element.

We have used the hard X-ray synchrotron beamline operated by the Bundesanstalt für Materialforschung und -prüfung (BAMline) at BESSY II to determine major and minor element contents in the silver point lines of the drawings. The special performances of the radiation obtained at the BAMline allow optimal discrimination between silver and paper backing. The sample mass in this case was less than 1 microgram.

Shown drawings are courtesy of Staatliche Museen Berlin, Kupferstichkabinett

Supported by the German Academic Exchange Service (DAAD) and the French Ministry of Research and Education.

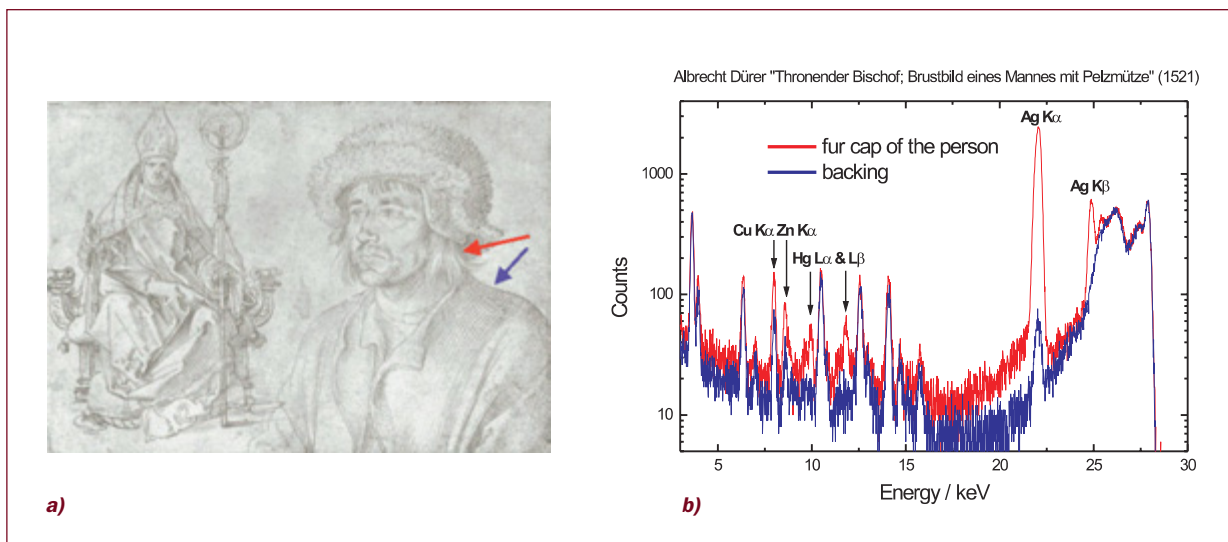


Fig. 1.
a) Albrecht Dürer drawing 'Thronender Bischof; Brustbild eines Mannes mit Pelzmütze' (realised probably in March 1521) from the Kupferstichkabinett Staatliche Museen zu Berlin (Inv.Nr. KdZ 34r),
b) Sy-XRF-spectra (28 keV excitation energy) of a silver point line and of the preparation layer indicated by the arrows.

In a French-German collaboration the new results will be compared to those measured in Paris and an international database on the chemical composition of drawings is to be created to facilitate the attribution of provenience and to provide new information on the material used for relisation of ancient drawings.

Up to now three sheets containing several silver point drawings of Dürer's travel book from the Kupferstichkabinett Berlin were analysed at the BAMline: 'Thronender Bischof; Brustbild eines Mannes mit Pelzmütze' (March 1521) (Fig. 1a), 'Liegender Hund; Hundekopf und Löwenkopf' (April 1521) and 'Brustbild eines Mannes aus Antwerpen; Der Krahenberg bei Andernach' (June 1521).

In the majority of the silver strokes, silver was affirmed to be the major element. Three other minor elements, Cu, Hg and in one case Zn could be attributed to the silver alloy (Fig. 1b).

Our results so far are consistent with those obtained in Paris on six other sheets of Dürer's travel book using PIXE. This includes

the surprisingly high mercury concentrations in the silver strokes of the drawings, which is possibly due to a special property of silver. Silver has a strong affinity to mercury and forms a very stable amalgam (hence it is used for tooth inlays) even with environmental mercury found in the earth's atmosphere. Therefore the presence of mercury in the silver strokes might be explained by an uptake due to the exposition to the atmosphere during the last 500 years.

The mercury contamination of small silver layers seems to be a general alteration phenomenon of these drawings. This observation has important consequences for the conservation of these drawings and allows also to distinguish original drawings from recent ones.

The new insights into the chemistry of Dürer's drawings obtained by synchrotron X-ray fluorescence encouraged us to setup further investigations of drawings from other artists or art objects of doubtful origin.

Contact:

Ina Reiche, Staatliche Museen zu Berlin, Rathgenforschungslabor
 ina.reiche@t-online.de

The first two novel protein structures determined at BESSY II

T. Maier, W. Saenger, J. Lodge and N. Sträter



Fig. 1:
Experimental setup for protein crystal diffraction at BAMline (Protein Structure Factory).

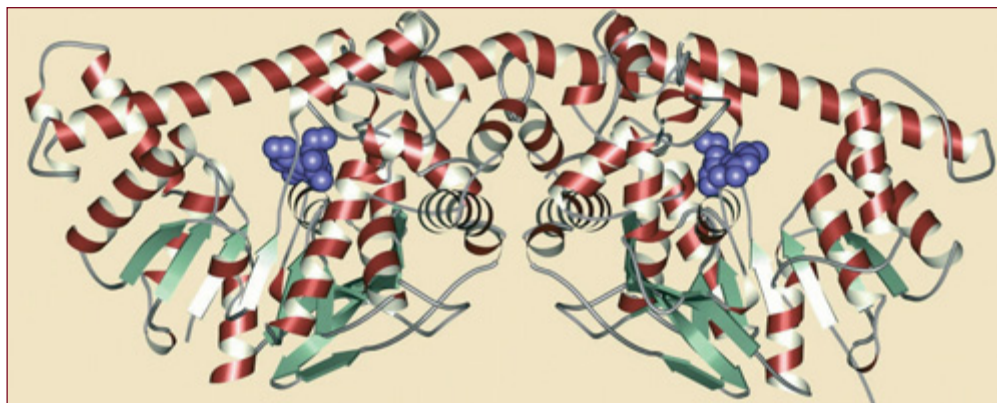


Fig. 2:
Fold of the dimeric glucosidase. The maltose substrate is shown in blue.

Protein X-ray crystallography is the key method to reveal full three-dimensional information of atoms in a protein molecule, which is in this resolution inaccessible by other methods. This precision is essential for an understanding of protein function, and a solid basis for the development of new drugs or industrial processes in biotechnology.

Protein X-ray crystallography requires single protein crystals, which can present problems. Protein crystals are difficult to grow, and once grown crystals are small and fragile as they contain up to 70% water. Diffraction data from single protein crystals are collected by using X-rays often generated at a rotating anode home source. But during the last decade synchrotron radiation has become the favoured X-ray source for protein crystallography for several reasons: At first, more accurate structures and better resolutions are obtained mainly due to the higher brilliance of the synchrotron X-ray beam compared to a rotating anode home source. The brilliance and the very small focus allow to collect data from tiny protein crystals (10-50 μm). In addition, the wavelength tunability greatly facilitates structure determination by increasing the anomalous scattering of metal ions, selenium or sulfur atoms, which is an elegant way for solving the so-called crystallographic phase problem.

Despite all the advantages, until recently synchrotron radiation dependent protein crystallography has not been available in Berlin due to the low ring energy of BESSY I. With the advent of BESSY II operation, a suitable X-ray source for protein crystallography is now in place. While the three experimental stations dedicated for protein crystallography are under construction, the first diffraction data of protein crystals have been collected at the BAMline of the Bundesanstalt für Materialforschung und -prüfung using the experimental set-up of the Protein Structure Factory (Fig. 1). Using these data we have determined the first two novel protein structures at BESSY II, a maltose-degrading enzyme from a thermophilic organism and a human lysosomal hydrolase.

Many of the industrially important enzymes are used in food processing, in particular in the degradation or processing of starch. In addition, starch serves as an important renewable raw material for chemical synthesis. But for these purposes the organic polymer starch has to be degraded to its monomeric building blocks, glucose.

For industrial applications it would be advantageous to use protein catalysts (enzymes) with an increased stability in order to work at higher temperatures. 'Heat stable' proteins are available from thermophilic ('heat resistant') organisms, mostly bacteria.

We have analysed the structure of an enzyme called glucosidase from a thermophilic organism, that degrades maltose (malt sugar) to glucose (Fig. 2). This enzyme still retains more than 50% of its activity when exposed 48 hours at 50°C. The determined structure is novel and structures of homologous enzymes of this family are currently not known. In order to characterise the catalytic mechanism, we have cocrystallised the glucosidase with maltose, which binds to the enzyme. Fig. 3 shows a maltose molecule bound to the enzymatically active site of the protein.

Lysosomes are organelles of animal cells, which are responsible for degradation of cell constituents and material taken up by the cell. Lysosomes therefore contain a battery of specific and non-specific degrading enzymes, called hydrolases, to be able to decompose all kinds of biomolecules e.g. proteins, carbohydrates, lipids and nucleic acids. Genetic defects in lysosomal enzymes often result in severe diseases caused by the accumulation of non-degraded substances.

In order to understand the causes of a fatal inborn error of metabolism in more detail, we determined the structure of a novel human lysosomal hydrolase bound to an inhibitor molecule (Fig. 4). Further analysis of this structure might help to develop strategies to prevent the outbreak of the disease in affected children.

The determination of two novel protein structures at the BAMline, which is not optimised for protein crystallography, raised the future prospect for the dedicated protein crystallography beamlines being under construction by the Protein Structure Factory at BESSY II.

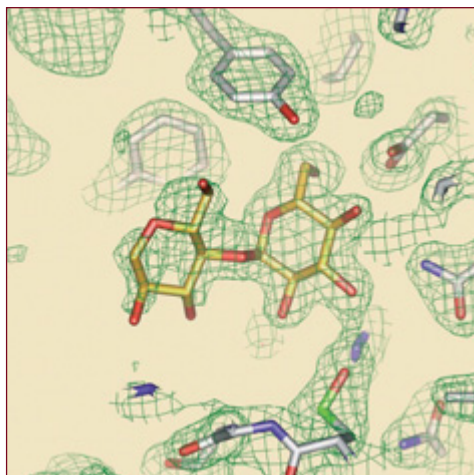


Fig. 3:
Electron density map (green) of a maltose molecule (yellow) bound to the catalytic site of the glucosidase.

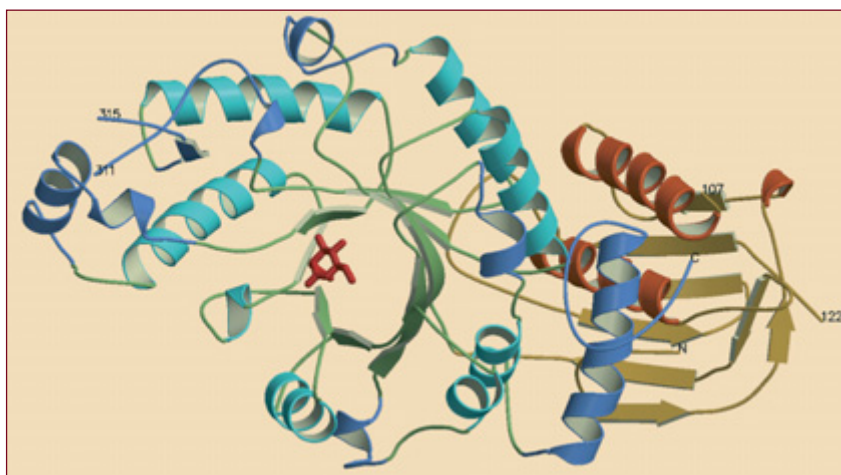


Fig. 4:
Cartoon representation of the lysosomal hydrolase. A bound inhibitor molecule is shown in red.

Contact:

Wolfram Saenger,
Norbert Sträter,
Institut für Chemie, Abteilung
Kristallographie,
Freie Universität Berlin
saenger@chemie.fu-berlin.de,
strater@chemie.fu-berlin.de

New photo resists for smaller chips

B. Löchel and H.-U. Scheunemann

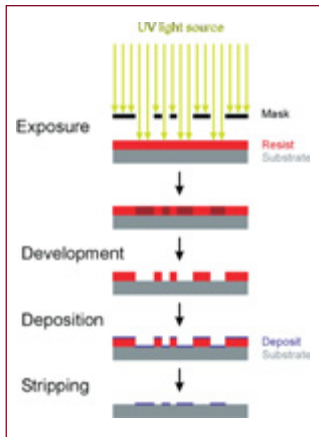


Fig. 1:
Main steps in a lithographic process.

For the production of microelectronic devices and microprocessors, presently factories apply optical lithography techniques for pattern transfer. In mass production, UV steppers with reduction optics using the mercury G-line (340 nm) were established. Special techniques employed during the lithography process allow to generate a minimum feature size of 180 nm. In order to overcome physical limits of optical pattern transfer, the wavelength of the applied light must be reduced.

Manufacturers are prepared to introduce optical steppers using 192 nm for the next chip generation and it is expected that using radiation 157 nm in wavelength, a feature size of 65 nm can be achieved as the ultimate limit in the year 2007. However, further integration of micro-processors will demand still more size reduction, i.e. a lithography technique using even shorter wavelength.

International investigations in this field are focussed on a wavelength of 13 nm, which requires a modified lithographical approach, the extreme UV lithography (EUVL). The tools and processes for EUVL are under investigation at present and microprocessor manufacturers hope to have the technique available in 5-6 years.

In lithography the pattern of a mask are demagnified by projection onto a semiconductor wafer covered with photo resist. A typical arrangement is shown in Fig. 1. After passing the mask, the light intensity is laterally inhomogeneous. In areas of high energy the photo resist on top of the substrate is modified by the incoming radiation and the pattern of the mask is reproduced as a latent picture in the resist layer. The following development step removes irradiated resist regions and leads to a resist mask covering the substrate surface. This mask will be used as a protecting layer for the subsequent silicon treating processes in which unprotected silicon areas will be altered by etching, metal depositing or doping.

After removing the resist, the entire procedure can be repeated by using another mask leading eventually to a silicon chip, or a wafer of silicon chips in the production process.

Lithography techniques require, that all materials and the entire equipment have to be adapted and optimized for the used radiation. In order to use 13 nm radiation, an adapted optical concept, suitable photo resists and new light sources are essential. In contrast to the currently used optical lithography, the mask and the entire projection optics must be reflective in EUV lithography (Fig. 2).

A special interest is set on the synthesis and optimization of photo resists for EUVL. Beside high sensitivity in the 13 nm range the resist should also have a high gradation, i.e. the slope of the gradation curve (Fig. 3) should be steep. Many companies and researchers are working in this field. For the investigation of suitable photo resists a light source delivering radiation of 13 nm is required but until appropriate plasma light sources will be available only synchrotron radiation can meet the demands of a clean and very stable light source.

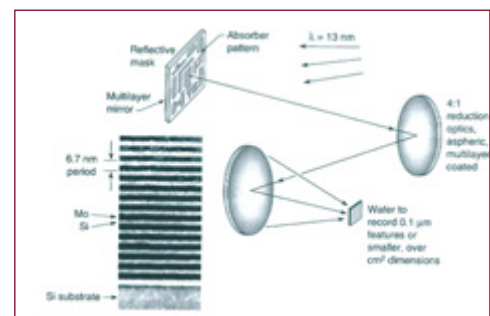


Fig. 2:
Principle set-up for EUV lithography using synchrotron light.



Fig. 4:
EUV beam line at BESSY:
 pre-mirror chamber on the right,
 multi layer mirror chamber in the
 middle, clean room hutch with
 exposure station on the left.

As a subcontractor of Infineon AG, Munich, BESSY built a special facility with an exposure tool for the development of EUV resists (Fig. 4). Synchrotron radiation from a bending magnet is first reflected by a pre-mirror (grazing incidence) to cut off high energy photons. The low energy part of the synchrotron spectrum is then reflected twice by coated multilayer mirrors at normal incidence optimized for reflection of 13 nm wavelength, which would be destroyed without cutting off high energy photons. Subsequently, the beam will pass the mask or will be reflected by the mask to the resist covered substrate.

In the exposure chamber simple open frame exposures of the new photo resists can be carried out. Clean room conditions and yellow light for the exposures are realised by using a hutch. For characterization of new photo resists an exact gradation of the intensity is necessary. Up to 15 different grey levels can be realized simultaneously by using a chopper disc during a single exposure. The facility was put into operation in December 2001 and characterization of the first photo resists is now in progress.

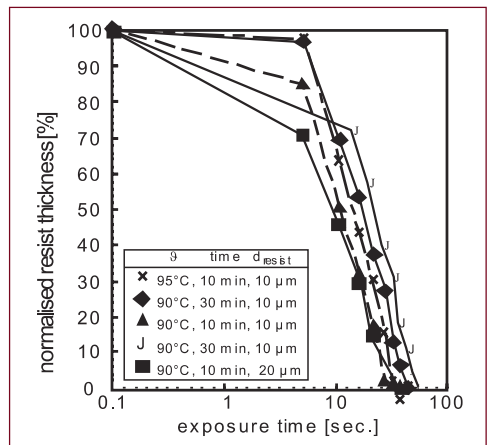


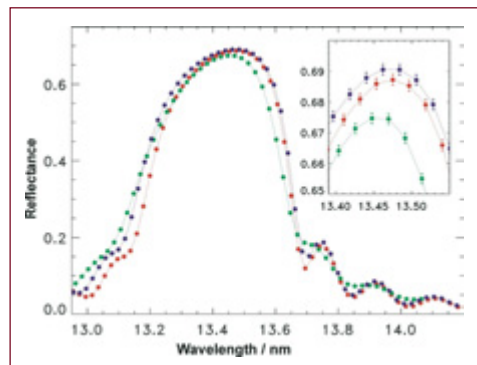
Fig. 3:
Gradation curves of a Novolak
photo resist for different pre-
bake conditions.

Contact:
 Bernd Löchel, BESSY GmbH,
 Berlin
 loechel@bessy.de

High-Accuracy Metrology for Extreme Ultraviolet Lithography

R. Klein, F. Melchert, F. Scholze, R. Thornagel, J. Tümmeler and G. Ulm

Fig. 1: Measured reflectance of Mo/Si multilayer mirrors coated by different coating processes. The relative uncertainty in the determination of the peak reflectance and center wavelength is 0.25 % and 0.025 %, respectively.



During the last decades, owing to a gradual reduction of the circuit size, electronic chips have become ever more powerful and more compact with the cost being lowered at the same time. The optical lithography techniques used for their production have however been pushed to the farthest possible extent. It is expected that using radiation 157 nm in wavelength, a feature size of 65 nm can be achieved as the ultimate limit in the year 2007 (according to the *International Technology Roadmap for Semiconductors*).

But following the so-called Moore's law, which postulates the doubling of power of electronic chips every 18 months and which has established as the industrial standard for progress and success, a new generation of lithography (NGL) systems is required.

The most promising candidate for this NGL is Extreme Ultraviolet Lithography (EUVL), which uses radiation of 13 nm wavelength. Similar to optical lithography, the patterns of a mask are demagnified by projection onto a semiconductor wafer covered with a photo resist. The mask and the entire projection optics have to be reflective and the required specifications for mask making, mirror shaping and wafer handling are unprecedented.

Along with the challenging technological development, a reliable metrology is essential. Synchrotron radiation sources are ideally suited for at-wavelength EUV metrology because they are clean, stable and reliable.

At the BESSY II electron storage ring, the Physikalisch-Technische Bundesanstalt (PTB) operates a laboratory [1] with several beamlines for high-accuracy at-wavelength metrology in the EUV spectral range using synchrotron radiation from bending magnets and from the EUV-optimized undulator U180 [2]. Many companies such as Carl Zeiss, Jenoptik Mikrotechnik GmbH, Infineon Technologies AG and Schott ML GmbH as well as many research groups rely on PTB's work.

As EUV transparent materials are lacking, the entire optics in an EUV projection system has to be reflective. To enhance the reflectance, normal incidence mirrors covered with multilayer coatings are used. Since the optics have to be optimized for high throughput, the reflectance of the mirrors has to be maximized. One important task is the determination of the reflectance with a low relative uncertainty to allow the multilayer production process to be optimized for maximum reflectance and uniformity of the reflectance along the mirror surface.

PTB operates a reflectometer at a bending magnet beamline equipped with a plane grating monochromator. The beamline is optimized to deliver radiation of high spectral purity, i.e. low higher order contribution and low scattered light content [3]. So it is possible to determine the reflectance with a relative uncertainty below 0.25 % in the EUV spectral range. In the year under review, the beamline was almost entirely booked out for EUV activities and more than 500 samples were analyzed for various cooperation partners. Fig. 1 illustrates the need for this high-accuracy reflectometry in order e.g. to distinguish very small differences in the reflectance of Mo/Si multilayers from different multilayer coating processes.

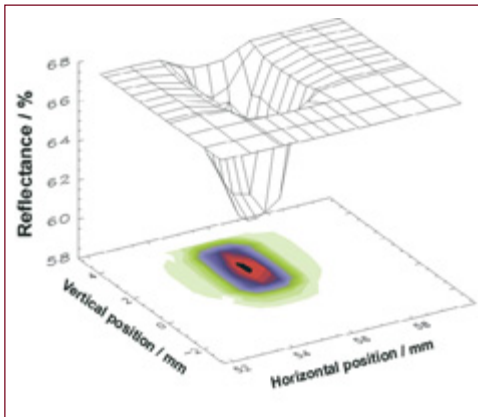
PTB is currently setting up an additional reflectometer which will be capable of handling mirrors up to 50 kg in weight and 550 mm in diameter or 1000 mm x 150 mm x 230 mm in size. The expected date for taking up operation is May 2002.

[1] G. Ulm et al.; *Proc. SPIE* 3444 (1998) 61–621

[2] R. Klein et al.; *J. Syn. Rad.* 5 (1998) 451-452

[3] F. Scholze et al.; *Proc. SPIE* 4344 (2001) 402-413

[4] R. Klein et al.; *Proc. SPIE* 4506 (2001) 105-112

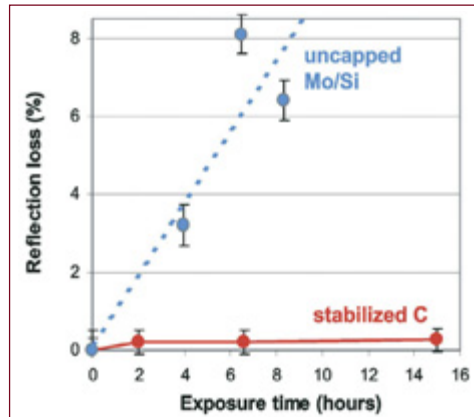

Fig. 2a

For mirror surface roughness characterization, scattering experiments are performed by measuring the radiation scattered into the dark field with a back-illuminated thinned CCD camera. This allows polishing procedures to be optimized and the very challenging specification for the mirror roughness to be tested.

In order to maintain sufficient optics throughput, reflection loss of the multilayer mirrors in an EUVL tool due to contamination has to be minimized.

To investigate processes which reduce the reflection and to develop strategies for preventing them or mitigating their effects, PTB operates two beamlines to simulate irradiation conditions for future lithography tools [4]. Both, undispersed undulator radiation from the U180 undulator and focused and filtered bending magnet radiation can be used. Both beamlines provide EUV radiation with power densities of several mW/mm^2 . A dedicated irradiation chamber with sample load lock and differential pumping allows components such as substrates, multilayer mirrors or filters to be exposed to EUV radiation under different vacuum conditions.

The components are characterized before and after irradiation in the PTB reflectometer described above. Fig. 2a shows a typical footprint of a degradation in reflectance for a Mo/Si multilayer mirror after irradiation, measured at the center wavelength of reflectance across the mirror surface. Fig. 2b shows as an example the mitigation of the reflection loss during illumination in a water enriched environment by adding a thin carbon capping layer (red line) on top of a Mo/Si multilayer mirror (blue line).


Fig. 2b

Crucial for the successful fabrication of EUV optics is the development of EUV system metrology. For testing and demonstration of the measurement methods a so-called Small Field Metrology Tool was set up at the PTB undulator beamline. The main item of this set-up is the Micro Exposure Tool (MET) projection optics built by Carl Zeiss in collaboration with the Lawrence Livermore National Laboratory (LLNL). At 13.4 nm wavelength, two multilayer mirrors will reduce reticle structures by a factor of five onto the wafer plane.

An illumination system allows efficient coupling of the 13 nm radiation emitted by the PTB undulator U180 to the projection optics. For testing and fast alignment and test of the detectors, it is also possible to couple a 248 nm KrF laser beam into the system. The whole set-up is completed by transfer systems for both the reticle and wafer stages and an EUV imaging sensor. The system illustrated in Fig. 3 is designed for a resolution of about 35 nm in the wafer plane.

EUVL is considered a lithography generation which will last many decades. The resolution obtainable will be gradually pushed to its theoretical limits, provided the necessary metrology keeps pace. The PTB low energy compact storage ring (200 MeV up to 600 MeV electron beam energy) planned in close cooperation with BESSY GmbH and scheduled to be put into operation in 2007, will be an ideal platform for investigating EUVL metrology questions of prime importance.

Fig. 2:
(a) A typical example of the degradation of reflectance in the irradiated spot of a Mo/Si multilayer mirror (ML) can be seen. The reflectance at different surface points was measured at the center wavelength of reflectance.

(b) Typical result for the mitigation of reflection loss during illumination in a water enriched environment is shown. The blue line shows the reflection loss for a normal Mo/Si ML, the red line for a Mo/Si ML covered with a thin carbon layer for protection (courtesy FOM Institute, Rijnhuizen).

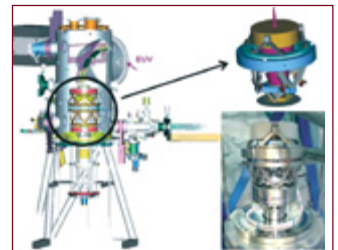


Fig. 3:
The left side shows a schematic drawing of the Small Field Metrology Tool used for characterization of the Micro Exposure Tool (MET) optics, shown enlarged on the upper right side. This system is designed to print patterns 35 nm in size. On the lower right side is a photograph of the MET optics (courtesy Carl Zeiss, Oberkochen).

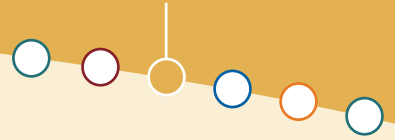
Contact:

Roman Klein, Physikalisch-Technische Bundesanstalt, Berlin
roman.klein@ptb.de

News & Events

3



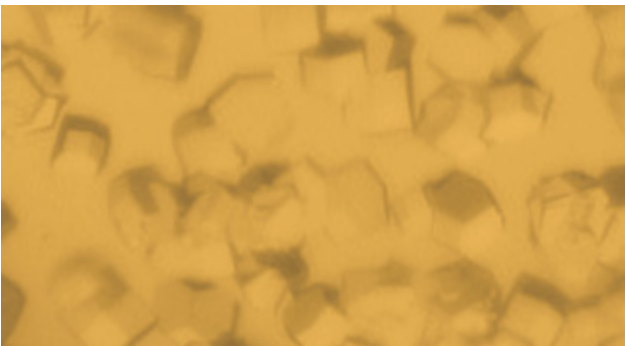


Prof. Dr. Wolfgang Gudat's term of office as scientific director of BESSY expired at the end of 2000.

His successor is Prof. Dr. Wolfgang Eberhardt formerly at Forschungszentrum Jülich. On the occasion of the official inauguration in July, Prof. Gudat handed over the official business of the BESSY light source symbolized by an oil lamp.



*The new scientific director
Prof. Dr. Wolfgang Eberhardt*



Construction works along the Albert-Einstein-Strasse were completed in 2001.

Prof. Dr. Hans-Olaf Henkel (picture right), president of the Wissenschaftsgemeinschaft Gottfried Wilhelm Leibniz, spoke at the ceremonial completion of the BESSY building extension in October.

Scientific talks were held by Prof. Dr. B. Keimer (Max-Planck Institute Stuttgart) and Prof. Dr. J. Stöhr, (Stanford Synchrotron Radiation Laboratory, USA).

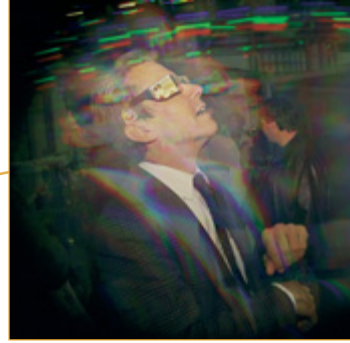


The new lecture hall is being used to promote scientific exchange: There are four for the 'User Treff' (USER/BESSY meetings regarding operations) and for 'Science on the Fly', informal seminars of research in progress.



Senator Adrienne Goehler was a fascinated visitor at BESSY.

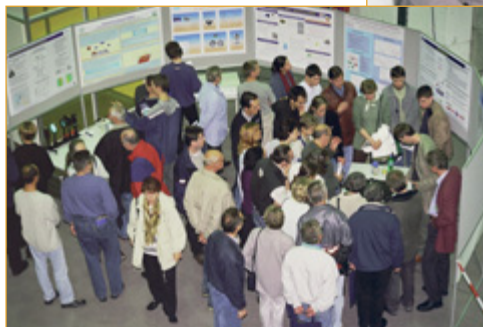
The inauguration of the Russian-German Laboratory, a joint venture of the University of St. Petersburg, the Freie Universität Berlin and BESSY, was accompanied by the 'Third Russian-German Workshop' on Synchrotron Radiation Research in November 2001.



Visitors



Almost 4,000 visitors took the opportunity during the 'Lange Nacht der Wissenschaft' to talk to BESSY researchers and to get detailed information about the facility and the research that is done there.





Workshops 2001

In 2001 BESSY enjoyed great popularity as ever: 76 groups – thereof 18 groups from primary and secondary schools and 16 groups from universities – visited BESSY to get a view inside the facility and the scientific work that is done there. Overall nearly some 1,500 participants attended guided tours at BESSY. The importance of BESSY for the WISTA and greater area of Berlin concerning science and technological development was also expressed by the visits of high ranking persons among them Klaus Wowereit (Mayor of Berlin), Adrienne Goehler (Berlin Senator of science, research and culture), Werner Müller (Federal Minister of Economy).

On September the 15th nearly 4,000 interested visitors joined the Open House which was arranged by BESSY in the framework of the '**Lange Nacht der Wissenschaft**' (Long Night of Science).



January,	12-17	Workshop on the Scientific Case of a BESSY VUV-Soft-X-Ray FEL
June,	18-19	Indo-German-Workshop on Nano-Materials & Technologies
September,	5-7	ESF Exploratory Workshop on Time Resolved Investigations of Structural Changes in Soft and Solid Matter with neutrons and X-rays
November,	8-9	Second BESSY II WLS Beamline User Seminar
November,	13-14	Innovation Forum Microtechnique
November,	18-20	Third Russian German Workshop on Synchrotron Radiation Research
December,	5	Scientia Users' Meeting
December,	5	XES Workshop
December,	5	IRIS Workshop
December,	17	BESSY Forum

Users' Meeting 2001

The poster session was held in the BESSY experimental hall. The posters will remain in the hall until next year's meeting so that the results of the experiments can be discussed by visitors and by other user groups the entire year.



As in the last years the best poster was honoured with a voucher for scientific literature. This year the poster prize was awarded to Lutz Kipp, University of Kiel.



At the 2001 BESSY Users' Meeting in early December the scientific director, Prof. Dr. Wolfgang Eberhardt, opened the meeting by reviewing some of the highlights of the 3rd year of BESSY II user operation. He mentioned among others the first protein structure resolved at BESSY marking the increasing importance of life sciences. Some more scientific results were selected for oral presentation to the BESSY community while the poster session with over 90 contributions gave a complete review. These results are summarized in the BESSY Annual Report CD.

However, the central issue of this meeting were the 'Visions of Science' related to the BESSY Free Electron Laser project. This laser based on the principle of stimulated amplification of spontaneous emission (SASE FEL) provides pulses as short as 20 fs with extremely high peak power and complete transverse coherence at photon energies up to 1,000 eV. The scientific potential of this source is significant as sketched by a number of speakers covering topics as far apart as the excitation and decay of free electrons and molecules, the functional-structural relationship of complex materials, novel characterization of materials and concepts for magnetic information storage and processing, the chemistry of radicals, and the dynamics of biological systems. The technical challenges to realize the source and to conduct experiments are significant. However, the experiences from the TTF FEL at DESY in Hamburg indicate the feasibility: 'The time is right for this project' (W. Eberhardt).

The vendor exhibition enabled the participants to stay in contact with suppliers of highly specialized components needed for state of the art research at BESSY.

Parallel to the Users' meeting a vendor exhibition was held in the Einstein- and Newton-Kabinett of the WISTA-building.



Ernst Eckhard Koch Prize

The Ernst Eckhard Koch Prize is annually awarded for an outstanding PhD thesis using synchrotron radiation at BESSY or HASYLAB. Like the years before, the prize was awarded on the Users' Meeting by the Society of Friends and Sponsors of BESSY. This year Karin Heister from the University Heidelberg received the prize for her thesis on self-assembled monolayers of large molecules on Au and Ag surfaces. The molecules investigated contain a sulfur head group, aliphatic and/or aromatic spacers and an endgroup which is chosen to be inert. She showed that the reconstructed gold surface is modified by the adsorption of the molecules while Ag does not show any modification of the surface as demonstrated by line shifts as small as 0.05 eV. She showed further that this result is independent of the details of the spacer part of the molecule. The radiation damage mechanism was identified to be mediated by secondary electrons. Lateral structuring by selective irradiation with synchrotron radiation was also demonstrated.



Karin Heister from the University of Heidelberg received the Ernst Eckhard Koch Prize 2001. The Prize was handed over by Prof. Dr. P. Zimmermann.



Dr. K. F. Beckstette, president of the jury, Technology Center Carl Zeiss, Oberkochen, the winners of the Innovation Award on Synchrotron Radiation Dr. Rolf Follath and Dr. Friedman Senf and the president of the Society of Friends and Sponsors of BESSY, Prof. Dr. P. Zimmermann (from left to right).

Innovation Award on Synchrotron Radiation

At this year's Users' Meeting the Society of Friends and Sponsors of BESSY awarded for the first time the Innovation Award on Synchrotron Radiation. It is granted for an excellent achievement which has contributed significantly to the further development of techniques, methods or uses of synchrotron radiation. The award which includes a monetary prize of € 2,550 was given to Rolf Follath and Friedman Senf, both from BESSY, for the development and manufacturing of high resolution plane grating monochromators. These monochromators yield the highest energy resolution in the XUV spectral region ever achieved, as well as a high photon flux and a very small focus.

Facility Report



4

In 2001 the BESSY light source has been operating during six user runs of four to five weeks each. The total beamtime delivered to users added up to more than 3,900 h. Installations were carried out during ten weeks of shutdown in April, July and August. Major additions to the storage ring were the installation of a 6 T superconducting wavelength shifter for micro-engineering and the replacement of ID vacuum chambers by 11 mm vertical aperture vessels. In machine-dedicated shifts special emphasis was set to further improvements of beam stability and improvements to beam lifetime.

Machine Status

Orbit Stability at the Highest Level

Orbit stability at a level well below 10% of the electron beam-size becomes more and more important for many experiments. Thus at the end of 2000 a powerful orbit correction system had been implemented. The new system uses the existing magnets and power supplies; but to allow sensitive correction of a fraction of about 10^{-6} radian all DACs were replaced by 24-bit units. Beam orbit is measured at 112 locations in horizontal and vertical direction and is corrected every 6 s using a Singular Value Decomposition (SVD) algorithm. Thermally induced drifts as well as remaining orbit displacements from undulator gap drives are thus compensated. The beam stays constant in space at a level of less than $5 \mu\text{m}$ at any location during a day with a constancy of the rms orbit of $\pm 25 \text{ nm}$ (Fig. 1).

At the beginning of each new user run the centers of all beam position monitors are recalibrated using beam-based alignment methods, ensuring a long-term reproducibility of the beam orbit better than $100 \mu\text{m}$ and/or $50 \mu\text{rad}$ over the year.

Tune Stabilization Feed Forward

The focusing effects of undulators during gap drives cause changes to the working point (tune) of the machine. Whereas the effect of a single undulator is negligibly small, ten such devices active in parallel sum up to yield an intolerably large tune shift. Thus, all IDs had to be characterized and a gap-dependent correction to the quadrupole power supplies has been generated. Each ID is connected to typically 32 pairs of quadrupoles to stabilize the tune globally.

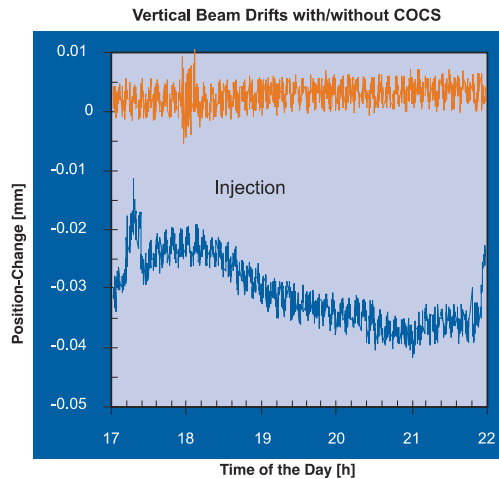


Fig. 1: Vertical photon beam stability during filling. Upper graph with closed orbit correction system (COCS) active, lower graph without stabilization.

Moreover, in order to compensate for the distortion in the optical function of the ring, local nearby quadrupoles are powered separately to minimize the beating of the amplitude functions. By this method the variations of the working point are reduced by a factor of more than 20 bringing back stable conditions.

Improving Beam Lifetime

Beam lifetime, which is already a factor of three higher than the design value, is still a subject of machine studies. Tuning of the harmonic sextupole magnet circuits did yield new field settings which resulted in a substantial increase in beam lifetime. Comparing the lifetime for the 'old' and the 'new' setting versus beam current a 25% improvement when all undulators are at open gap position is seen (Fig. 2).

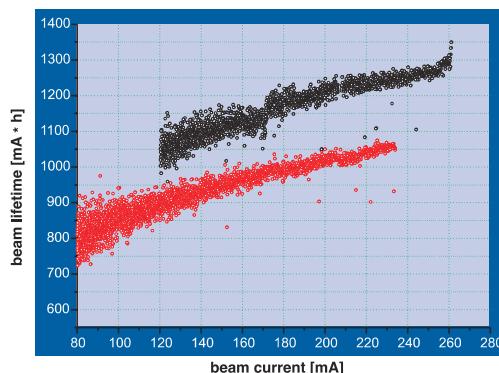


Fig. 2: Beam lifetime vs. beam current for the 'old' harmonic sextupole setting (lower red dots) and the improved setting (upper black dots).

Fig. 3:
Filling pattern of the ring in single-bunch mode (left) and in hybrid mode with 310 bunches filled to 0.6 mA/bunch and the 10 mA single-bunch in the empty clearing gap (right).

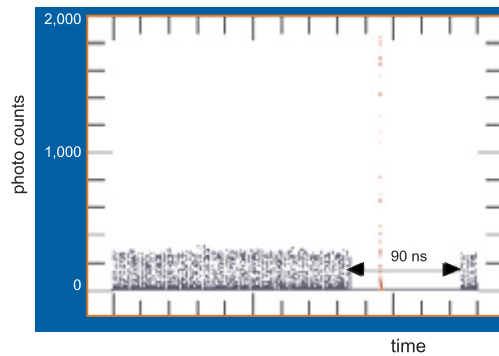
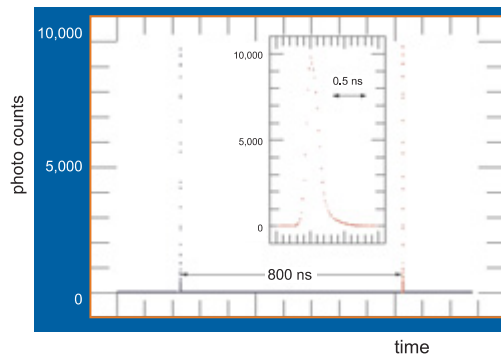


Fig. 4:
Photo of the 6 T wavelength shifter, formerly operated at BESSY I, that replaced the 4 T device.

Filling modes

Standard filling mode throughout the year was the multi-bunch mode where 320 out of the 400 rf-buckets available are filled and an 80 ns long 'empty' clearing gap is generated by a knock-out kicker. The ring was filled typically to current values of 250 mA: Eight hours after injection the current had decreased to 110 mA and a new injection was started.

For the first time single-bunch mode was scheduled for a two-week period. One rf-bucket was filled to 15 mA circulating current. The injection rates were about 2 mA/min. As beam lifetime for this current is only about 2 h due to the large charge density in the bunch, an rf-quadrupole field was used for slightly increasing the vertical beam-size; thus the Touschek effect was reduced and lifetime increased to 4 h typically.

During the single-bunch period also a hybrid mode was offered to users. In this mode 310 buckets of the ring are filled to 200 mA – similar to multibunch mode – while in the clearing gap one bucket is filled to 10 mA (Fig. 3). The technique used was to switch

the electron gun parameters from multi-bunch to single-bunch by reloading appropriate settings from file. Total injection time to fill the machine in hybrid mode was 30 min typically.

Hardware Changes

During three installation phases of altogether ten weeks all necessary installations were done in the machine tunnel, such as the integration of a 6 T wavelength shifter (Fig. 4), the replacement of a cavity, the replacement of a dipole chamber for an IR-beamline, the substitution of ID-chambers by 11 mm high vessels at U49-1 and U180, and the installation of connecting chambers to four front-ends.

Current Activities and Future Plans

The 3rd harmonic cavities successfully used for bunch-lengthening are being replaced by new high-power versions to allow operation at considerably higher voltages for further increase of beam lifetime. A superconducting 3rd harmonic cavity, presently under fabrication, is expected to be installed in early 2003 to exploit this technique to the limit.

A second 7 T wavelength shifter for protein structure analysis and a 7 T multipole wiggler for material research are in a well advanced production state at BINP (Novosibirsk). Installation of the devices is scheduled in 2002.

As space for future insertion devices is of most importance the last non-occupied straight section will be cleared from the many diagnostic elements in the course of the next 18 months.

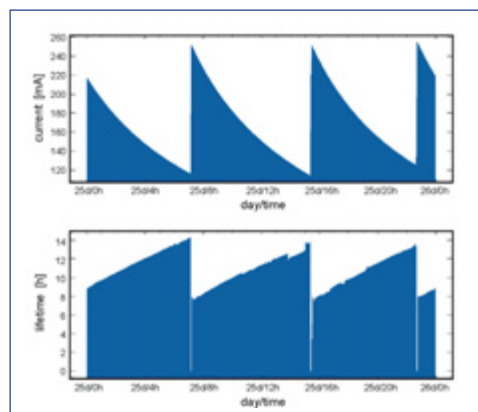
A typical day at BESSY

Operation energy:
1.7 GeV

Filling:
250 mA at injection

Eight hours after injection:
110 mA left

Beam lifetime:
7 to 14 h



Beamline Developments

Since the start of the new facility BESSY II three years ago, 36 beamlines have been put into operation, an average of one beamline per month. At the end of 2001, 21 insertion device beamlines together with 8 undulators and 2 wavelength shifters have been installed. Additionally 15 bending magnet beamlines were put into operation. The main emphasis is now shifting toward improving the quality of operation of the beamlines, educating the user community in exploiting all the capabilities of the existing beamlines, and to the construction of special beamlines which will provide unique features such as, for example, fs pulses of circularly polarized soft X-rays for the investigation of magnetization dynamics on ultrashort timescales.

Recent Installations of Beamlines

Installation and commissioning of undulator based PGM's have become a highly standardized procedure. The experiences gained in the last three years with this monochromator type enabled us to put the U49/2-PGM-1 successfully into user operation with only four weeks of commissioning. The beamline shows a very high resolving power combined with a small spot size and excellent flux values even at photon energies of more than 2 keV (Fig. 5).

With the first grating delivered after more than 2 years of delay the U125/2-SGM finally went into operation in 2001. Due to the absence of two additional gratings, the energy range is still limited, nevertheless first experiments could be performed on this monochromator which is operated by the Berlin universities.

An additional hard X-ray beamline, the BAM/PTB-KMC at 7T-WLS/1 went into user operation in 2001. This beamline, devoted to materials research and detector calibration, also serves as source for protein crystallography at BESSY II.

With the excellent results obtained at the newly installed German-Russian-PGM, the virtues of the BESSY collimated PGM design, which resulted in beamlines of

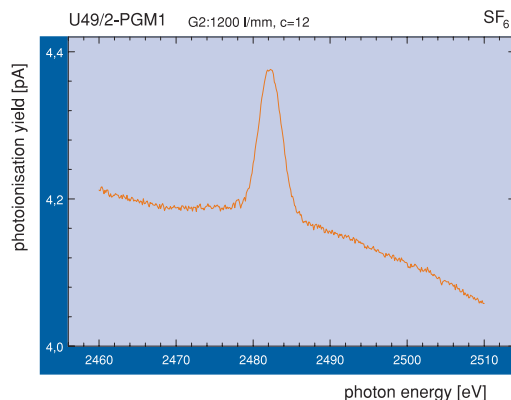


Fig. 5: Even at energies as high as 2.5 keV the U49/2-PGM shows reasonable results. The pronounced structure in the photoionisation yield of SF₆ at the sulphur K-edge is clearly visible

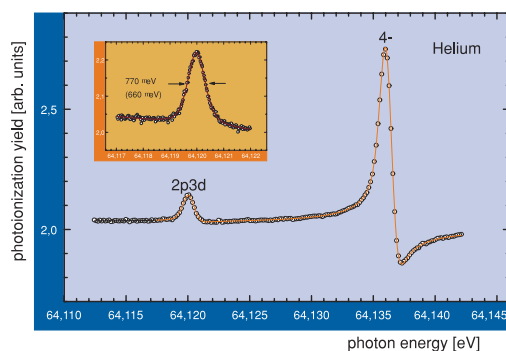


Fig. 6: After Doppler correction the He 2p3d resonance shows a line width of 660 meV resulting in a resolving power of 100,000 achieved at the German-Russian PGM on Dipole DIP16.1A.

unprecedented performance at our undulator sources, have been implemented on a bending magnet, DIP16.1A. A resolving power of 100,000 has been demonstrated at 65 eV and flux and focus size have reached their design values (Fig. 6).

The IR-system installed at dipole-frontend DIP2.2 went successfully into operation. The focussing system delivers 60 mrad (h) and 40 mrad (v) infrared radiation from 5,000 cm⁻¹ to 50 cm⁻¹ to an Fourier Transform Spectrometer and an IR-Microscope (Fig. 7).

After adaptation to the new source and careful set-up even almost 20 year old monochromators like the 3m-NIM-2 show now an outstanding resolving power of 60,000 at 11 eV. Focus size of 400 μm x 100 μm and flux values in the 10¹⁰ range meet or even exceed the design values (Fig. 8). This increase in performance reflects the improvement in the source parameters of the new source BESSY II.

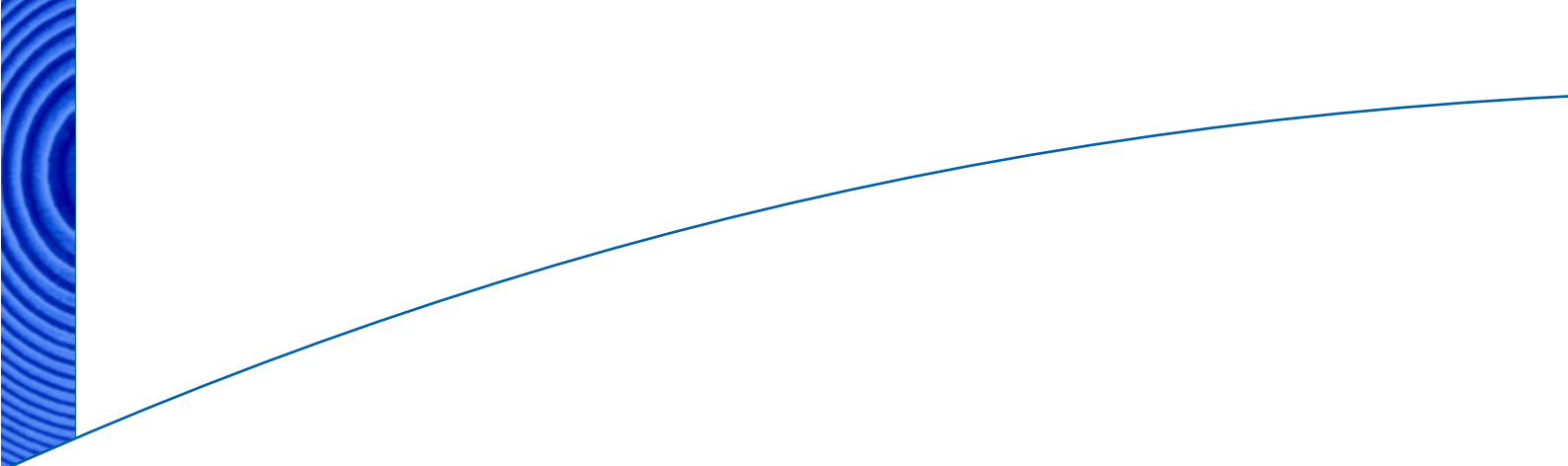
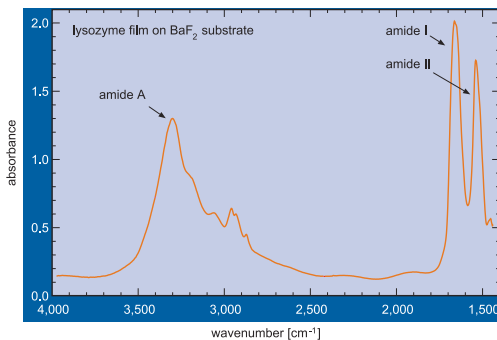


Fig. 7:
Fourier Transform Infrared (FT IR) spectrum of the protein lysozyme measured at the commissioned infrared beamline

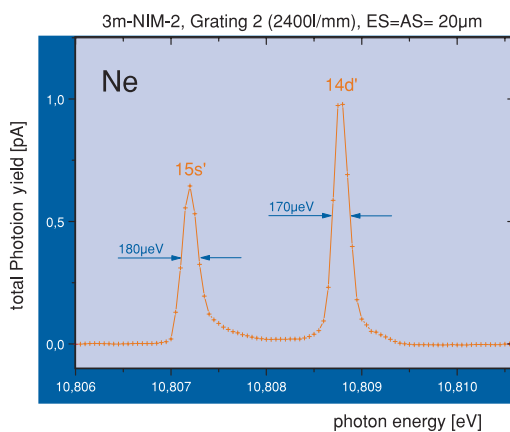


Improvements of Beamline Operations

In order to maintain and improve the performance of the BESSY-beamlines, a permanent process of characterization and optimization during regular commissioning shifts has become a major task of the experimental systems group. The close cooperation of specialists for undulators, beam position diagnostics, optics, computer control and accelerator scientists provides the foundation for the successful improvement of the beamlines. Now users have full control over gap and shift of all undulators, thus it is possible to scan on top of the undulator harmonic with an exactly defined degree of polarisation.

The in-beamline ionisation chambers have proven to be an indispensable tool. Using a well established procedure it is now possible to obtain an absolute energy scale calibration for our PGM's with an uncertainty of less than 0.1%.

Fig. 8:
A resolving power of 60,000 at 11 eV was achieved with the almost 20 year old 3m-NIM-2.



For optimization of focal position and spot size a focus test chamber, based on a high resolution fluorescent screen combined with a microscope-CCD-system has been developed. The test chamber can be adjusted in all three directions under vacuum. Thus, the results of alignment actions can be monitored online and quantitative values of the focus size are automatically determined.

UE56-Dual-Beam-Mode

The implementation of the dual-beam-mode of the UE56-PGM was one of the most demanding tasks we had to perform on our beamlines. This requires an identical photon energy of both beams in addition to a complete geometrical overlap with homogeneous intensity. Ionisation chamber, focus test system and in-beamline dichroism detectors had to be used for this purpose.

A severe problem was the inhomogeneity of the focus in the horizontal direction (Fig. 9 left). Even with the best mirrors available a significant intensity modulation remained, which was different for both beams due to the fact that they pass over different portions of the optical components. The solution to this problem was a modification of the last mirror chamber, allowing for well defined micro-oscillations of the refocussing mirror. They produce an almost uniform intensity distribution without enlarging the spot size by more than 10% (Fig. 9 right).

For an appropriate usage of this dual beam mode, e.g. for MCD measurements, the data acquisition and beamline control software was adopted to give the users full access to the chopper for switching of the helicity. First MCD spectra recorded with this technique show an improved quality (Fig. 10) compared to spectra recorded successively.

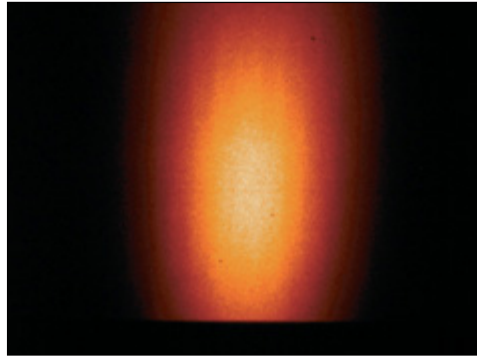
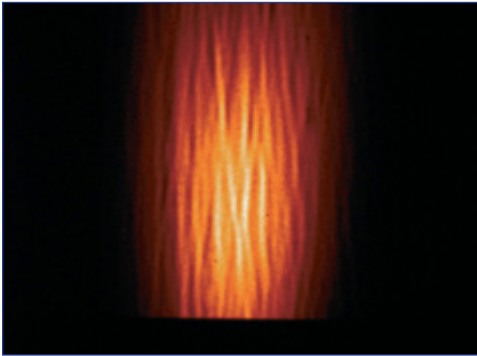


Fig. 9:
Intensity distribution in the focus of the UE56/1-PGM without (left) and with (right) micro-oscillation of the refocussing mirror.

RF-Carbon-Decontamination

Carbon contamination of the optical components results in a substantially reduced intensity at photon energies above the carbon K-edge. This is a severe problem for all beamlines working in this energy range.

Since several years BESSY has good experience with removing carbon contamination by in situ applying an Ar/O₂ low-energy rf-discharge in the mirror chambers.

All chambers of the BESSY-beamlines are equipped such that the cleaning procedure can be applied readily. Fig. 11 shows the result of a cleaning procedure at the U125/1-PGM. Before cleaning, the flux at the carbon K-edge dropped more than an order of magnitude. After cleaning almost no intensity loss could be detected.

Future Developments

In the near future (2002-2004) we are planning the following upgrades of the experimental capabilities for the user community at BESSY:

- Construction of a bending magnet beamline for testing of optics components at wavelength.
- Fs-slicing to provide fs pulses with circular polarization at the transition metal L-edges for investigations of the dynamics of magnetic storage media.
- A low energy undulator beamline with a high resolution electron spectroscopy endstation for investigations of high T_c materials and other correlated electron systems.
- A micro-focus insertion device beamline (2-30 keV) for materials and environmental sciences.
- Additional endstations for high resolution XPS and photoemission microscopy with spin detection.

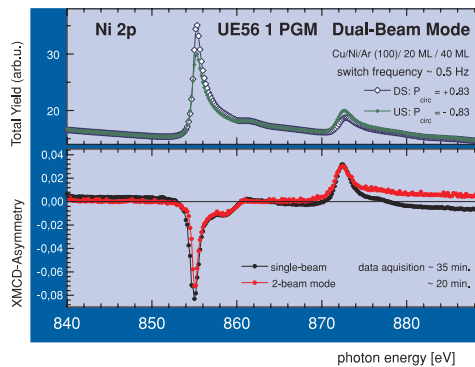


Fig. 10:
Comparison of MCD-spectra recorded in dual-beam-mode and successively.

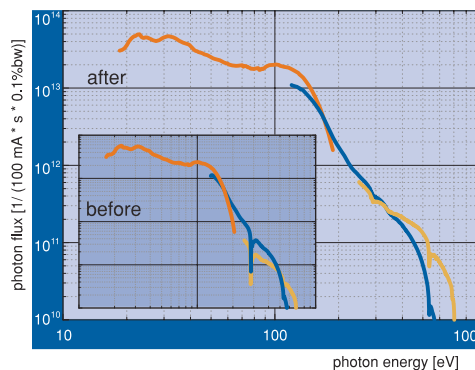


Fig. 11:
Photon flux of the U125/1-PGM before and after carbon decontamination.

BESSY-FEL



5



Following the successful commissioning of BESSY II, the BESSY GmbH now plans to extend its capabilities with the construction of an Free Electron Laser (FEL) based on the principle of Self-Amplified Spontaneous Emission (SASE). The project aims for BESSY's traditional spectral range of the vacuum ultraviolet and soft X-ray, i.e., $20 \text{ eV} \leq h\omega \leq 1 \text{ keV}$. Compared to modern synchrotron sources the FEL produces 1,000 times shorter ($\leq 20 \text{ fs}$) and coherent pulses with selectable patterns with an up to nine orders of magnitude higher peak power. Hence, it is expected to provide the foundation for a complete new field of scientific research complementary to BESSY II.

FEL Design

The BESSY-FEL will be setup in close cooperation with the foundation Deutsches Elektronen-Synchrotron (DESY), Hahn-Meitner-Institute Berlin (HMI) and Max-Born-Institute (MBI). Its site will be adjacent to BESSY II in Berlin-Adlershof. A study group funded by the 'Zukunftsfonds des Landes Berlin' is presently working out the detailed R&D issues of the project as the basis for the final proposal to be submitted by end of 2003. Considering a construction phase for the SASE-FEL of four years, the experimental program with this unique future light source can start as early as in the year 2008.

An overview of the project is shown in Fig. 1. The FEL will be sited on a 500 m long straight along the Teltow-canal at the WISTA site south-west of BESSY II. The central part is a super-conducting linear accelerator of the TESLA type. In the first phase of the project an electron beam with an energy up to 2.25 GeV will be inserted into three separate undulators to ensure a flexible selection of the photon energy. Downstream of the undulators a distance of (at least) 100 m to the experimental stations ensures sufficient space for the construction of optical beam lines and a sophisticated experimental environment.

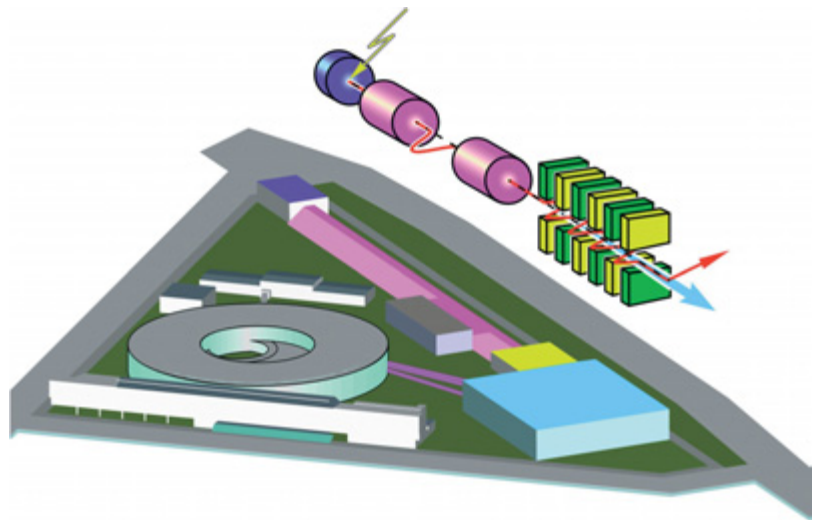


Fig. 1: Animation of the BESSY site with location of the planned BESSY FEL

The range of brilliance expected for the BESSY-FEL is displayed in Fig. 2. The radiation generated by the FEL has a peak brilliance of up to 7×10^{31} Photons/(s mrad² mm² 0.1% bandwidth).

For comparison the 3rd generation light source BESSY II is shown as well as the operation regimes of the DESY Tesla Test Facility (TTF), and the hard X-ray sources (TESLA-XFEL) as planned at Hamburg and the Linac Coherent Light Source (LCLS) at SLAC. In terms of output power, the performance data of the SASE-FEL projects compared to present high power lasers as well as sources using higher harmonic generation are shown on the right panel of Fig. 2. It is evident that in the photon energy range $E \geq 20$ eV there is a lack of powerful sources; only the FELs can deliver powerful pulses with ≤ 20 fs pulse length in this wavelength regime.

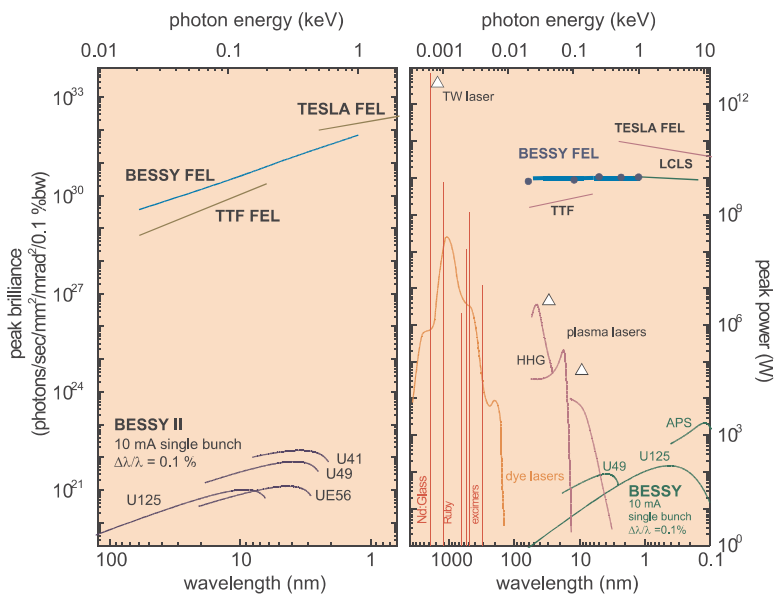
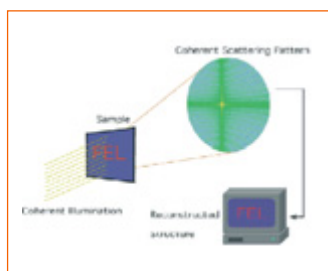


Fig. 2: Expected brilliance of the BESSY FEL in comparison with several radiation sources

FEL - Visions of Science

With its short and coherent pulses of enormous peak power, the BESSY-FEL opens a whole new field of scientific research and will serve both the synchrotron radiation and the laser communities. The impact of the new source on future scientific challenges has been discussed during a workshop in Holzhausen and is published in 'Visions of Science: The BESSY SASE-FEL in Berlin-Adlershof' (see attached CD). Some areas of research which can highly benefit from the new source are described below.



Magnetization dynamics of nanostructures on the fs time scale

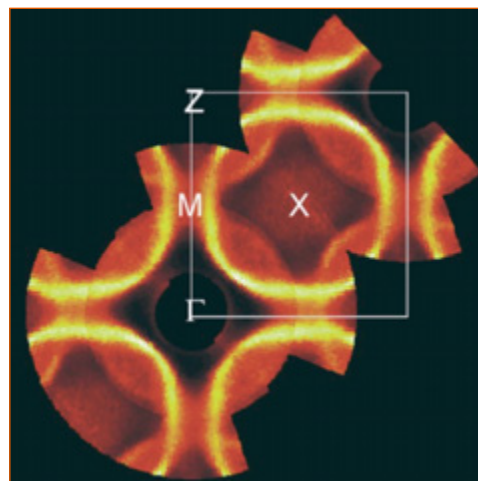
Magnetic data storage is continuously increasing in density and speed. In order to explore and expand the limits of this important technology the BESSY SASE-FEL will enable studies of the magnetization dynamics of small magnetic nanostructures and clusters on the femtosecond (fs) time scale in conjunction with nm spatial resolution. Dichroic effects in the soft X-ray regime are an ideal probe to monitor the magnetic moments with elemental specificity in space and time.

Femtochemistry – understanding the dynamics and formation of a chemical bond

On the fs time scale the nuclei in a molecule or solid are 'standing still'. Typical vibrational periods are between 20 and several 100 fs. Therefore spectroscopy with fs time resolution allows one to observe the effects of the motion of the nuclei on the electronic structure in a molecule, a solid, or adsorbate on a surface. In pump-probe experiments the development of the electronic states in a dissociating or desorbing molecule can be followed, yielding insights into the transition states and the nature of barriers determining the pathways for chemical reactions. Thus, the dynamics of the complete electronic structure can be observed using photo-emission as a tool.

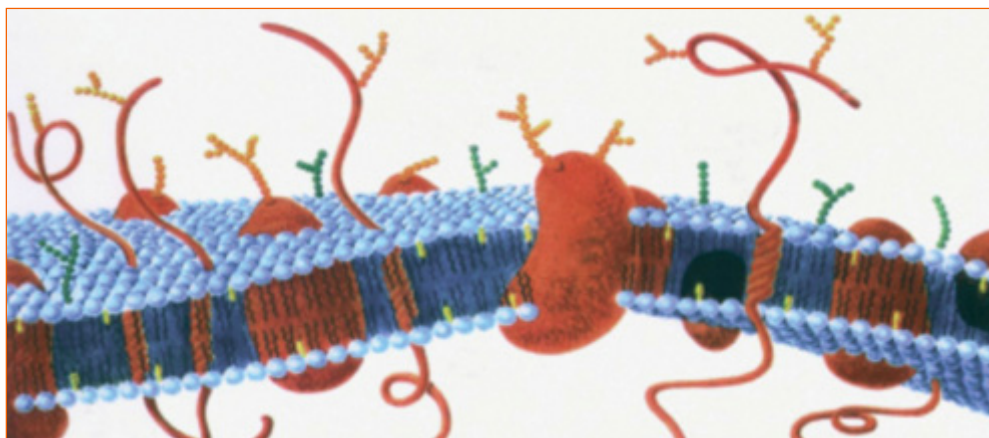
Atoms and molecules – new fundamental limits

Novel exotic states of matter can be prepared by Bose condensation of atoms in electrodynamic and optical traps. The BESSY SASE-FEL offers unique possibilities for spectroscopy and selective preparation or excitation of dilute assemblies and condensates of atoms in various traps. Thus elementary steps for the experimental realization of quantum computers may be explored. Furthermore, linear and non-linear interaction of radiation with atoms and molecules serves to test fundamental theoretical models with the highest possible precision.



The nature of complex solids

High-temperature superconducting oxides are already employed in several high-tech applications. However, the mechanism of superconductivity in these highly correlated materials is not yet understood and accordingly at the forefront of research in solid state physics. In general, these oxides exhibit a wealth of phenomena. Apart from the high temperature superconductivity of the cuprates this includes also the colossal magnetoresistance phenomenon of the manganates.



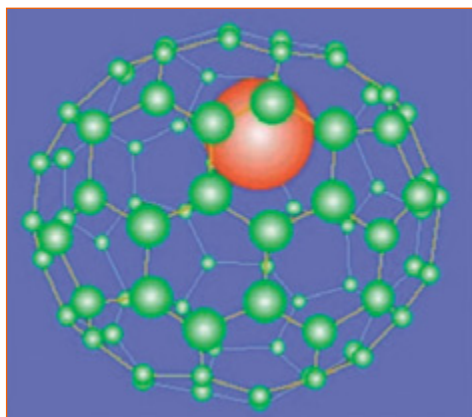
These materials exhibit complex phase diagrams with interesting stationary and dynamic phases. Resonant inelastic soft X-ray scattering, which can be carried out also in the presence of magnetic fields, as well as electron spectroscopy with ultimate energy and momentum resolution, hold the promise to furnish decisive data to resolve some of these mysteries of modern physics. With the FEL the resolution capabilities for electron spectroscopy and soft X-ray scattering will be enhanced by orders of magnitude in the spectral and spatial domain.

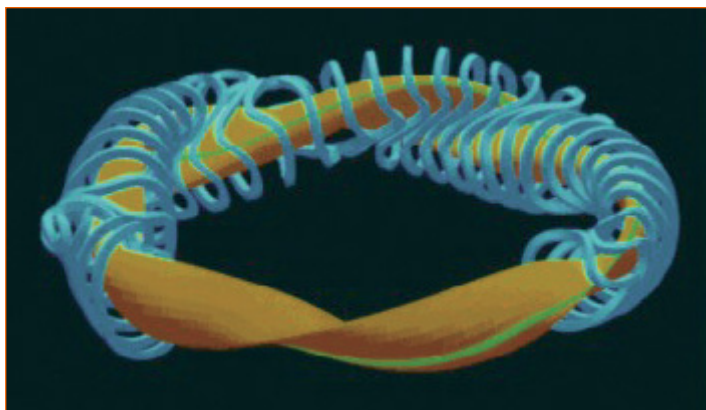
Clusters as new materials

Clusters of almost any element of the periodic table may be assembled with an exactly defined number of atoms thus preparing the way to the development of new materials tailored with exceptional precision. The fullerenes are presently the best known example of such cluster materials. Upon condensation, the fullerenes form a semi-conducting solid, the third modification of carbon apart from graphite and diamond. Upon doping the C_{60} solid with alkali atoms, superconductivity has been observed at transition temperatures exceeding 30 K. The FEL with a photon energy in the VUV and soft X-ray range and pulse energy comparable to present day lasers will be a unique tool for characterising atomic geometry and electronic structure of the individual building blocks of these exciting new materials.

Dynamics in biological systems

The BESSY soft X-ray FEL opens the unique possibility to combine microscopy with a resolution in the nm range, spectroscopy with high energy resolution and accordingly high chemical selectivity, and a superb time resolution in the fs range in investigations of biological systems in their natural wet environment. This will open a new route to an understanding of functional systems such as ion channels, molecular motors and pumps embedded in cellular membranes. Furthermore, the dynamics of various steps in biological functional cycles in photosynthesis or in enzymatic reactions may be followed and resolved in real time.





Characterization of fusion plasmas

The diagnostics of elementary processes in fusion reactors relies on the analysis of the characteristic radiation emerging from the reactor. Important parameters for these diagnostics are absolute cross sections and lifetimes of highly excited states of multiply charged ions, which currently are only partially known. Using the FEL a reliable database may be established in studies of dilute plasmas or on ion beams to provide a better understanding and diagnostics for the development of this future energy source.

Ultrahigh resolution spectroscopy

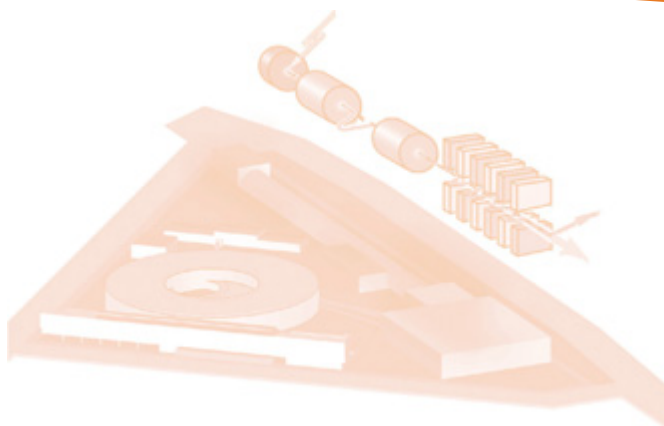
The dramatic increase in brightness of the FEL opens up the possibility to perform investigations of the electronic structure with a resolution comparable to the thermal energy scale (K) rather than meV. This allows one to investigate energy gaps in superconductors, phase transitions, Kondo resonances, and other many body phenomena with unprecedented spectroscopic precision.

New perspectives on catalysis

Spectroscopy of catalysts under 'real conditions', i.e. under a gaseous atmosphere or submerged in a liquid is one of the visions to advance research in catalysis from the study of model systems towards real catalysts. Photons are able to penetrate this environment and to carry spectroscopic information. Using sum frequency generation (IR + VUV), for example, a specific vibrational mode can be detected originating at a specific atom selectable via the chemical shift of its core electrons. Resonant inelastic X-ray scattering is another probe that allows one to distinguish the electronic structure at atomic centers according to their chemical environment, promising new insights into local electronic interactions at the reaction centers in this complex environment with a high potential for impact on industrial technology.

Nanofabrication of materials using soft X-rays

Materials with a structural size on the nm size scale offer extraordinary possibilities for atomic scale engineering of materials which is synonymous with tailoring the electronic, optical, magnetic, chemical or even mechanical properties. Already today, thin film systems, where one dimension is reduced to the nm size scale, form the basis of the high-tech electronics and information industries with revenues in the multibillion Dollar range. These systems have an impact on everybody's daily life. Laterally or even 3-D structured materials with controlled features in the nm range are still largely a challenge for the future. At the BESSY SASE-FEL, feature sizes may be realized much smaller than envisioned for the next step in industrial applications of EUV lithography (at 13.5 nm), corresponding to a wavelength limit as short as 1.2 nm. The FEL, where the high power is concentrated in an extremely narrow spectral range, is an ideal source for nanolithography.



Materials and processes observed under technologically relevant conditions

Electrochemical reactions, thin film growth, corrosion, and friction are, apart from catalysis, technologically and economically highly relevant processes, where surfaces are in contact with a gas or a liquid. The FEL photons have sufficient intensity to penetrate this liquid or gaseous environment. This opens the field for spectroscopic investigations of these surfaces under process conditions using the methods of resonant inelastic soft X-ray scattering for the investigation of the electronic structure with not only elemental but even chemical specificity.

Time resolved spectroscopy – reaching the attosecond range

Intrinsically the FEL has pulses of about 200 fs in length. Advanced seeding concepts which will be explored in close collaboration with scientists from the Max-Born-Institut hold the promise to reach pulse lengths shorter than 20 fs. Ultimately for soft X-ray pulses the time resolution could be pushed into the attosecond region, far beyond the limits of lasers at photon energies in the visible optical spectrum.

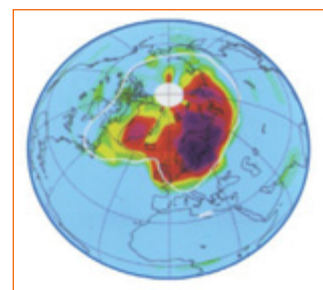
New Frontiers in photon-related spectroscopies and coherence

The FEL offers a fully transverse coherent beam with about 10^9 degenerate photons within the coherence volume. Exploiting the coherence opens the pathway for new 'imaging' techniques, where the individual rather than the statistical properties of the sample can be probed in time-resolved single shot experiments in life, environmental, materials and chemical sciences. Furthermore, photons are able to penetrate

through solids, liquids, and gases and thus resonant (inelastic) scattering offers a unique, element and chemical environment selective probe of the electronic structure.

Environmental chemistry and analysis

Chemical and biological processes occurring at the complex interfaces between organic and anorganic matter, aqueous solutions, and gases control the composition of the environment and determine the migration and toxicity of pollutants in the biosphere. Understanding these processes and their dynamics at the molecular size scale in their natural environment is a key factor for the development of better models for the spreading of pollutants and to develop better strategies for environmental remediation. Soft X-rays from the FEL uniquely enable a characterization of these systems and processes in their natural state with nm spatial and sub ps time resolution.



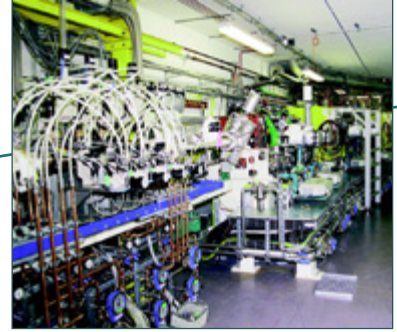
Chemistry of radicals

Understanding the factors and key processes influencing the global change in climate is one of the most important scientific problems of present times. The chemistry of radicals as well as photo-physical reactions on the surfaces of suspended nanoparticles play an important role in understanding the processes and interactions in the upper atmosphere. The FEL, possibly in conjunction with an ion storage device, will furnish a new spectroscopic tool to study these processes, reaction pathways, cross sections and the formation of elusive chemical species in unprecedented fashion. Furthermore, the FEL offers fascinating prospects for the study and the simulation of the processes and reactions occurring in interstellar clouds in the presence of intense VUV and X-ray radiation.

Facts & Figures

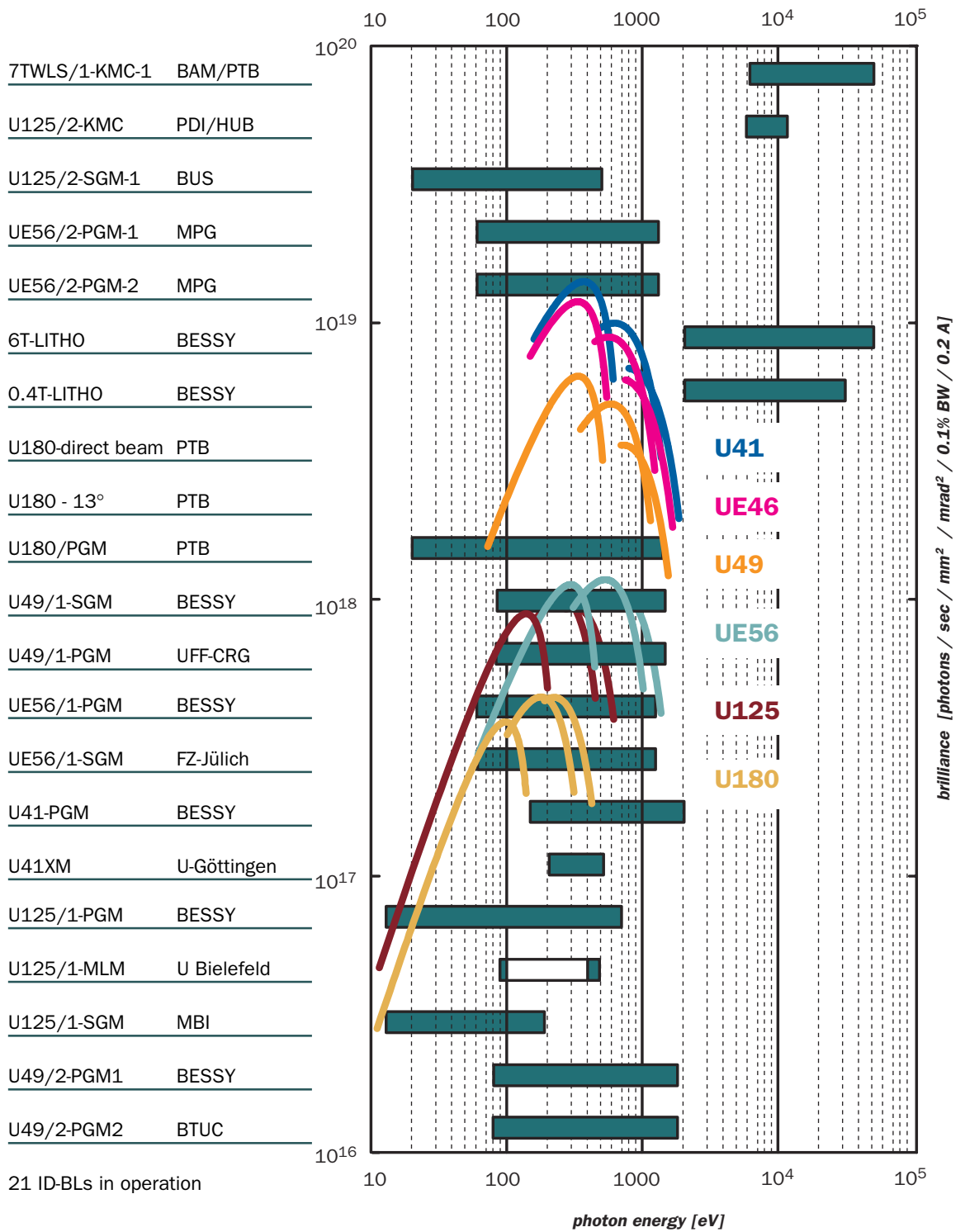
6





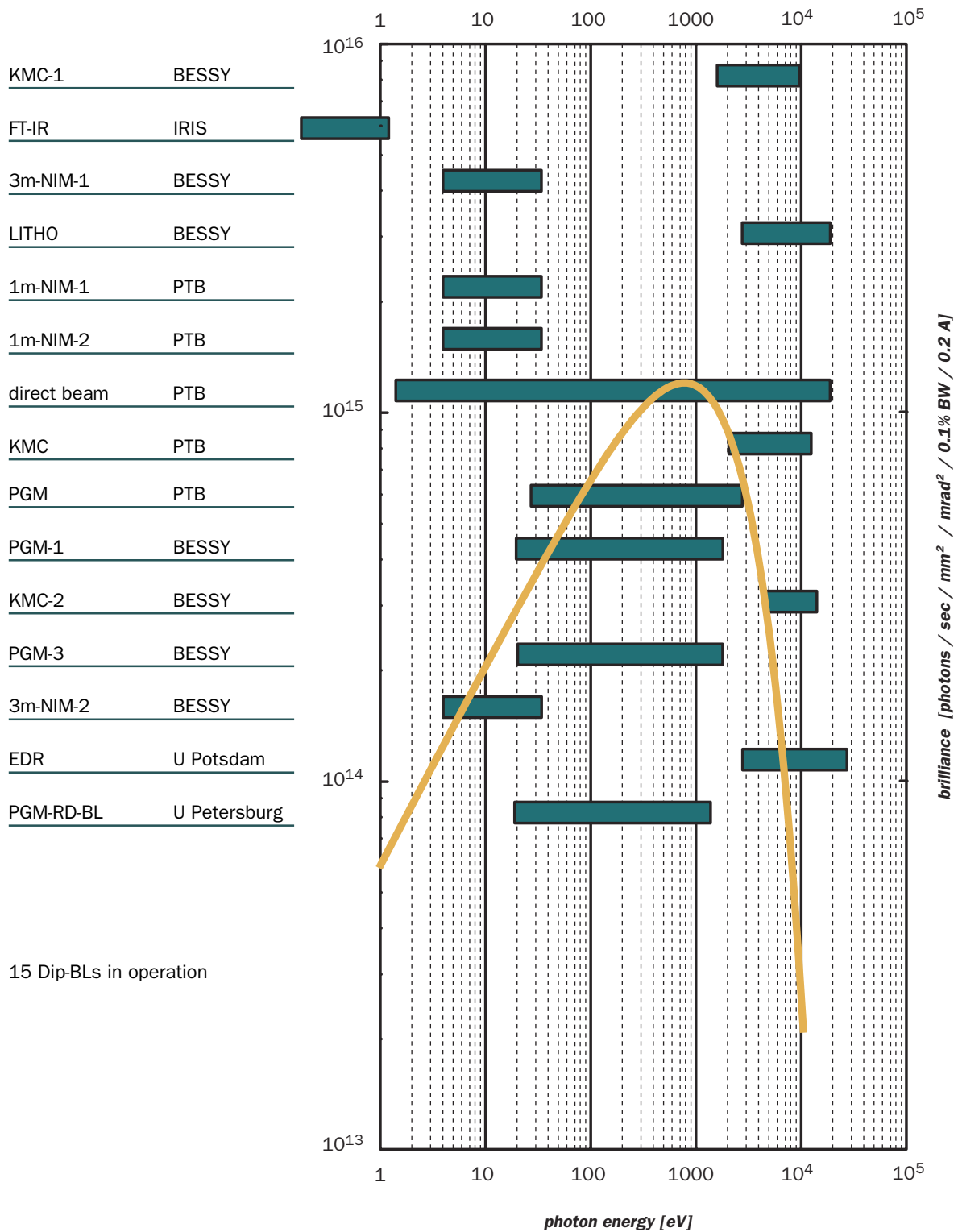
ID Beamlines at BESSY II

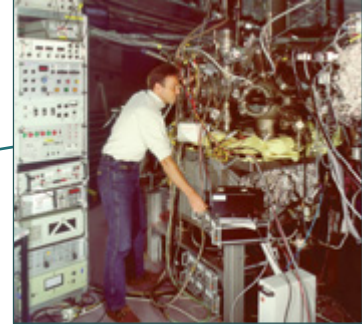
(January 2002)



DIPOLE Beamlines at BESSY II

(January 2002)





Beamlines on Insertion Devices

<i>Insertion Device</i>	<i>Monochromator</i>	<i>Energy Range (eV)</i>	<i>Contact Persons</i>	
7 T WLS/1	KMC 1	6 k – 50 k	H. Riesemeier (BAM) B. Müller (BAM)	A. Erko
U 125 - 2	KMC	6 k – 12 k	W. Braun (PDI) A. Erko	B. Jenichen (PDI)
U 125 – 2*	NIM	< 10 – 35	A. Ehresmann (U KI) G. Reichardt	I. Packe P. Rotter
U 125 - 2	SGM	20 – 500	R. Püttner (FUB)	G. Reichardt
UE 56-2	PGM 1	60 – 1 300	W. Mahler (MPG) B. Zada (MPG)	H.-C. Mertins
UE 56-2	PGM 2	60 – 1 300	W. Mahler (MPG) B. Zada (MPG)	H.-C. Mertins
6 T WLS	LITHO	> 2 000	B. Löchel H. Köhrich	H.-U. Scheunemann M. Bednarzik
0.4 T	LITHO	> 2 000	B. Löchel H. Köhrich	H.-U. Scheunemann LM. Bednarzik
U 180/(U 49*)	-	direct beam	R. Klein (PTB)	
U 180/(U 49*)	13°		R. Klein (PTB)	A. Gottwald (PTB)
U 180/(U 49*)	PGM	20 – 1 900	B. Beckhoff (PTB)	
U 49 -1/(UE 52*)	SGM	85 – 1 600	F. Senf	T. Zeschke
U 49 -1/(UE 52*)	PGM	85 – 1 600	T. Schmidt (U Wü)	C. Jung
UE46*	PGM	120 – 1 700	H. Rossner (HMI) D. Schmitz (HMI)	F. Senf
UE 56 -1	PGM	60 – 1 300	H.-C. Mertins J. Schmidt	T. Zeschke
UE 56 -1	SGM	60 – 1 300	S. Cramm (FZJ)	
U 41	PGM	170 – 1 800	C. Jung	M. Mast
U 41	XM	~ 200 – ~600	P. Guttman (U Gö)	
U 125 -1	PGM	20 – 700	P. Bressler	F. Eggenstein
U 125 -1	Multilayer	80 – 700	M. Pohl (U Bi)	
U 125 -1	SGM	15 – 180	B. Winter/T. Gießel/ W. Widdra (MBI)	R. Follath
7T WLS/2*	KMC-1	4.5 k – 17.5 k	U. Müller (PSF)	K. Höppner (PSF)
7T WLS/2*	KMC-2	4.5 k – 17.5 k	U. Müller (PSF)	K. Höppner (PSF)
7T WLS/2*	KMC-3	13.7 k	U. Müller (PSF)	K. Höppner (PSF)
U 49 -2	PGM 1	85 – 1 600	R. Follath	J.-S. Schmidt
U 49 -2	PGM 2	85 – 1 600	P. Hofmann (BTUC)	D. Batchelor

* *under construction*

Beamlines on Dipole Magnets

<i>Monochromator</i>	<i>Energy Range (eV)</i>	<i>Contact Persons</i>	
KMC-1	1.7 k – 10 k	F. Schäfers M. Mertin	F. Neißendorfer
FT-IR	IR	F. Bartl (HUB)	U. Schade
3m-NIM-1	4 – 35	T. Schroeter I. Packe	G. Reichardt
LITHO	direct beam	B. Löchel H.-U. Scheunemann	H. Köhrich M. Bednarzik
1m-NIM-1	3 – 35	M. Richter (PTB)	
1m-NIM-2	3 – 35	M. Richter (PTB)	
	direct beam	R. Thornagel (PTB)	
KMC	1.7 k – 10 k	M. Krumrey (PTB)	
PGM	30 – 1 800	F. Scholze (PTB)	
HE-SGM*	200 – 700	A. Lippitz (BAM)	O. Schwarzkopf
PGM-1	20 – 1 900	T. Kachel	F. Eggenstein
KMC-2	4.5 k – 15 k	A. Erko	I. Packe
PGM-3	20 – 1 900	T. Kachel	F. Eggenstein
3m-NIM-2	4 – 35	T. Schroeter I. Packe	G. Reichardt
EDR	2 k – 12 k	J. Grenzer (U Po)	A. Erko
TGM-7*	8 – 120	C. Pettenkofer (HMI)	S. Tiefenbacher (HMI)
TGM-4*	8 – 120	K. Godehusen	M. Mast
PGM-RD-BL	30 – 1 500	D. Vyalikh (FUB) S. Molodtsov (TUD)	A. Shikin
CP-NIM*	4 – 35	F. Neißendorfer M. Mertin	F. Schäfers

* *under construction*

*BAM
Bundesanstalt für
Materialforschung und -
prüfung*

*BTUC
Brandenburgische Technische
Universität Cottbus*

*FUB
Freie Universität Berlin*

*FZJ
Forschungszentrum Jülich*

*HMI
Hahn-Meitner-Institut*

*HUB
Humboldt-Universität zu
Berlin*

*MPG
Max-Planck-Gesellschaft*

*PSF
Proteinstrukturfabrik*

*PTB
Physikalisch-Technische
Bundesanstalt*

*TUB
Technische Universität
Berlin*

*TUD
Technische Universität
Dresden*

*U Bi
Universität Bielefeld*

*U Gö
Universität Göttingen*

*U KI
Universität Kaiserslautern*

*U Po
Universität Potsdam*

*U Wü
Universität Würzburg*

*For general information on beamlines see BESSY website under
www.bessy.de*



Experimental stations

The aim of BESSY is to make the unique opportunities offered by synchrotron radiation accessible to a large user community. Thus, those scientists who plan to perform experiments at BESSY but do not have dedicated experimental equipment find below a list of experimental stations available for common use. The list merges setups which are already available with those designed to exploit the enhanced performance of BESSY II.

In addition to the stations already available several new experimental stations are under construction for future use at BESSY. These experiments will be put into operation during 2003. For further information on the experimental stations please contact W. Braun (braun@bessy.de) or Ch. Jung (jung@bessy.de)

Experimental systems available at BESSY	UPS / XPS	Microscopy	Electron yield	Fluorescence	X-ray emission	Contact
HIRES – high resolution electron spectrometer	•		•			rader@bessy.de
PHOENEXS – photoemission and near edge X-ray spectroscopy	•		•	•		bressler@bessy.de
Multi-user-multi-purpose measuring station	•		•	•		tepper@bessy.de
Fluorescence spectrometer				•	•	ruediger.mitdank@physik.hu-berlin.de
Two-photon-photoemission experiment	•					bwinter@mbi-berlin.de
XPEEM photoemission microscopy		•				pohl@physik.uni-bielefeld.de
HIRE-PES – highest energy resolution photoemission	•					christoph.jannowitz@physik.hu-berlin.de
Soft X-ray emission spectrometer					•	eisebitt@bessy.de
ROSA – rotatable spectrometer apparatus	•				•	szargan@rz.uni-leipzig.de
SMART – spectro-microscope with highest spatial resolution	•	•				thomas.schmidt@physik.uni-wuerzburg.de
XM – X-ray microscopy		•				guttman@bessy.de

IRIS – infrared spectroscopy experiment	schade@bessy.de
Infrared ellipsometry	hinrichs@isas-berlin.de
VUV / XUV ellipsometry	norbes@gift.physik.tu-berlin.de
Scattering experiments in the VUV / XUV range	eugen.weschke@physik.fu-berlin.de
X-ray diffraction during molecular beam epitaxy	ploog@pdi-berlin.de
Reflectometry	schaefers@bessy.de
Polarimetry	mertins@bessy.de

Experiments under construction	UPS / XPS	Microscopy	Electron yield	Fluorescence	X-ray emission	Absorption	Scattering
Investigations on stored nano particles	•			•			•
X-ray emission on organic substances and biomaterials			•		•		
So-Li-AS – the solid-liquid-analysis system	•						
Photoemission microscope for time resolved spectroscopy in the ps-regime	•	•					
High resolution spinpolarization photoelectron spectroscopy	•						
UVIS – circular dichroism spectroscopy for biological investigations						•	

User operation

Operation Statistics

Throughout the year 2001 the source delivered photon beam to the experiments for 3,900 h about 10% more scheduled resulting from the trouble-free night operation where the machine is run without human intervention.

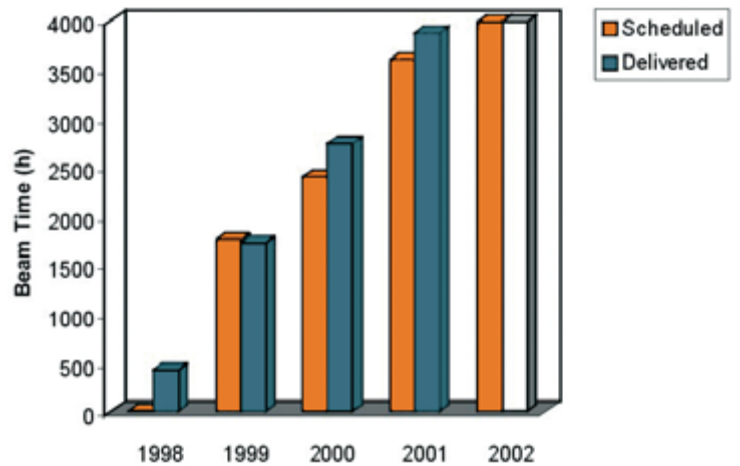
The general operation schedule was made up of six periods of user operation adding up to a total of 28 weeks of user operation on a basis of seven days per week, 24 h a day. The storage ring operated during additional 13 weeks for dedicated machine development as well as for undulator and beamline commissioning.

Failures and Preventive Maintenance

The overall availability of the BESSY light source was 94%. About half of the down-time was associated with technical malfunctions, the other half originated from injection.

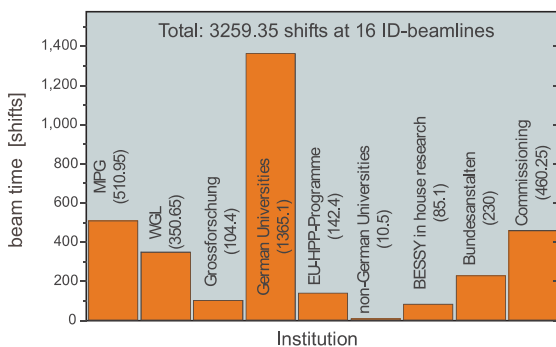
The major hardware problem was one rf-resonator which developed a vacuum leak in a damping antenna. To replace the device the rf-section had to be vented, rf-cavities needed one week of re-conditioning.

Annual operation times from 1998 to 2001

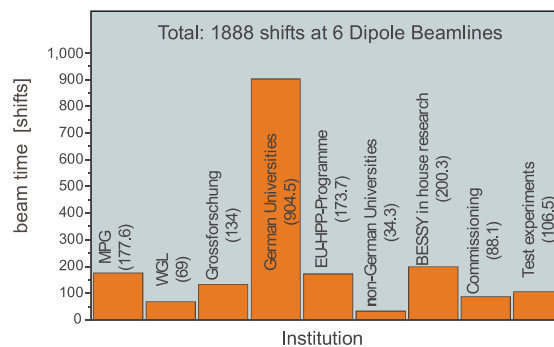


Allocation of beam time at BESSY II (2001)

Insertion Device Beamlines



Bending Magnet Beamlines

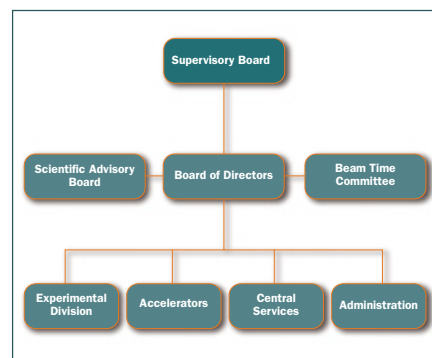


Number of User Runs: 160
Projects in the EU-HPP-Programme: 20
Average beam time per User Run: 32.2 shifts

MPG = Max-Planck-Gesellschaft
 WGL = Wissenschaftsgemeinschaft Gottfried Wilhelm Leibniz,
 Grossforschung = Members of Helmholtz Gemeinschaft,
 Bundesanstalten = BAM, PTB

Advisory Boards

(January 2002)



Supervisory Board

Prof. Dr. J. Treusch (Chairman)	Forschungszentrum Jülich
Prof. Dr. A. Goldmann (Vice-Chairman)	Gesamthochschule Kassel
ORR C. Brandt	BMBF
Prof. Dr. E. O. Göbel	PTB Braunschweig
M. Meinecke	Max-Planck-Gesellschaft München
Prof. Dr. R. Maschuw	Forschungszentrum Karlsruhe
Dr. D.-M. Polter	Fraunhofer Gesellschaft München (FhG)
Prof. Dr. W. Saenger	Freie Universität Berlin
Prof. Dr. J. Schneider	DESY Hamburg
MinRat Dr. J. Schöttler	BMW
Prof. Dr. M. Steiner	Hahn-Meitner-Institut, Berlin (HMI)
Ltd. Senatsrat J. Stoehr	Senatsverwaltung WFK, Berlin

Financial Committee

Dr. H. Krech (Chairman)	DESY Hamburg
Dr. W. Buck	PTB Berlin
OAR H. Diermann	BMBF
R. Kellermann	Forschungszentrum Jülich
A. Röhr	Max-Planck-Gesellschaft, München
Dr. R. Schuchardt	Senatsverwaltung WFK, Berlin

Scientific Advisory Committee

Prof. Dr. M. Grunze (Chairman)	Universität Heidelberg
Prof. Dr. V. Saile (Vice-Chairman)	Forschungszentrum Karlsruhe
Prof. Dr. D. S. Chemla	Advanced Light Source, Berkeley, USA
Prof. Dr. M. Eriksson	MAXLab Lund, Schweden
Prof. Dr. H.-J. Freund	Fritz-Haber-Institut, Berlin
Prof. Dr. K.C. Holmes	MPI für medizinische Forschung, Heidelberg
Prof. Dr. Y. Petroff	Lawrence Berkeley Lab, Berkeley, USA
Prof. Dr. W. Sandner	Max-Born-Institut, Berlin
Prof. Dr. G. Schütz	MPI für Metallforschung, Stuttgart
Prof. Dr. J. Stöhr	Stanford Synchrotron Radiation Laboratory, USA
Dr. A. F. Wrulich	Paul-Scherrer-Institut Villigen, Schweiz

Permanent Guests:

ORR C. Brandt	BMBF
Prof. Dr. R. Gerhardt-Mulhaupt	Universität Potsdam
Prof. Dr. H. Hahn	TU Darmstadt
Dr. T. Möller	HASYLAB/DESY Hamburg
Dr. R. Schuchardt	Senatsverwaltung WFK, Berlin

Beam Time Committee

Prof. Dr. J. Fink (Chairman)	IFW Dresden
Prof. Dr. H.-P. Steinrück (Vice-Chairman)	Universität Würzburg
Prof. Dr. D. Arvanitis	Universität Uppsala
Prof. Dr. H. Bertagnolli	Universität Stuttgart
Prof. Dr. M. Grunze	Universität Heidelberg
Prof. Dr. E. Rühl	Universität Osnabrück
Prof. Dr. K.-H. Schartner	Universität Gießen
Prof. Dr. R. Schlögl	Fritz-Haber-Institut Berlin
Prof. Dr. G. Schütz	MPI für Metallforschung, Stuttgart

Contact

Scientific Director

Prof. Dr. Wolfgang Eberhardt

Secretary: Ines Maupetit

phone +49 (0)30 / 6392 4633

fax +49 (0)30 / 6392 2989

Eberhardt@bessy.de, Maupetit@bessy.de

Technical Director

Prof. Dr. Eberhard Jaeschke

Secretary: Nikoline Hansen

phone +49 (0)30 / 6392 4651

fax +49 (0)30 / 6392 4632

Jaeschke@bessy.de, Hansen@bessy.de

Administration

Thomas Frederking

Secretary: Katrin Rosenblatt

phone +49 (0)30 / 6392 2901

fax +49 (0)30 / 6392 2920

Frederking@bessy.de, Rosenblatt@bessy.de

Beam time Coordination

Dr. Walter Braun, Dr. Gerd Reichardt

Secretary: Stine Mallwitz

phone +49 (0)30 / 6392 2904

fax +49 (0)30 / 6392 4673

Braun@bessy.de, Reichardt@bessy.de,

Mallwitz@bessy.de

User Office

Daniela Baum, Maha Krämer

phone +49 (0)30 / 6392 4734

fax +49 (0)30 / 6392 4746

Baum@bessy.de, MahaKraemer@bessy.de

Public Relations

Regina Bost, Dr. Heike Henneken,

Dr. Markus Sauerborn

phone +49 (0)30 / 6392 2907

fax +49 (0)30 / 6392 2925

pr@bessy.de

Photo Credits:

FOM Institute, Rijnhuizen, NL

Graffinity AG, Heidelberg

IBM Corporation, USA

Institut für Röntgenphysik
der Universität Göttingen

Institut für Kristallographie
der FU Berlin

Licht&Schatten GmbH, Berlin

Staatlichen Museen Berlin,

Kupferstichkabinett

J. Waters, JPL, USA

Carl Zeiss, Oberkochen

Mauritius GmbH, Berlin

